Investigations on Startup Instabilities and Power Ramping Procedures for Natural Circulation Boiling Systems

A Thesis Submitted in
Partial Fulfillment of the Requirements
for the Degree of

Doctor of Philosophy

by

S. P. Lakshmanan

Department of Mechanical Engineering
Indian Institute of Technology Guwahati

May 2010

TH-831_05610306

To my parents

TH-831_05610306

TH-831_05610306

Acknowledgment

I express my deepest gratitude to my supervisor, Dr. Manmohan Pandey, for his inestimable guidance and support, for the constant inspiration I drew from his critical thinking and approach, and for providing an excellent working atmosphere. His thoughtful suggestions and ideas were vital for the framework and outcome of this research. It has been a rewarding experience for me in working with him all these years, and has inspired me enough in different aspects of research and life, for the years to come.

My sincere and heartfelt thanks to Prof. Kannan N. Iyer for giving me the opportunity to work with him in his laboratory. It was an enriching experience. The understanding and confidence I gained over various aspects of experimental studies are very valuable.

I would like to thank my doctoral committee members, Prof. Anoop. K. Dass, Prof. Subhash C. Mishra and Dr. Vijay S. Moholkar, for their valuable suggestions and encouragement during my research work. I also extend my sincere thanks to Prof. P. Mahanta for his help and advice as my administrative supervisor. I am very thankful to Dr. S. K. Gupta for his expert advice and suggestions on my research topic. Special thanks to Mr. S. K. Pradhan for his help with RELAP5 code.

I would like to acknowledge Indian Institute of Technology Guwahati for providing me with the funds and facilities for carrying out my research. I am thankful to Atomic Energy Regulatory Board for providing me partial financial support during my research work. I would also like to acknowledge Indian Institute of Technology Bombay and Indian Institute of Technology Gandhinagar for the facilities during my research related visits.

I would like to thank all my colleagues in our research team, especially Mr. Durga Prasad and Mr. Pradeep Kumar, for their discussions, suggestions and help in my research work. I extend my thanks to Lab Assistant Mr. Rahul for his help during the conduct of startup experiments in the test facility.

I am thankful to many friends across different IITs. Special mention to my dear friends Santosh, Satheesh, Subraminian and Vijay at IIT Guwahati, for being with me in good and as well as difficult times through these years; Vivek and Bhoomek for their

TH-831_05610306

friendship and help during my stay at IIT Bombay. Many thanks to my teammates in the sports field for their friendship and company.

I wish to extend my special thanks to Smt. Divya Pandey for her kind hospitality and I appreciate her efforts for making me feel at home. I wish I stay in touch with her family for long.

I am very grateful to my beloved parents Shri. R. Periasamy and Smt. P. Chandrakala, for their immeasurable love, understanding and unwavering support, which has made this feat possible. Last but not least, my love to my sister Ananthi, as she never agrees with any gesture of thanks from me.

TH-831_05610306

Abstract

The thesis contains studies on startup instabilities and methods of power ramping in natural circulation boiling water systems. Numerical models of a test facility and its prototype have been developed using RELAP5 code. Startup transients in both single and double channel systems have been analyzed and their structural nature has also been determined. Numerical simulations on power ramping have been performed and suitable startup procedures for the boiling systems have been evolved. Experimental observations in a test facility have been used for model validation and analysis.

In the recent past, the use of natural circulation in boiling water reactors (NCBWRs) has been highly recognized for its inherent passive safety feature and the potential for improved economy in nuclear power generation. However, the use of natural circulation has generated concern regarding operating conditions, especially related to the startup phase of the reactor. During startup, an NCBWR is susceptible to flow oscillations when the system has to pass from single-phase to two-phase operation. The startup instabilities are often induced by the phenomena of geysering in the heated channel and flashing in the riser section, which may result in mechanical vibrations, system control problems and critical heat transfer issues. A proper understanding of these instabilities through experimental and numerical studies is of primary importance before attempting to devise an appropriate startup procedure.

For numerical simulation of two-phase flow instabilities, a thermal-hydraulic system code such as RELAP5 can be employed. However, the use of such codes to simulate the transients during startup conditions is yet to be fully established. Although earlier reports suggested that RELAP5 cannot deal with flashing instabilities, recent studies towards enhancing the predictive performance of the code under low-pressure subcooled conditions indicate promising results. In the present work, numerical models of a natural circulation test facility and its prototype (a pressure tube type NCBWR)

TH-831_05610306

have been developed with RELAP5 code and verified for their grid independence. The model of the test facility has been validated for its steady state as well as transient predictions with the help of experimental observations. The transient predictions and parametric trends obtained by the numerical model of the prototype have been compared with those of the numerical model of the test facility. Thus, the ability of RELAP5 code to predict the transients during startup of a natural circulation boiling water reactor has been verified.

It is important to get an insight of the phenomena behind the low-pressure low-power transients that occur during startup of a natural circulation boiling system. The RELAP5 model developed for the test facility and its prototype is used to record additional system parameters that were not included in the data obtained from experiments. The flow oscillations observed during experimental and numerical studies are analyzed and classified. It is inferred that the low amplitude oscillations are not condensation induced geysering instabilities, but a density wave instability supported by flashing. The similarity between the nature of startup transients observed in the test facility and the prototype has also been examined, and a different kind of startup oscillations is found in the prototype where only flashing exists. The effect of flashing is more pronounced in the prototype due to the strong variation of saturation temperature, as the length scale is 4 times that of the model. The understanding of transient phenomena can be enhanced by doing a time series analysis of the data recorded during an experimental or numerical study. The computation of power spectral density, Lyapunov exponents and Poincaré sections helps in understanding the structural behavior of flow signals. The data obtained from experimental observations and numerical simulations are analyzed to identify the structural nature of flow oscillations. The power spectral density estimated using fast Fourier transform (FFT) algorithm illustrates the chaotic nature of the signals. The nonlinear time series analysis (TISEAN) package has been used for the estimation of Lyapunov exponents and Poincaré sections. The Poincaré section and the Lyapunov exponent confirm the chaotic nature of the flow oscillations.

TH-831_05610306

The above understanding on the transport mechanism and the structural nature of the observed flow oscillations is attained through a single channel analysis. However, single channel models are inadequate to model out-of-phase instabilities, especially when there are hundreds of parallel-channels involved, as in the case of the pressure tube type NCBWR studied here. Hence, startup transients in parallel-channel natural circulation boiling systems have been simulated numerically using RELAP5. The parallel-channel RELAP5 model is an extension of the single-channel model. The existence of in-phase and out-of-phase flashing instabilities in the parallel-channel systems is investigated through simulations under equal and unequal power boundary conditions and flow restrictions in the channels. Under unequal power, flow reversal is observed in one channel when there is a sudden surge in flow through the other channel due to flashing. The effect of flow resistance on Type-I oscillation has also been explored. Presence of additional loss coefficient in one channel results in out-of-phase flow oscillations in parallel-channel systems.

A normal startup procedure for an NCBWR can be divided into four distinct phases: Phase I - Single-phase core heat up, Phase II - Net vapor generation in core, Phase III - Saturated chimney, and Phase IV - Power ascension to full power. The transition through Phase II and Phase III is important, where the instabilities like geysering and flashing are highly dominant. Phase IV also assumes importance in taking the system to the operating pressure in a reasonable time, especially in test facilities where the system has to be pressurized on a daily basis. In view of these, the present work attempts to propose suitable startup procedures for reactors and test facilities. A number of numerical experiments are carried out using various power ramps, to identify the suitable heat-up rate. It is inferred that, using a suitable heat-up rate, the reactor can be pressurized to the desired operating conditions in a reasonable time, without considerable void generation in the core, albeit with the occurrence of flashing in the riser section. Though flashing helps in steam production, the amplitude of flow oscillations induced by flashing is the event of concern. Therefore, the feasibility of a complete single-phase startup is also examined and is found not attractive considering the time factor and the requirement of additional components that involve modifications in the design of the PHT. A startup procedure completely bypassing the

TH-831_05610306

unstable two-phase region has been conceptualized and numerically simulated. A powering procedure for the test facility, addressing Phase IV of the startup, has been devised with the help of its RELAP5 model and demonstrated experimentally, which results in saving considerable amount of time in raising the system pressure to the desired operating condition.

TH-831_05610306

Publications from this Work

International Journals

1) Lakshmanan, S. P., Pandey, M., Kumar, P. P., Iyer. K. N., Study of startup transients and power ramping of natural circulation boiling systems, Nuclear Engineering and Design, 239, pp.1076-1083, 2009.

2) Lakshmanan, S. P., Pandey, M., Analysis of startup oscillations in natural circulation boiling systems, Nuclear Engineering and Design, 239, pp.2391-2398, 2009.

3) Lakshmanan, S. P., Pandey, M., Numerical investigations on power ramping procedure for a natural circulation boiling water reactor, Nuclear Engineering and Design. 240, pp.860-867, 2010.

4) Lakshmanan, S. P., Pandey, M., Numerical investigation of startup instabilities in parallel-channel natural circulation boiling systems, Science and Technology of Nuclear Installations (accepted).

Conference Proceedings

5) Lakshmanan, S. P., Kumar, P. P., Pandey, M., Iyer. K. N., Simulation for startup transients in a natural circulation boiling loop, ASME Int. Conf. Nuclear Engineering (ICONE-16), Orlando, Florida, USA, Log. ICONE16-48406, 2008.

6) Lakshmanan, S. P., Pandey, M., Review of the state of the art on startup transients in natural circulation boiling water systems, National Conference on Recent Advances in Mechanical Engineering (NCRAME-2008), NIT Silchar, Assam, India. Paper No.22, 2008.

7) Lakshmanan, S. P., Pandey, M., Numerical experiments on power ramping in a natural circulation boiling water reactor, 13th Int. Topical Meeting on Nuclear Reactor Thermal Hydraulics (NURETH-13), Kanazawa, Japan, N13P1194, 2009.

8) Lakshmanan, S. P., Pandey, M., Numerical study of startup instabilities in a parallel-channel natural circulation boiling system, 20th National and 9th International ISHMT-ASME Heat and Mass Transfer Conference Mumbai, India, 10HMTC277, 2010.

TH-831_05610306

TH-831_05610306

Contents

Abstract iii
Publications from this work vii
List of figures xi
List of tables xiv
Nomenclature xv

1. Introduction 1
1.1. Motivation 1
1.2. Major objectives 2
1.3. Organization of thesis 3

2. Review of Literature 5
2.1. Introduction 5
2.2. Flow instabilities during startup 5
2.3. Experimental facilities 14
2.4. Modeling of startup transients 15
2.5. Startup procedures 18
2.6. Summary 19

3. Numerical Models 21
3.1. Introduction 21
3.2. Code description 22
3.3. Test facility 28
3.4. RELAP models 29
3.4.1. Nodalization schemes 29
3.4.2. Nodal sensitivity studies 31
3.5. Model validation 33
3.6. Verification of NCBWR model 37
3.7. Summary 40

4. Analysis of Startup Oscillations 41
4.1. Introduction 41
4.2. Analysis of startup oscillations 42
4.2.1. Flow instabilities in NCTF 42
4.2.2. Flow instabilities in NCBWR 46
4.3. Time series analysis 47
4.3.1. Power spectrum analysis 48
4.3.2. Poincaré section 51
4.3.3. Lyapunov exponent 53
4.4. Summary 55

5. Startup Oscillations in Parallel-Channel Systems 57
5.1. Introduction 57

TH-831_05610306

5.2. Description of parallel-channel systems 57
5.3. Numerical model 59
5.4. Results and discussion 60
5.4.1. Single channel power input 60
5.4.2. Double channel power input 62
5.4.3. Effect of loss coefficients 66
5.5. Summary 69

6. Power Ramping Procedure for NCBWR 71
6.1. Introduction 71
6.2. Numerical experiments on reactor heat-up rate 72
6.2.1. An initial startup test 72
6.2.2. Simulations for various heat-up rates 73
6.3. Startup of NCBWR under single-phase condition 81
6.4. Conceptualization of a new startup procedure 82
6.4.1. RELAP5 simulation procedure 84
6.4.2. Numerical demonstration of startup procedure 85
6.4.3. Point of bleed 86
6.5. Summary 88

7. Ascension to Full Power 89
7.1. Introduction 89
7.2. Power ramping procedure for the test facility 90
7.3. Prediction of stability boundary using RELAP5 model 90
7.4. Experimental demonstration of power ramping procedure 92
7.5. Scale-up for NCBWR 94
7.6 Summary 95

8. Conclusions 97

Appendix A 101
Appendix B 107
Appendix C 113

References 119

TH-831_05610306

List of Figures

2.1. Stability map for 5 MW reactor at 1.5 MPa (Jiang et al., 1995), Operating point of the reactor shown by *
2.2. Stability map showing Type-I and Type-II instabilities (Furuya, 2006).
2.3. Geysering instability and oscillations of inlet velocity (Aritomi et al., 1993).
2.4. Effect of system pressure on large bubbly flow region (Chiang et al., 1994).
2.5. Flashing instability accompanied with geysering (Jiang et al., 1995).
2.6. Stability maps for different pressures (Manera and van der Hagen, 2003).
2.7. Geysering-induced flashing instability (Jiang et al., 1995).
3.1. Schematic of difference equation nodalization scheme.
3.2. Schematic view of Natural Circulation Test Facility (NCTF) loop.
3.3. RELAP5 nodalization scheme for NCTF loop.
3.4. Nodal sensitivity study for transient simulation of NCTF.
3.5. Nodal sensitivity study for transient simulation of NCBWR.
3.6. Mass flow rate observed during experiment and RELAP5 simulation.
3.7. Comparison of system pressure rise in the experiment and simulation.
3.8. Transients observed for various initial pressures of NCTF.
3.9. Transients observed for various initial pressure of the prototype.
3.10. Transients observed for various inlet loss coefficients.
3.11. Transients observed for various outlet loss coefficients.
4.1. Mass flow rate and heater exit void fraction in NCTF simulation.
4.2. Mass flow rate and riser exit void fraction in NCTF simulation.
4.3. Core void fraction study for one geysering cycle.
4.4. Core exit and riser inlet void fraction along with mass flow rate during NCTF simulation.
4.5. Startup simulation of the prototype using RELAP5.
4.6. Mass flow rate and void fraction in NCBWR simulation.
4.7. Fourier power spectrum for flow oscillations in NCTF.
4.8. Fourier power spectrum for flow oscillations in NCBWR.
4.9. Poincaré section for flow oscillations (using TISEAN).

TH-831_05610306

4.10. Lyapunov exponent for flow oscillations (using TISEAN). (a, b, c) effect of embedding dimension. (d, e, f) effect of reconstruction delay.
5.1. Schematic and major dimensions of PHT loop.
5.2. RELAP5 nodalization scheme for PHT loop.
5.3. Prediction for single channel power input in test facility
5.4. Prediction for double channel power input with equal power.
5.5. Core inlet flow rate for 10% power difference between channels in NCTF.
5.6. Core inlet flow rate for 50% power difference between channels in NCTF.
5.7. Core inlet flow rate for 10% and 50% power difference between channels in NCBWR.
5.8. Downcomer flow rate for 10% and 50% power difference between channels in NCBWR.
5.9. Effect of loss coefficient on startup oscillations in parallel-channel NCTF.
5.10. Effect of loss coefficient on startup oscillations in parallel-channel NCBWR.
6.1. System parameters during startup with constant 2 MW power input.
6.2. Heat-up rate for the startup of NCBWR.
6.3. System parameters during startup (Case-1A).
6.4. System parameters during startup (Case-1B).
6.5. System parameters during startup (Case-1C).
6.6. System parameters during startup (Case-2A).
6.7. System parameters during startup (Case-2B).
6.8. System parameters during startup (Case-3A).
6.9. System parameters during startup (Case-3B).
6.10. System parameters during single-phase startup.
6.11. RELAP5 nodalization scheme for startup.
6.12. System parameters during startup.
6.13. System parameters during startup simulation with bleeding at inlet header.
6.14. System parameters during startup simulation with bleeding at steam drum bottom.
7.1. Comparison of Type-II boundaries obtained by power law fit and RELAP5.
7.2. Type II boundary prediction by RELAP5.
7.3. System parameters during startup experiment in NCTF.

TH-831_05610306

7.4. Comparison of system pressure rise in the NCTF experiment under different startup procedures.

7.5. System parameters during startup simulation for the prototype using RELAP5.

TH-831_05610306

List of Tables

3.1. Model to prototype scaling ratio.

3.2. Nodal sensitivity study for steady state condition.

3.3. Comparison of steady state mass flow rate.

3.4. Type-II boundary predictions.

TH-831_05610306

Nomenclature

A	cross-sectional area (m^2)
B_x	body force in x coordinate direction (m/s^2)
C	coefficient of virtual mass
DS	energy dissipation function (W/m^3)
f_w	wall drag coefficient (s^{-1})
f_i	interface drag coefficient (s^{-1})
g	gravitational acceleration (m/s^2)
h	specific enthalpy (J/kg)
p	pressure (Pa)
Q_w	wall heat transfer rate (W/m^3)
Q_i	interface heat transfer rate (W/m^3)
t	time (s)
T_{sub}	subcooling temperature (K)
u	specific internal energy (J/kg)
V	volume (m^3)
v	velocity (m/s)
x	axial coordinate (m)

Greek Symbols

α	void fraction
Γ	volumetric mass exchange rate (kg/m^3s)
ρ	density (kg/m^3)

Subscripts

g	Vapor
l	Liquid
i	Liquid vapor interface
w	Wall

TH-831_05610306

Abbreviations

AHWR	Advanced Heavy Water Reactor
BWR	Boiling Water Reactor
ESBWR	Economic Simplified Boiling Water Reactor
GE	General Electric
HEM	Homogeneous Equilibrium Mixture
LWR	Light Water Reactor
NC	Natural Circulation
NCTF	Natural Circulation Test Facility
PHT	Primary Heat Transport

TH-831_05610306

Chapter 1
Introduction

1.1. Motivation

In nuclear power plant development, the current trend is to emphasize on improved economy by system simplification along with increased safety features. In line with this, the designers of nuclear power plant systems and components are fundamentally interested in the principle of natural circulation (NC), where no external sources of mechanical energy are used for the fluid motion. This can result in simplified systems, reduced cost and most importantly, a very high safety level as they possess inherent passive safety features. NC mode for core heat removal is used in existing reactors (like the Russian boiling water reactor VK-50 or the Dodewaard reactor in the Netherlands) as well as in future generation III+ boiling water reactors (BWRs), like ESBWR from GE and the Indian AHWR. With respect to plant safety, application of passive systems/components based on natural circulation is intended to simplify the safety systems and to improve their reliability, to mitigate the effect of human errors and equipment failures. Such systems typically do not require or accommodate repair or maintenance work during operation.

The accomplishment of the objectives of achieving a high safety level and reducing the cost through the reliance on NC mechanisms requires a thorough understanding of the flow mechanisms. NC systems are usually characterized by smaller driving forces in comparison to the systems that use an external source of energy (forced circulation) for the fluid motion. Hence, the system is generally less stable due to the regenerative feedback which is inherent in the NC process. In natural circulation boiling water reactors (NCBWRs), the presence of riser (used to enhance circulation flow) induces new region of instability (Type-I) especially at low-pressure low-power startup conditions. The phenomena causing flow instabilities under such conditions are

TH-831_05610306

dependent on system parameters such as pressure, inlet subcooling, flow resistance, geometry, power etc. Therefore, the level of knowledge on the thermal-hydraulic phenomena for the specific geometric conditions and governing heat transfer conditions should be deeper when natural circulation is involved.

Similarly, thermal-hydraulic system codes have been qualified through the comparison of predicted results and experimental data. The quality of recorded experimental data and the precision level of the available system codes, or the expected uncertainty in these predictions, are generally evaluated as satisfactory for the needs of the current reactors. However, the demand posed by the more extensive use of the NC in the design of evolutionary and innovative water cooled reactors requires a re-evaluation of the code capabilities considering the new phenomena and conditions involved. The flow is susceptible to gravity-driven instabilities, especially, at low-pressure low-power operating conditions (startup) because of the high sensitivity of the flow to perturbations. These conditions are very challenging for numerical codes to predict.

1.2. Major Objectives

- To develop a numerical model of the NC boiling system, using a system code (RELAP5) for predicting the transient that occur at low-pressure low-power startup conditions, and confirm the code's ability in predicting flashing and geysering instabilities.

- To investigate the characteristics of the flow oscillations observed during startup of a system with a particular geometric configuration: Analyze and classify the instabilities and also study the structural nature of the transients using time series analysis.

- To investigate the existence of in-phase and out-of-phase Type-I instabilities that could occur during startup of a parallel-channel boiling system. To make

TH-831_05610306

observations under similar and different conditions (power, flow restriction) in the channels.

- To identify a suitable heat-up rate, focusing on a minimal void generation in the core region and faster reactor pressurization. To conceptualize and study a startup procedure, whereby the unstable two-phase region is completely avoided.

- To conceptualize and demonstrate a power ramping procedure that could make the daily startup of test facilities a smooth and faster process.

1.3. Organization of Thesis

A review of literature on low-pressure low-power instabilities observed in natural circulation system is presented in Chapter 2. The chapter also discusses the experimental and numerical studies carried out under low-pressure conditions, and the methods employed for startup of NCBWRs.

Chapter 3 deals with numerical modeling of transients under low-pressure startup conditions, especially the simulation of flashing and geysering type instabilities. Thermal-hydraulics system code, RELAP5 is used for the simulations, and the major interest here is to validate the system code application for low-pressure conditions, by comparing the prediction with experimental observations.

Chapter 4 presents the efforts and methods used for a better physical insight of the instabilities observed during startup of a test facility. Additional parameters predicted by the numerical models are used to clarify and classify the phenomenon observed during experiments, and further, a comparison is made between the behaviour of instabilities in a scaled model and the prototype. A non-linear time series analysis is also carried out for assessing the structural nature of the transients.

TH-831_05610306

Having studied the transients in a single channel system, the investigation is extended for a parallel-channel system, which is presented in Chapter 5. The existence of in-phase and out-of-phase oscillations under equal and unequal boundary conditions between channels are studied for both model and prototype configurations.

The issue of startup procedure is addressed in Chapter 6 and 7. In Chapter 6, numerical experiments on different heat-up rates are carried out and a new startup procedure is proposed and studied, illustrating the method to avoid the low-pressure instabilities (flashing) that occur during startup of NCBWR. The focus is essentially on the early phases of startup (Phase II and III).

Chapter 7 deals with the later part of startup (Phase IV/ ascension to full power) which is of a greater interest during the daily startup of test facilities. A unique method by integrating numerical predictions and experimenting, is formulated and demonstrated experimentally, which results in a faster pressurization of the system and yet with assured safety.

TH-831_05610306

Chapter 2

Review of Literature

2.1. Introduction

A proper understanding of the system behavior and other important parameters during startup of a NCBWR is of primary importance in thermal hydraulic safety analysis. The use of natural circulation has introduced operational uncertainties, especially related to the startup phase of the reactor, when the system has to pass from single-phase to two-phase operation. Natural circulation systems may exhibit thermal-hydraulic instabilities under low-pressure low-power startup conditions. At low-pressures, a natural circulation loop typically has three operation ranges: (A) single-phase stable region, (B) two-phase unstable region and (C) two-phase stable region as shown in Fig. 2.1. The instabilities in the region between single-phase and stable two-phase NC mode are mainly induced by the phenomenon of geysering in the heated channel and flashing in the riser section (i.e. steam production in adiabatic conditions). The findings and understanding obtained through various experimental and analytical research reported in the literature is summarized in this chapter.

2.2. Flow Instabilities during Startup

In an early work by Fukuda and Kobori (1979), thermal-hydraulic instabilities for both natural and forced two-phase circulation were classified into two major categories: Type-I and Type-II, which has been generally accepted. A boiling water reactor is susceptible to Type-I instabilities when it starts from low-pressure and low-temperature conditions, as originally pointed out by Aritomi et al. (1992), and also at higher pressure and low-quality conditions. Figure 2.2 shows a typical stability map in the non-dimensional plane of the phase change number and the subcooling number for a natural circulation system consisting of a heated core, adiabatic chimney and a

TH-831_05610306

downcomer. The straight line in the figure indicates the operational points where the flow quality at the core exit is zero. Therefore, this line divides the stability map into two regions: a single phase flow region ($N_{sub} \geq N_{pch}$) and a boiling two-phase flow region ($N_{sub} < N_{pch}$). The instabilities during startup are classified into two major categories: geysering instabilities and instabilities induced by void flashing. The term instabilities induced by void flashing is used to emphasize the important role of void flashing in Type-I instabilities encountered in a low-pressure two-phase NC system with a long unheated riser.

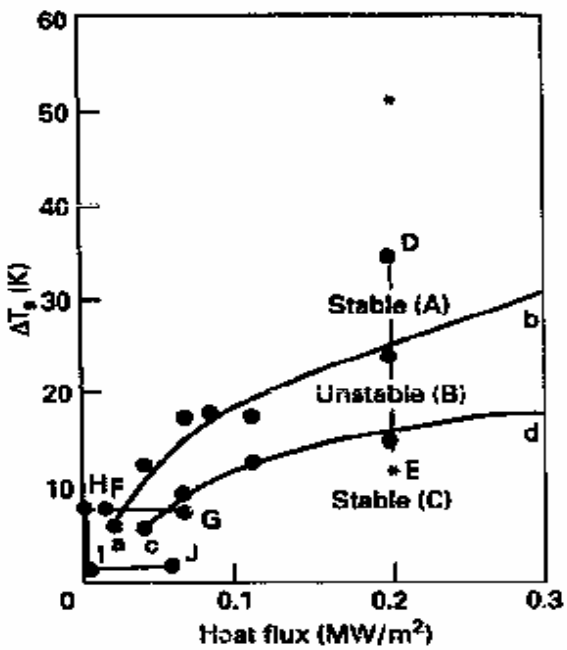

Figure 2.1. Stability map for 5 MW reactor at 1.5 MPa (Jiang et al., 1995), Operating point of the reactor shown by *

TH-831_05610306

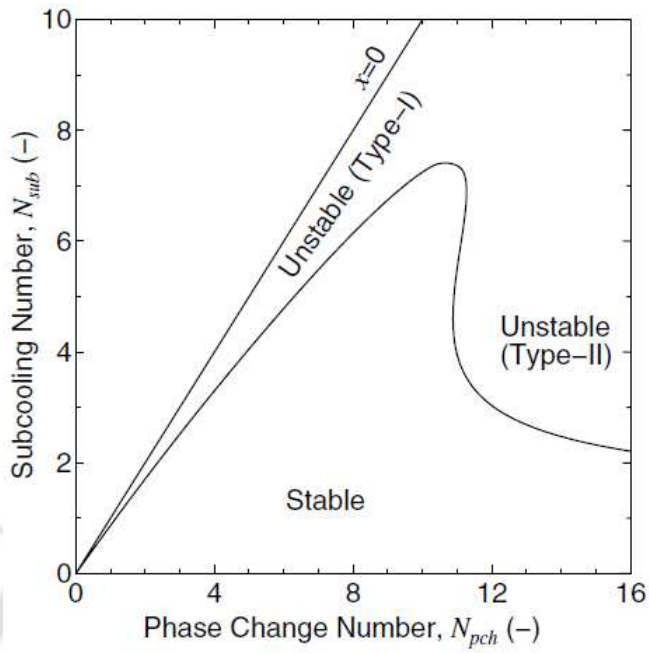

Figure 2.2. Stability map showing Type-I and Type-II instabilities (Furuya, 2006).

2.2.1. Geysering instability

Under certain thermal-hydraulic conditions, geysering instabilities can occur in a two-phase NC loop at low-pressure and low-power. Fundamental studies in the area of geysering instability have been conducted by Aritomi et al. (1993) and Wu et al. (1996). Based on the studies and observations of these researchers, the process of geysering, its mechanism and the effect of various system parameters on geysering are discussed here.

The geysering process can be described as follows (Fig. 2.3). Voids are generated in the channel's heated section. As voids move upward at low system pressure, they grow into large bubbles due to the decrease in hydrostatic pressure head and can cover most of the cross section of the channel. Large bubbles are then condensed in the riser or upper plenum, where the fluid is still subcooled. With the bubble collapse and subsequent decrease in pressure, the subcooled liquid reenters the heated channel and restores the nonboiling condition. This causes reduction of flow rate and flow reversal can also take place if the condensation rate of bubbles is greater than the circulation flow. This

TH-831_05610306

process repeats periodically and causes flow oscillations as can be seen in the lower part of Fig. 2.3. Therefore, bubble formation, growth, and collapse phenomena are crucial in the occurrence of geysering instability.

Different forms of geysering have been observed in different test facilities. Periodic oscillations due to geysering were observed by Aritomi et al. (1993) in the experiment conducted on their test facility. Wang et al. (1994) reported a quasi-periodic type of geysering oscillation (three oscillations followed by another oscillation of larger magnitude) as cited by Paniagua et al. (1999). In contrast, flow oscillations due to geysering observed by Jiang et al. (1995) behaved in a manner of irregular pulses. Chaotic oscillations were observed at higher inlet subcooling in the experimental results shown by Wu et al. (1996).

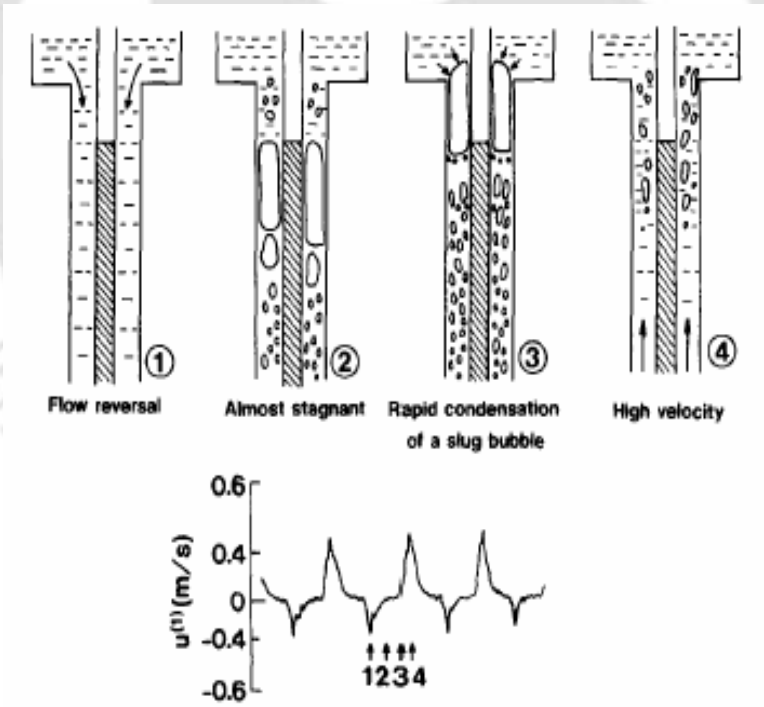

Figure 2.3. Geysering instability and oscillations of inlet velocity (Aritomi et al., 1993).

TH-831_05610306

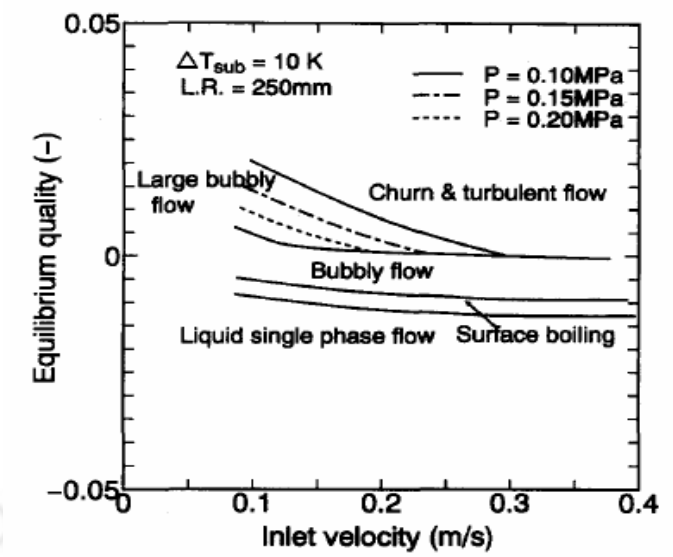

Figure 2.4. Effect of system pressure on large bubbly flow region (Chiang et al., 1994).

The characteristics of geysering are affected by various system parameters such as system geometry, pressure, subcooling at core inlet, heat flux, etc. At a given heating power, geysering is sensitive to system pressure and inlet subcooling. An increase in system pressure tends to suppress geysering and reduce oscillation amplitude (Subki et al., 2003; Paniagua et al., 1999). It has been found that geysering disappears when the system is started up at a pressure greater than 0.3 MPa (Jiang et al., 1995). This value of the threshold pressure was also found by numerical computation (Paniagua et al., 1999). The reason for stabilization is that an increase in pressure can suppress the formation of large bubbles, as confirmed experimentally (Chiang et al., 1994). The large bubbly flow region becomes rather small at 0.2 MPa compared to 0.1 MPa (Fig. 2.4). A decrease in inlet subcooling also tends to suppress geysering, and geysering disappears when the inlet subcooling is low enough that the liquid at inlet of riser reaches its saturation temperature (Jiang et al., 1995).

2.2.2. Flashing instability

Flashing-induced flow oscillation can occur during startup of a NCBWR. At startup, both system pressure and heating power are low. The low system pressure implies large differences in saturation temperature (due to the hydrostatic pressure difference)

TH-831_05610306

between the inlet and the outlet of the adiabatic section and difference can easily exceed 10 K. At low-powers, the coolant, which is heated up in the heated section of the NC loop, may not reach saturation conditions in the core itself. Due to the strong variation of saturation temperature along the system, flashing can occur in the adiabatic section leading to an enhancement of the natural circulation flow rate (Fig. 2.5). The occurrence of flashing will cause a decrease of the pressure below the location of bubble formation. The decrease in local pressure will trigger additional steam formation, leading to a large increase in the flow rate (Jiang et al., 1995). The increase of flow rate will cause a subsequent decrease of the coolant temperature entering the adiabatic section, so that the process of flashing may eventually stop and the flow rate will be low again. The coolant temperature entering the adiabatic section will therefore increase, leading to a new flashing cycle. In this way, a self-sustained flow oscillation will take place. A detailed study on flashing-induced instability and their difference from other type of instabilities has been done by Manera and van der Hagen (2003) and Furuya et al. (2005) in their experiments conducted on CIRCUS and SIRIUS-N facilities, respectively.

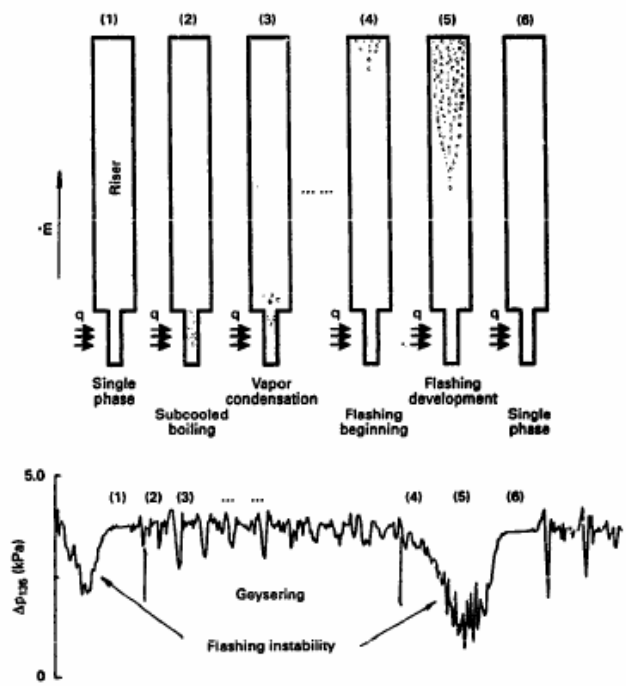

Figure 2.5 Flashing instability accompanied with geysering (Jiang et al., 1995).

TH-831_05610306

Flashing-induced instability phenomena are complicated and there are different views about their nature. Jiang et al. (2000) regarded void flashing as a thermal equilibrium process and stated that it starts at the exit of the riser and develops downward. In contrast, Manera and van der Hagen (2003) pointed out that void flashing is a nonequilibrium process and void flashing fronts develop both downward and upward in the riser. They also classified flashing instabilities as a type of density wave instability. Earlier, Chiang et al. (1994) had suggested that flashing-induced oscillations are similar to density wave oscillations but a different type of instability. Furuya et al. (2005) reported two types of instabilities: an intermittent oscillation at higher channel inlet subcooling and a sinusoidal oscillation at lower subcooling. They suggested these instabilities to be flashing-induced density wave oscillations.

The effect of system pressure and inlet subcooling on flashing induced instability was studied and reported by Manera and van der Hagen (2003). It was observed that, the amplitude of oscillation increases as the inlet subcooling increases and the range of inlet subcooling for which oscillations occur, increases with power and decreases with pressure. There is a pressure feedback from the steam drum that limits the amplitude of oscillation. Fig. 2.6 illustrates their conclusion that, the unstable transition region between stable single-phase region and stable two-phase region shrinks as the pressure is increased.

2.2.3. Geysering-induced flashing instability

The phenomenon of geysering-induced flashing instability was reported by Jiang et al. (2000). During geysering, a gradual increase in riser fluid temperature is observed and some vapor is left in the upper part of the riser. As geysering continues, the liquid reaches its saturation temperature near the exit of the riser, where flashing occurs. The increase in flow rate due to flashing will lead to a subcooled condition in the core and at the inlet of the riser. Thus, a condition for the occurrence of geysering is created. Therefore, the flow oscillates with a few geysering pulses of lower amplitude followed by a higher amplitude flashing pulse (Fig. 2.7).

TH-831_05610306

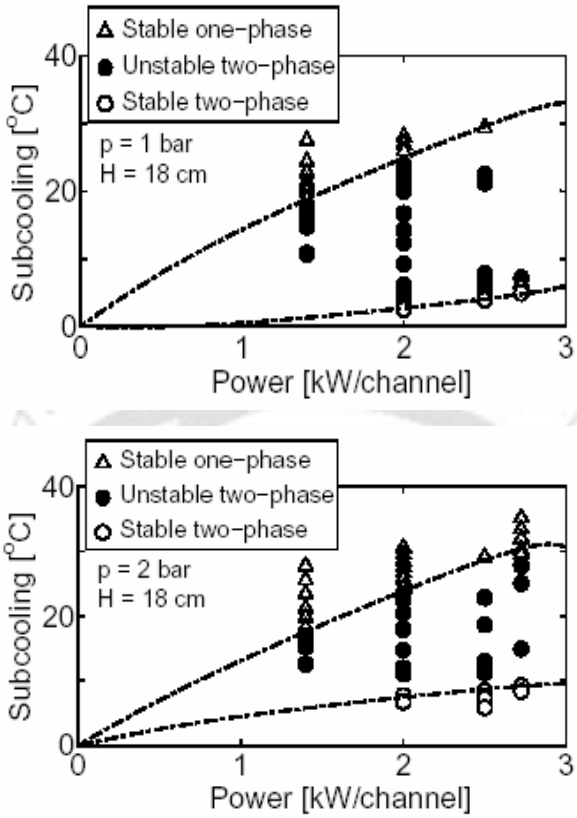

Figure 2.6. Stability maps for different pressures (Manera and van der Hagen, 2003).

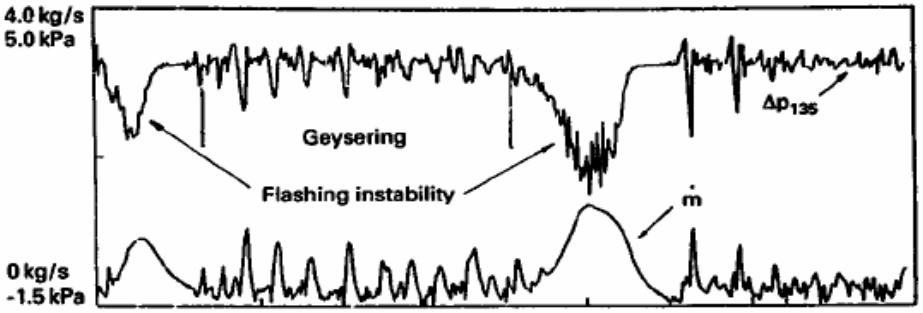

Figure 2.7. Geysering-induced flashing instability (Jiang et al., 1995).

TH-831_05610306

2.2.4. Density wave oscillations

Apart from geysering and flashing instabilities, density wave oscillations can also occur under low-pressure low-power conditions. These oscillations are due to multiple regenerative feedbacks between flow rate, vapor generation and pressure drop (Boure et al., 1973). A small flow fluctuation at the channel inlet may create an enthalpy perturbation. When this enthalpy perturbation reaches the boiling boundary of the channel, it would transform into a two-phase mixture density perturbation resulting in pressure drop fluctuation in the two-phase region. A feedback between the pressure drop and the inlet velocity may result in a self-excited oscillation (Subki et al., 2003).

2.2.5. Low-pressure instabilities in parallel-channel systems

The nature of transients under low-pressure conditions is mostly explained through single channel studies. A limited number of investigations have been done to study the low-pressure transients that could occur in parallel-channel natural circulation boiling systems. An experimental study using a double-channel natural circulation loop was carried out and the transport mechanism of various types of instability under startup conditions was discussed (Subki et al., 2003). In-phase and out-of-phase flow oscillations were reported. Out-of-phase flow oscillations were also reported through an experimental observation (Pan et al., 1999) as cited in Lee and Pan (2005). Chen et al. (1999) carried out experiments in a double-channel system under equal and unequal power conditions. They reported the existence of out-of-phase oscillations even under equal power condition in channels, and similar observation was also reported through the experimental studies by Subki et al. (2003). Through a numerical study, the nonlinear dynamics and stability boundary of a double-channel natural circulation boiling loop was analyzed (Lee and Pan, 2005; Durga Prasad et al., 2008). In-phase and out-of-phase behaviour in systems having common heater and two parallel risers were studies through an experimental investigation by Marcel (2007), and suggested that, in a multiple riser configuration, NCBWRs might encounter a chaotic region during low-pressure startup phase.

TH-831_05610306

2.3. Experimental Facilities

A number of boiling channel natural circulation test facilities have been constructed to study thermal-hydraulic instabilities that could occur in a BWR. The Natural Circulation Test Facility (NCTF) (Iyer and Kandengal, 2003) is a scaled model designed to investigate various phenomena involved right from startup to operating condition of a pressure tube type NCBWR (Sinha and Kakodkar, 2006). Purdue University Multi-Dimensional Test Assembly (PUMA) is a low-pressure facility that can simulate the transients at a pressure below 1.03 MPa (Ishii et al., 1996). It is a scaled facility for the proposed simplified boiling water reactor (SBWR) designed by GE. The PANDA large-scale facility (Auban et al., 2004) under the NACUSP project (Kruijf et al., 2003; Aguirre et al., 2005) is also aimed at investigating system behavior at varied operating conditions with a special interest in the phenomenon involved during startup of the reactor. Thus, a part of the research in these facilities is directed towards getting an insight into the transients at low-pressure low-power conditions in natural circulation boiling systems.

An experimental facility (CIRCUS) under the umbrella of NACUSP project was developed at the Delft University of Technology, Netherlands. It was designed and built to study the thermal–hydraulic stability of a NCBWR at low-pressure conditions typical for startup. The experiments in the facility resulted in a better understanding of flashing-induced instabilities and numerical modeling of low-pressure instabilities using system codes (Manera, 2003). The facility is also equipped to study the effect of parallel risers, inlet friction and inlet subcooling. The Central Research Institute of Electric Power Industry (CRIEPI) in Japan has constructed a natural circulation test facility (SIRIUS-N), in cooperation with GE and the Interfaculty Reactor Institute, Delft University of Technology. Experiments were focused on investigating Type-I instabilities and the phenomenon of flashing-induced instabilities during startup of NCBWR (Furuya, 2006). The Chinese Institute of Nuclear Energy and Technology (INET) has developed a 5 MWt nuclear heating reactor, which is in operation since 1989 (Wang, 1993). This natural circulation reactor operates at a low-pressure (15 bar),

TH-831_05610306

low-steam quality (less than 1% at the core exit), and is cooled by natural circulation. A test loop (HRTL-5), simulating the design and geometry of this reactor, was built at INET to simulate the thermal-hydraulic stability of the test reactor (Jiang et al., 2000). A review article by Durga Prasad et al. (2007), also lists the experimental test facilities existing around the world that involve study of flow instabilities under natural circulation condition.

2.4. Modeling of Startup Transients

For accurate modeling of two-phase flow systems, a 6-equation model is used, where the two phases are treated as two separated fluids for which mass, momentum and energy balances are solved separately. This type of model is implemented in some of the codes (RELAP5, TRAC, MONA) and allows considering thermal nonequilibrium and slip between the phases. Simplified models are developed in order to gain more insight of a given process. However, not many of these models have been reported in literature, which can deal with startup instabilities. Use of homogeneous equilibrium mixture (HEM) model is preferred when a lower level of complexity is desired. Inada et al. (2000) reported a lumped parameter model for startup transients in NCBWR based on HEM formulation. It includes pressure-dependent thermodynamic properties along the vertical axis of the system but excludes single-phase natural circulation (flow rate is different from zero only when steam is present in the system). Though the model is able to predict stability boundaries fairly well compared with experimental data, the code cannot be used to simulate startup transients since it has been developed in frequency domain. van Bragt et al. (2002) extended the model by Inada et al. (2000) in time domain, but the energy balance is linearized to derive a simple differential equation for the dynamics of the boiling boundary. In this way, important non-linear effects might be excluded and again single-phase circulation is not taken into account.

2.4.1. Numerical codes

Chatoorgoon (1986) developed a simple time-domain code SPORTS, based on HEM formulation, which includes single-phase natural circulation and pressure-dependent

TH-831_05610306

thermodynamic properties along the axis of the system. It was shown that the code is able to reproduce flashing instabilities at low-pressure and low-power, but a systematic parametric study and comparison with experimental results remains to be done. Even state-of-the-art thermal-hydraulic codes (RELAP, RAMONA-4B and TRACG) have often shown unsatisfactory and sometimes even contradictory results (Manera, 2003). Startup transient simulations for GE SBWR have been done using RAMONA-4B code (Cheng et al., 1998). Oscillations, especially geysering and flashing type instability as observed in the test facilities, were not found in these simulations. The inability of finding flashing-induced oscillations is not surprising, since in this code, local physical properties are evaluated on system averaged transient pressure without taking into account the effect of local pressure. Paniagua et al. (1999) developed a modified version of RAMONA-4B called TWOPHASE that includes local pressure dependencies and an explicit numerical scheme to avoid numerical damping of the solution. Their simulations with TWOPHASE code show occurrence of geysering type instabilities, and the results were in good agreement with the experimental results. Cheung and Rao (2000) performed simulations of the startup of the ESBWR with TRACG code and found that no instabilities occur during the entire startup procedure (as reported in Manera, 2003). Flashing induced instabilities were modeled by Manera et al. (2005) using a code FLOCAL, which is a 4-equation drift flux model and allows for the liquid and vapor to be in thermal nonequilibrium with different velocities. A list of other thermal hydraulic and neutronic codes that can be used in modeling and studying a two-phase system was reported by Durga Prasad et al. (2007).

2.4.2. RELAP5 code

RELAP5 is a light water reactor (LWR) transient analysis code, developed at the Idaho National Engineering Laboratory (INEL). Its specific applications include simulations of transients in LWR systems such as loss of coolant, anticipated transients without SCRAM, and operational transients such as loss of feed water, loss of off-site power, station blackout and turbine trip. It can also be used for simulation of a wide variety of hydraulic and thermal transients in both nuclear and non-nuclear systems involving mixtures of steam, water, noncondensable, and solute. A comprehensive validation

TH-831_05610306

study on the numerical techniques involved in the RELAP5 code is given by Shieh et al. (1994). Validation studies, especially in testing the codes capability for predicting operating transients and accident scenarios were carried out and reported in the literature. Assessment of the application of RELAP5/MOD3 to simulate loss of feed water scenario was carried out by D'Auria et al. (1993). The influence of nodalization refinement on the codes prediction was also emphasized. Kaliatka and Uspuras (2000) developed a RELAP5/MOD3 model of the main circulation circuit (MCC) of RBMK-1500 graphite moderated BWR. They carried out benchmark analysis of three different events which occurred at Ignalina nuclear power plant, and the numerical results compared well with plant data. In their subsequent analysis Kaliatka and Uspuras (2002) studied loss-of-coolant accident conditions in RBMK-1500 reactor using RELAP5 code. Based on the results, a management strategy was developed and implemented so that the plant is adequately protected from such accidents. Urbonas et al. (2003) validated RELAP5 with the experimental data of Electrogorsk E-108 test facility. Different phenomena such as oscillatory flow pattern and CHF were studied using RELAP5 models and E-108 test facility. They also compared specific RBMK tests (oscillatory behaviour, critical discharge, and CHF) with the RELAP5 models. RELAP5/MOD3 code was employed to simulate a natural circulation experiment in IIST facility, to investigate the event of decay heat removal in a pressurized water reactor (Ferng and Lee, 1994). However, the application of RELAP code to low-pressure two-phase conditions, especially for simulating the startup transients in a BWR is yet to be benchmarked, and studies in this direction are underway.

In order to model the dynamics of a subcooled flow boiling and condensation in a channel, an 1-D system code generally employees various sub-models that account for wall to liquid heat transfer, the rate of vapor generation and condensation (wall heat flux partitioning), flow regime transition (bubbly to slug), and the drift between phases using drift flux models. Due to the evolution of RELAP5 under high-pressure application, it may not be effective to use certain sub-models of the code in the original form for low-pressure subcooled conditions. Tiselj and Cerne (2000) showed that RELAP5 code cannot deal with flashing, since the results become strongly dependent on the integration time step used for the simulations. Some of the major limitations

TH-831_05610306

identified (Hari and Hassan, 2002) in the original code are, the treatment of umbrella restriction (RELAP5 team, vol-IV, 2001), which significantly effects the calculation of the volumetric interfacial heat transfer coefficient; the parameter, pumping factor (ratio of quenching heat flux to evaporation heat flux) under the wall heat partitioning model, which is important in predicting the rate of evaporation; the transition limit from bubbly to slug flow. New models to address these issues were developed and incorporated in the RELAP5 code, and the performance of the refined code when tested with experimental observation showed good prediction of axial void fraction (Hari and Hassan, 2002; Koncar and Mavko, 2003). Refinement done to the subcooled boiling models of system codes (Tu and Yeoh, 2002; Yeoh and Tu, 2002; Dilla et al., 2006), resulted in testing of different existing correlations and new correlations were proposed. Hence, the above mentioned studies, towards enhancing the predictive performance of the code under low-pressure subcooled conditions indicate promising results.

Numerical simulations of startup transients in a natural circulation test facility (PUMA) using RELAP5/SCDAP/MOD3.4 (Lakshmanan and Pandey, 2007), showed trends similar to those observed in experiments (Appendix A), although, it was not supported with a quantitative validation due to lack of sufficient information on the experimental and measurement data. In view of assessing system codes for low-pressure and low-power applications, experiments were conducted in the available large-scale test facilities (PANDA, PUMA) (Auban et al., 2004; Kuran et al., 2006).

2.5. Startup Procedures

A general startup procedure for NCBWR design has been discussed by Kuran et al. (2006). The startup procedure is divided into four distinct phases: Phase I - Single-phase core heat up, Phase II - Net vapor generation in core, Phase III - Saturated chimney and Phase IV - Power ascension to full power. The nature of transition through Phase II and Phase III is important, where the instabilities like geysering (in Phase II) and flashing (in Phase III) are highly dominant. From literature, it appears that a consensus has been reached that the above mentioned Type-I instabilities can be

TH-831_05610306

suppressed or avoided by having an increased system pressure around 15–20 bar (Chiang et al., 1994; Manera and van der Hagen, 2003; Subki et al., 2003). A rational startup procedure is required to overcome the startup instabilities. Literature on startup procedures proposed by various authors conveys that different methodologies can be adopted in raising the system pressure to the desired level. For example, one of the procedures is to externally pressurize the system by steam produced in a separate boiler or by nitrogen. External pressurization can even be applied upto full operating pressure of 70 bar with maintaining a low-power level to control the heat up rate and to allow boiling only at operating pressure (Bagul et al., 2008). This procedure needs an external boiler of adequate volume, power and the related connecting piping to the reactor vessel. Manera (2003, 2005) proposed a procedure for creating a steam cushion in the system without using steam pressurized in external vessels. This is done by allowing flashing to occur only above the riser exit, with no void generation in the core and riser section. However, avoiding flashing could be a problem when dealing with very high chimney. The startup procedures proposed so far, concentrate on the Type-I instabilities, and no method has been reported for faster pressurization of system (Phase-IV), that is very important in daily startup of test facilities.

2.6. Summary

During the start up of a NCBWR, it is evident that an unstable operational region exists between the stable single-phase and the two-phase region, where the phenomena of geysering and flashing are significant. Experimental and analytical approaches have been carried out in view of overcoming this unstable region. Increase in system pressure has a suppressing effect on these instabilities, although, the methods (startup procedures) employed for increasing the pressure need to be explored further. A good number of experimental investigations have been, and are being carried out for the better understanding of the low-pressure instabilities in natural circulation boiling systems. In numerical modeling, simple mathematical models based on homogeneous equilibrium mixture (HEM) and lumped parameter formulations, which are used for handling a lower level of complexity, are not adequate, as the effects of pressure

TH-831_05610306

dependency, velocity slip between phases and thermal nonequilibrium condition between liquid and vapor phases are essential for effective simulation of transients during startup. Thermal-hydraulic system codes based on two-fluid and drift flux formulation can be employed for the prediction of startup transients. However, the applicability of such codes under low-pressure conditions is to be confirmed by validating with experimental results. In doing so, the validated numerical model can be used for predicting additional system information required for a better interpretation of the physical phenomenon occurring at low-pressure conditions. Based on such predictions and understanding, appropriate startup procedures for NCBWRs and test facilities can be devised.

TH-831_05610306

Chapter 3

Numerical Model

3.1. Introduction

The fluid behaviour in a system can be described using the basic conservation equations of mass energy and momentum in differential form. A boiling system consists of distinct or co-existing single-phase and two-phase regions. In single-phase region, the application of conservation equations is straightforward. A lumped parameter approach (van Bragt and van der Hagen, 1998a; van Bragt et al., 2002) based on the basic one-dimensional unsteady state equations of mass, momentum and energy can be used to study the dynamic behaviour of the system. However, the behaviour of fluid in two-phase region is rather complicated, especially during the low-pressure startup conditions where complex nonequilibrium phenomena like flashing are expected. In such cases, the models based on simple lumped parameter approach are not adequate and more sophisticated models that include slip between phases, thermal nonequilibrium, local properties and better discretization schemes, are preferred. Such models are implemented in some of the system codes (RELAP, TRACG, ATHLET, etc). However, the use of system codes to simulate the transients during startup conditions is yet to be fully established, especially their ability to predict certain low-pressure thermal-hydraulic phenomena like geysering and flashing.

The current chapter deals with two issues: one, development of numerical models with RELAP5/SCDAP/MOD3.4 (RELAP/SCDAP, 1997) code; and the other, its ability to predict transients occurring at low-pressure low-power conditions. RELAP5 models for the natural circulation loops of NCTF and NCBWR are developed along with nodal sensitivity studies, and their predictions are verified with experimental data. The RELAP5 model of the test facility is validated for its steady state as well as transient predictions with the help of experimental observations (Section 3.5). The transient

TH-831_05610306

predictions and parametric trends obtained by the RELAP5 model of the prototype are compared with those of the numerical model of the test facility (Section 3.6).

3.2. Code Description

3.2.1. Mathematical model

The RELAP5 hydrodynamic model is a one-dimensional, transient, two-fluid model for flow of a two-phase steam-water mixture that can contain noncondensable components in the steam phase and/or a soluble component in the water phase. The RELAP5/SCDAP/MOD3.4. thermal-hydraulic model solves eight field equations for eight primary dependent variables. The primary dependent variables are pressure (p), phasic specific internal energies (u_g, u_f), vapor volume fraction (void fraction) (α_g), phasic velocities (v_g, v_f), noncondensable quality (X_n), and boron density (ρ_b). The independent variables are time (t) and distance (x).

The differential form of the one-dimensional transient field equations that form the basis for the hydrodynamic model for a liquid/vapor system, without considering noncondensable and solute components are presented here. The basic field equations for the two-fluid nonequilibrium model consist of two phasic continuity equations, two phasic momentum equations, and two phasic energy equations. The equations are recorded in differential stream tube form with time (t) and one space dimension (x) as independent variables, and in terms of time and volume-average dependent variables.

Mass Continuity:

<u>gas phase</u>

$$\frac{\partial(\alpha_g \rho_g)}{\partial t} + \frac{1}{A}\frac{\partial(\alpha_g \rho_g v_g A)}{\partial x} = \Gamma_g \tag{3.1}$$

<u>liquid phase</u>

$$\frac{\partial(\alpha_l \rho_l)}{\partial t} + \frac{1}{A}\frac{\partial(\alpha_l \rho_l v_l A)}{\partial x} = \Gamma_l \tag{3.2}$$

TH-831_05610306

Momentum conservation:

gas phase

$$\alpha_g \rho_g A \frac{\partial(v_g)}{\partial t} + \frac{\alpha_g \rho_g A}{2} \frac{\partial(v_g{}^2)}{\partial x} = \alpha_g A \frac{\partial p}{\partial x} + \alpha_g \rho_g A B_x - \alpha_g \rho_g A f_{wg} v_g + \Gamma_g A (v_{gi} - v_g) - \alpha_g \rho_g A f_{ig} (v_g - v_l) - C \alpha_g \alpha_l \rho_m A \left[\frac{\partial(v_g - v_l)}{\partial t} + v_l \frac{\partial v_g}{\partial x} - v_g \frac{\partial v_l}{\partial x} \right] \quad (3.3)$$

liquid phase

$$\alpha_l \rho_l A \frac{\partial(v_l)}{\partial t} + \frac{\alpha_l \rho_l A}{2} \frac{\partial(v_l{}^2)}{\partial x} = \alpha_l A \frac{\partial p}{\partial x} + \alpha_l \rho_l A B_x - \alpha_l \rho_l A f_{wl} v_l - \Gamma_l A (v_{li} - v_l) - \alpha_l \rho_l A f_{il} (v_l - v_l) - C \alpha_l \alpha_g \rho_m A \left[\frac{\partial(v_l - v_g)}{\partial t} + v_g \frac{\partial v_l}{\partial x} - v_l \frac{\partial v_g}{\partial x} \right] \quad (3.4)$$

Energy conservation:

gas phase

$$\frac{\partial(\alpha_g \rho_g u_g)}{\partial t} + \frac{1}{A} \frac{\partial(\alpha_g \rho_g u_g v_g A)}{\partial x} = -p \frac{\partial \alpha_g}{\partial t} - \frac{p}{A} \frac{\partial(\alpha_g v_g A)}{\partial x} + Q_{wg} + Q_{ig} + \Gamma_{ig} h_g^* + \Gamma_w h_g^{'} + DS_g \quad (3.5)$$

liquid phase

$$\frac{\partial(\alpha_l \rho_l u_l)}{\partial t} + \frac{1}{A} \frac{\partial(\alpha_l \rho_l u_l v_l A)}{\partial x} = -p \frac{\partial \alpha_l}{\partial t} - \frac{p}{A} \frac{\partial(\alpha_l v_l A)}{\partial x} + Q_{wl} + Q_{il} - \Gamma_{il} h_l^* - \Gamma_w h_l^{'} + DS_l \quad (3.6)$$

where,

Q_{wg} and Q_{wl} are the phasic wall heat transfer rates per unit volume

Q_{ig} and Q_{il} are the phasic interface heat transfer rates per unit volume

h^*_g and h^*_l are the phasic enthalpies associated with bulk interface mass transfer

h'_g and h'_l are the phasic enthalpies associated with wall (thermal boundary layer) interface mass transfer

DS_g and DS_l are the phasic energy dissipation terms

TH-831_05610306

The terms f_{wg} and f_{wl} are part of the wall frictional drag, which are linear in velocity, and are products of the friction coefficient, the frictional reference area per unit volume, and the magnitude of the fluid bulk velocity. The interfacial velocity (v_{gi} and v_{li}) in the interface momentum transfer term is the unit momentum with which phase appearance or disappearance occurs. The coefficients f_{ig} and f_{il} are part of the interface frictional drag; two different models (drift flux and drag coefficient) are used for the interface friction drag, depending on the flow regime (RELAP5 team, Vol-I, 2001).

3.2.2. Numerical scheme

The difference equations are based on the concept of a control volume (or mesh cell) in which mass and energy are conserved by equating accumulation to the rate of mass and energy in through the cell boundaries minus the rate of mass and energy out through the cell boundaries plus the source terms. This model results in defining mass and energy volume average properties and requiring knowledge of velocities at the volume boundaries. The velocities at boundaries are most conveniently defined through the use of momentum control volumes (cells) centered on the mass and energy cell boundaries. This approach results in a numerical scheme having a staggered spatial mesh. The scalar properties (pressure, energies, and void fraction) of the flow are defined at cell centers, and vector quantities (velocities) are defined on the cell boundaries. The resulting one-dimensional spatial noding is illustrated in Fig. 3.1. The term cell means an increment in the spatial variable, x, corresponding to the mass and energy control volume. A semi-implicit numerical solution scheme is employed, based on replacing the system of differential equations with a system of finite difference equations partially implicit in time. The semi-implicit numerical solution scheme uses a direct sparse matrix solution technique (Curtis and Reid, 1971) for time step advancement. The method has a material Courant time step stability limit.

RELAP5 solution scheme is designed to converge based on the material Courant limit (i.e., the numerical algorithms limit the solution time-step size based on the mass flow transit time through each component cell). A variety of checks on the solution are used

TH-831_05610306

to control the time step that includes Courant limit check, mass error checks, material properties out of defined ranges, water property errors.

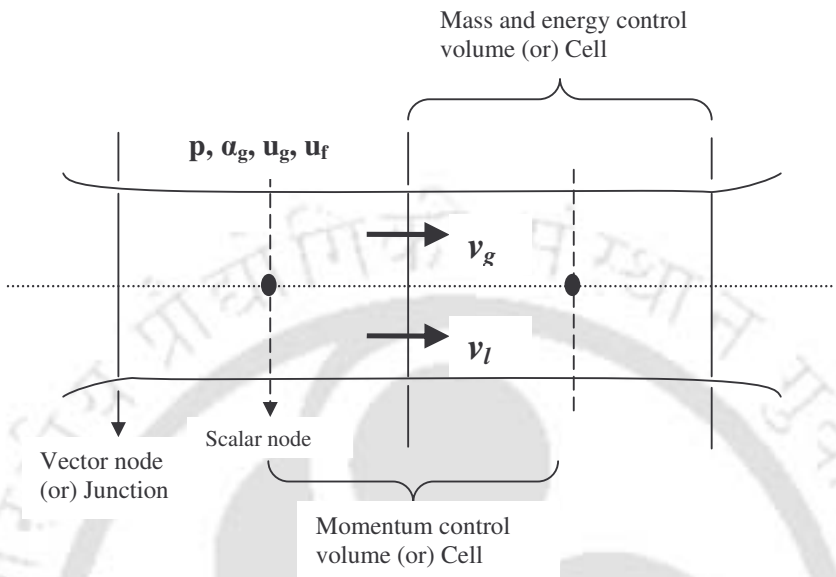

Figure 3.1. Schematic of difference equation nodalization scheme.

The original material Courant limit is evaluated for each hydrodynamic volume using the phasic volume velocities and the phasic volume fractions, and it is given by

$$(\Delta t_c)_i = \Delta x_i \frac{\max(\alpha_{li}^n, \alpha_{gi}^n)}{\max(|\alpha_{li}^n, v_{gi}^n|, |\alpha_{li}^n, v_{gi}^n|)} \qquad i = 1, 2, ..., N \tag{3.7}$$

The N volumes are divided into five subsets, i.e., the 1st, 6th, 11th,... volumes belong to the first subset, the 2nd, 7th, 12th,... volumes belong to the second subset, etc. The minimum Courant limits for each of the five subsets are rearranged in ascending order, i.e.,

$$\Delta t_c^1 \le \Delta t_c^2 \le \Delta t_c^3 \le \Delta t_c^4 \le \Delta t_c^5 \tag{3.8}$$

Thus, Δt_c^1 is the Courant limit for the entire system. For the semi-implicit scheme, Δt_c^2 is used for limiting the time step size. Thus, partial violation of the material Courant

TH-831_05610306

limit is allowed for this scheme. For the nearly-implicit scheme, 20 times Δt_c^2 is used for limiting the time step size for the transient mode, and 40 times Δt_c^2 is used for limiting the time step size for the steady-state mode.

The Courant limit check is made before a hydrodynamic advancement takes place, which may reduce the time step, but it does not cause a time step to be repeated. All the other checks may cause all or part of the time advancement to be repeated at a smaller time step. The mass error is measured to check the validity of density linearization calculated by

$$\varepsilon_m = \max\left(\frac{|\rho_{mi} - \rho_i|}{\rho_i}\right)$$

and the overall system mass error, estimated by

$$\varepsilon_{rms} = \frac{\sum_{i=1}^{N}\left[V_i\left(\rho_{mi} - \rho_i\right)\right]^2}{\sum_{i=1}^{N}\left[V_i\left(\rho_i\right)\right]^2}$$

where ρ_{mi} is the density of the i-th volume obtained from the mass continuity equation and ρ_i is the total density of the i-th volume calculated from the state relationship. If either ε_m or ε_{rms} is greater than 8×10^{-3}, the time step is rejected and repeated with one half of the time step size. Otherwise, the time step is accepted, and the next time step size is doubled if both ε_m and ε_{rms} are less than 8×10^{-4}.

3.2.3. Constitutive model

The constitutive relations include models for defining flow regimes and flow-regime related models for interphase drag and shear, the coefficient of virtual mass, wall friction, wall heat transfer, interphase heat and mass transfer. In an earlier version (RELAP5/MOD2), all constitutive relations were evaluated using volume-centered conditions. Junction parameters such as interfacial friction coefficients were obtained as volume-weighted averages of the volume-centered values in the volumes on either side of a junction. The procedure for obtaining junction parameters as averages of volume parameters was adequate when the volumes on either side of a junction were in

TH-831_05610306

the same flow regime and the volume parameters were obtained using the same flow regime map (i.e., both volumes were horizontal volumes or both volumes were vertical volumes). Problems were encountered when connecting horizontal volumes to vertical volumes. Such problems have been eliminated in RELAP5/MOD3 by computing the junction interfacial friction coefficient using junction properties so that the interfacial friction coefficient would be consistent with the state of the fluid being transported through the junction (RELAP5 team, vol-I, 2001). The approach has been used successfully in the TRAC-B code (Weaver et al., 1986; Taylor, 1984) also. The independent variables in the flow regime maps for the volumes and junctions are somewhat different as a result of the finite-difference scheme and staggered mesh used in the numerical scheme as discussed earlier.

The phasic interfacial friction force calculations in RELAP5/MOD3 are done using two different models; the drift flux method and the drag coefficient method. As mentioned earlier, the constitutive models are flow regime dependent, the drift flux approach is used in the bubbly and slug flow regimes for vertical flow. The drift flux model specifies the distribution coefficient and the vapor drift velocity. The drag coefficient method is used in all flow regimes except for bubbly and slug flows in vertical components. The model uses correlations for drag coefficients and for the computation of the interfacial area density and is the model used by previous versions of RELAP5 for all flow regimes.

The wall friction calculations are based on a two-phase multiplier approach, in which the two-phase multiplier is calculated from the Heat Transfer and Fluid Flow Service (HTFS)-modified Baroczy correlation (Chaxton et al., 1972). The individual phasic wall friction components are calculated by apportioning the two-phase friction between the phases using a technique derived by Chisholm (Chisholm, 1967) from the Lockhart-Martinelli model (Lockhart and Martinelli, 1949). The partitioning model is based on the assumption that the frictional pressure drop may be calculated using a quasi-steady form of the momentum equation.

TH-831_05610306

3.3. Test Facility

The natural circulation loop studied here is a part of Natural Circulation Test Facility (NCTF) developed at IIT Bombay (Iyer and Kandengal, 2003). The test facility is a scaled model designed to simulate a pressure tube type reactor which is driven by natural circulation. The NCTF consists of two loops with four risers connected to two drums. While one simulator with its riser, drum, downcomer and feeder represents one loop (Fig. 3.2), the other loop with three simulators, three risers, one drum, one downcomer and three feeders represent the other three loops of the prototype. Hence, a total of 4 risers simulate the 452 risers in the prototype. A brief discussion on the major components of the test facility is presented in Appendix B. The length scale used in the NCTF model is ¼ and the time scale is accelerated by a factor of 2. The models to prototype scaling ratios are given in Table 3.1.

The current study is confined to the single loop natural circulation system shown in Fig. 3.2, representing 113 channel of the prototype. Experiments are being conducted to study and predict the system behavior at a wide rage of operating conditions including startup. In the present work, emphasis was given on experiments to validate the RELAP5 model, study the nature of instabilities at low-pressure low-power conditions, and also to identify the method of power ramping for the startup of the test facility.

Table 3.1: Model to prototype scaling ratio.

Parameter	*Model to prototype ratio*
Elevations	¼
Power	1/2702.6
Number of fuel rods	1/663
Linear heating rate	2/1
Core hydraulic diameter	1/1
Cross sectional area	1/1351.3
Feed flow	1/2702.6
Length of links	¼
Number of risers/feeders	1/51
Number of downcomers	¼

TH-831_05610306

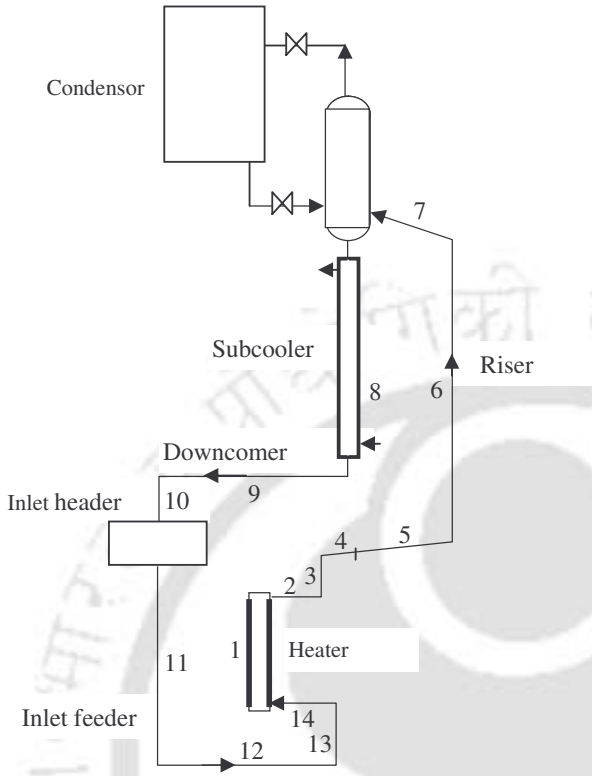

Link No.	*Inner Diameter (mm)*	*Length (mm)*	*Change in elevation (mm)*
1	32.50	1200	1200
2	18.90	200	0.0
3	18.90	430	430
4	18.90	530	66
5	32.50	4115	514
6	32.50	5890	5890
7	32.50	1010	160
8	15.58	6614	-6614
9	15.58	1640	0.0
10	15.58	200	-200
11	24.30	2040	-2040
12	24.30	1615	0.0
13	24.30	990	990
14	24.30	310	0.0

Figure 3.2. Schematic view of Natural Circulation Test Facility (NCTF) loop.

3.4. RELAP Models

RELAP5 models have been developed for the NCTF loop and the prototype. The RELAP5 model of NCTF is validated with experimental observations of the test facility. The RELAP5 model of NCBWR is verified by comparing with the results of NCTF.

3.4.1. Nodalization schemes

The test facility described in Section 3.3 was nodalized in RELAP5 as shown in Fig 3.3. The core and the riser sections are modeled as *pipe* components. A *simple separator* model is used for modeling the steam drum, and the downcomer is modeled

TH-831_05610306

as a *pipe* component. A *trip valve* is used for modeling the steam control valve. A *time dependent junction* between the source and the mixer facilitates the control of feed water supply, which is equal to the mass flow rate of steam exit from the drum to sink. The heater element is modeled as a *heat structure*. The length of each axial heat structure node is consistent with the length of the hydrodynamic component. To account for the effect of thermal capacitance, *heat structures* are applied for all the components of the loop. Experimentally measured loss coefficient values of various links of the loop have been applied. The subcooler in NCTF is modeled by employing a heat structure associated with the downcomer.

In the interest of observing the startup transients in a prototype, a RELAP5 model of NCBWR is developed. The models employed for simulating NCTF and NCBWR are similar in the sense that the same RELAP5 components have been used and the loss co-efficient values used in the NCTF model have been applied for the NCBWR model also.

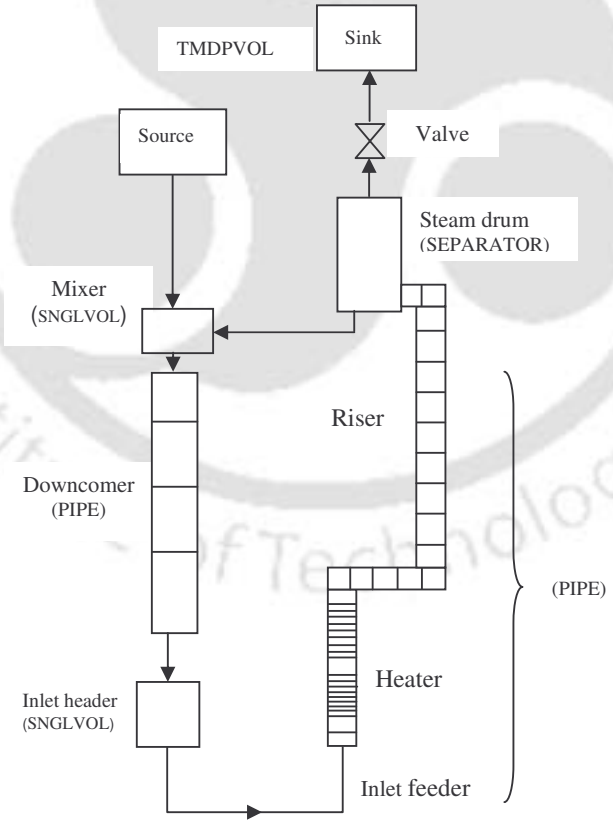

Figure 3.3. RELAP5 nodalization scheme for NCTF loop.

TH-831_05610306

For the heater heat structure, stainless steel thermal properties were used in the NCTF model, whereas zirconium-niobium alloy (Sinha and Kakodkar, 2006) are used in the NCBWR model. The heat structures in other components that account for the thermal capacitance use thermal properties of stainless steel.

3.4.2. Nodal sensitivity studies

In order to decide the number of nodes in the core (or heater) and the riser sections, nodal sensitivity studies are carried out for the RELAP5 models of the test facility and the prototype. During these numerical simulations, the steam outlet valve is kept open for simulating the steady state condition and closed while simulating the transient condition. In the steady state, the power inputs in the NCTF and NCBWR simulations were 17 kW and 120 MW, respectively, and the inlet subcoolings were 9ºC and 15ºC, respectively. The results of nodal sensitivity analysis for the steady state models are presented in Table 3.2. It is found that the NCTF nodalization scheme with 8 core nodes and 16 riser nodes (8C 16R), and NCBWR nodalization scheme with 32 core nodes and 36 riser nodes (32C 36R), differ from finer schemes by less than 2%. Hence, these schemes can be selected for numerical simulations of the test facility and the prototype.

It is also essential to verify the nodal sensitivity of the RELAP5 models in predicting the transient during startup. Transient simulations were carried out with the same nodal schemes as chosen for the steady state study. Figures 3.4 and 3.5 report the transient results for the NCTF and NCBWR models, respectively. In the transient simulations of NCTF model, oscillations obtained with 8C 16R scheme were similar to those of the finer schemes (8C 32R and 16C 16R), whereas some additional oscillations were observed when coarser schemes (4C 16R and 8C 8R) were employed (Fig. 3.4). The additional oscillations are spurious oscillations that arise due to the inadequacy of the numerical model when coarser nodalization is used. Considering both the steady state and transient studies, the nodalization scheme with 8 core nodes and 16 riser nodes (8C 16R) was selected for the NCTF model. Though there is no significant difference in the prediction of the NCBWR model when the number of core nodes is increased from 16 to 64, an increase in the number of riser nodes from 18 to 36 shows a change in the

TH-831_05610306

nature of oscillations (Fig. 3.5). Further increasing the number of riser nodes to 72 does not show much difference in the nature of oscillations. Hence, considering both the steady state and transient studies, the scheme with 32 core nodes and 36 riser nodes (32C 36R) was chosen for the NCBWR model. The simulations for the test facility and the prototype were done for a real time 500 s, and the relative CPU time required for different schemes is given in Table 3.2. It can be seen that the nodalization schemes selected for NCTF and NCBWR consume considerably less CPU time compared to the finer schemes.

Table 3.2: Nodal sensitivity study for steady state condition.

NCTF model			*NCBWR model*		
Scheme	*Mass flow rate (kg/s)*	*Relative CPU time*	*Scheme*	*Mass flow rate (kg/s)*	*Relative CPU time*
4C 16R	0.2124	0.89	16C 36R	501.5	0.77
8C 16R	0.2048	1.00	32C 36R	510.2	1.00
16C 16R	0.2010	1.26	64C 36R	515.4	1.51
8C 8R	0.2130	0.91	32C 18R	505.7	0.78
8C 16R	0.2048	1.00	32C 36R	510.2	1.00
8C 32R	0.2027	1.34	32C 72R	512.5	1.46

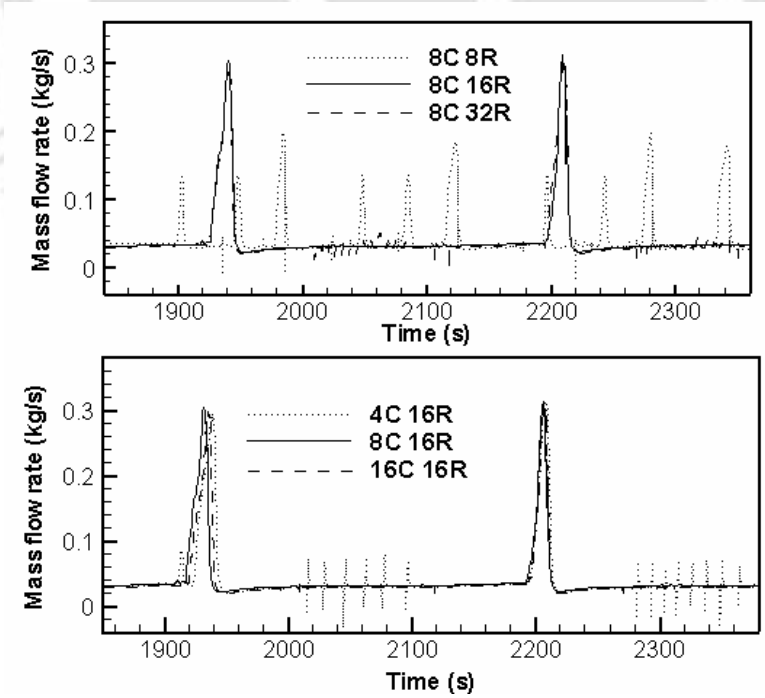

Figure 3.4. Nodal sensitivity study for transient simulation of NCTF.

TH-831_05610306

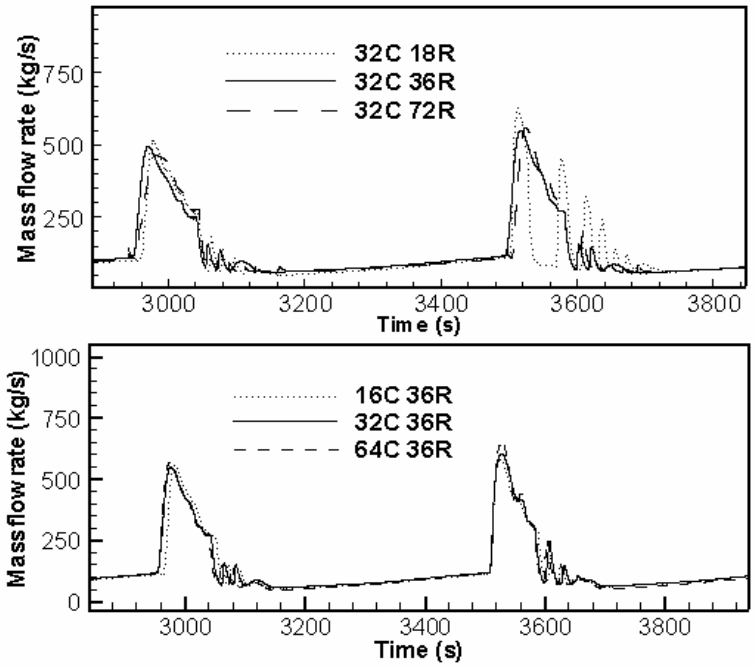

Figure 3.5. Nodal sensitivity study for transient simulation of NCBWR.

3.5. Model Validation

The above explained NCTF model has been validated by checking the predicted mass flow rate with various experimental data points. Fluid temperatures are measured with calibrated insertable K-type thermocouples. The heater inlet and outlet temperatures measured have uncertainty of 0.5% and 0.8%, respectively. Power measurements have an overall uncertainty less than 4 %. The pressure measurements are carried out with calibrated pressure transmitter having an overall uncertainty of 0.25 %. Flow measurements are carried out using orificemeter with an overall uncertainty of less than 1%. The mass flow rate, pressure, and temperature reported in the subsequent sections shall be presumed as measured at the inlet of the core, if not otherwise mentioned. To start with, it is intended to verify the model's ability to predict the state of the system at a given pressure, power and subcooling condition, by comparing with the steady state conditions recorded during various experiments. The predicted steady states of the system for different pressure, power and temperature conditions are listed in Table 3.3. The table also gives the percentage deviations between experimental and predicted

TH-831_05610306

mass flow rate, which are comparable with the deviations reported under previous studies with system codes (D'Auria et al., 1993; Ferng and Lee, 1994). The stability boundary predictions of the RELAP5 model were also done against the experimental predictions. The power at the boundary above which the system moves into an unstable Type-II region is predicted numerically, and compared with the experimental results. A good agreement is found between the results, as given in Table 3.4.

Transient predictions are very important in the context of the present study. Hence, the ability of RELAP5 model to reproduce the transients observed in the experiments is to be verified. Simulations were done with the same input power and initial conditions as that in the experiment, and the transients were observed. The initial temperature of the working fluid was 80ºC and the power was increased in steps of 1.5 kW every 15 min. The transients during the startup were observed both experimentally and numerically, and the flow signatures are shown in Fig 3.6a. A magnified view of these oscillations observed at low-pressures low-power condition during the startup is shown in Fig. 3.6b, where the signatures of geysering and flashing oscillations are evident.

Table 3.3: Comparison of steady state mass flow rate.

Pressure (bar)	*Power (kW)*	T_{sub} (°C)	*Mass flow rate (kg/s)*		*% deviation*
			Exp	*RELAP5*	
15	27.7	11.5	0.14	0.180	28.5
15	24	9.6	0.14	0.178	27.1
15	20.2	7.9	0.15	0.179	19.3
15	16.6	6.4	0.16	0.196	22.5
15	14.2	5.8	0.16	0.192	20.0
8	9.3	5.0	0.17	0.205	20.5
8	11.4	5.6	0.17	0.200	17.6
8	14.2	6.4	0.16	0.180	12.5
8	17.1	7.6	0.15	0.190	26.7
8	19.3	8.6	0.14	0.170	21.4
8	21.4	10.1	0.13	0.160	23.0
2	7.6	16.7	0.19	0.170	11.8
2	8.2	17.0	0.20	0.185	8.1
2	8.7	17.1	0.21	0.190	10.5

TH-831_05610306

Table 3.4: Type-II boundary predictions.

Pressure (bar)	*Subcooling (°C)*	*Power at Type-II boundary (kW)*	
		Experimental	*RELAP5*
25	9	39.5	40.0
25	18	43.4	42.5
15	14	34.0	33.0
15	5	26.6	26.0
8	12	24.1	24.0

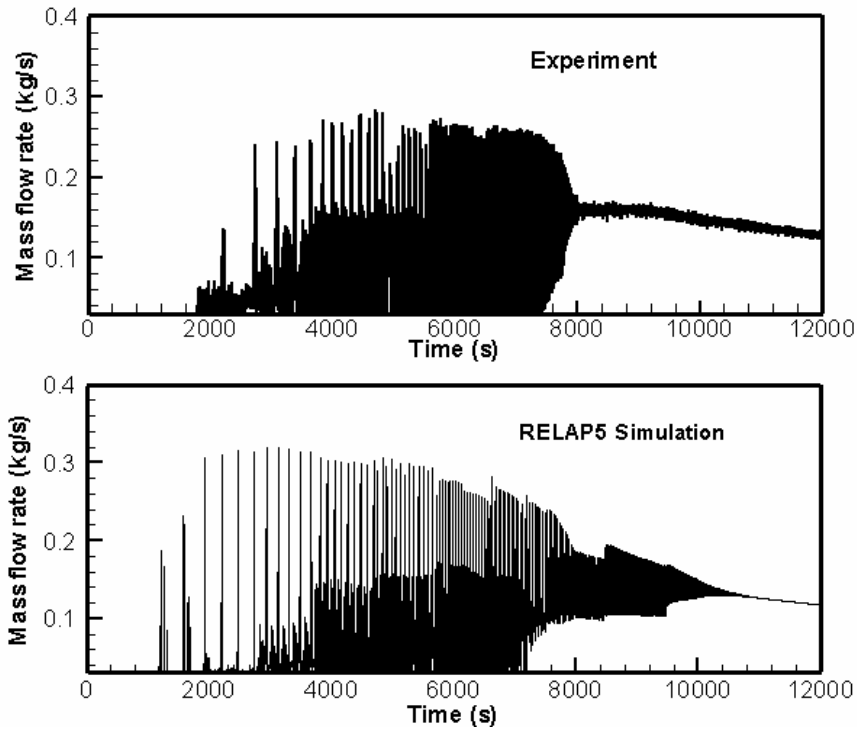

Figure 3.6a. Mass flow rate observed during experiment and RELAP5 simulation.

TH-831_05610306

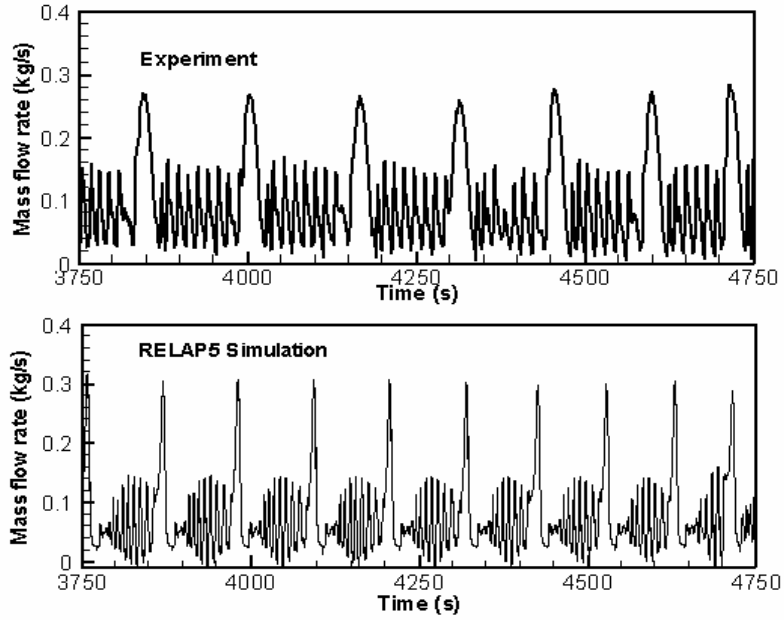

Figure 3.6b. Mass flow rate observed during experiment and RELAP5 simulation.

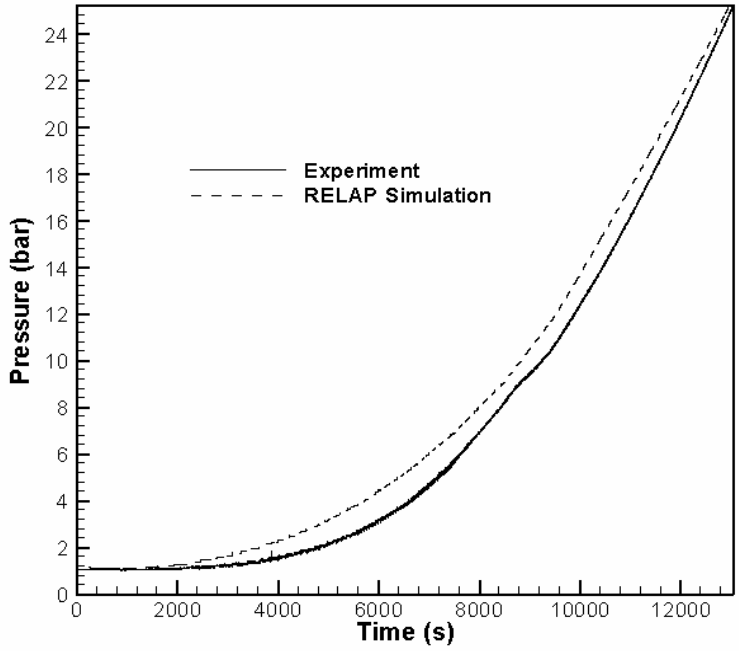

Figure 3.7. Comparison of system pressure rise in the experiment and simulation.

It is inferred that the flow oscillates by few geysering peaks with lower amplitude, followed by a flashing peak with higher amplitude. It is evident from Table 3.3 and Fig.

TH-831_05610306

3.6b, that RELAP5 model slightly over-predicts the frequency and amplitude of oscillations. This is due to the low frictional pressure drop calculation in the RELAP model, which allows the density/enthalpy waves to travel faster through the heater and riser section. However, it is inferred that RELAP5 model is capable of predicting the phenomenological and structural nature of oscillations (as further discussed in Chapter 4), at low-pressure low-power conditions during startup. The variation of pressure with time obtained by the numerical simulation was compared with that observed in the experiment and a good agreement was found between the two (Fig. 3.7).

3.6. Verification of NCBWR Model

Numerical models of NCTF and NCBWR were verified for their nodal sensitivity (Section 3.4) and the NCTF model was validated with experiments (Section 3.5). In order to verify the nature of transients predicted by the NCBWR model, numerical simulations are carried out with both RELAP5 models and compared. Effect of system parameters, viz., initial pressure, inlet and outlet loss coefficients, is studied. Simulations for different initial pressures show that, for both RELAP5 models, higher initial pressure results in suppression of oscillations (Figs. 3.8 and 3.9).

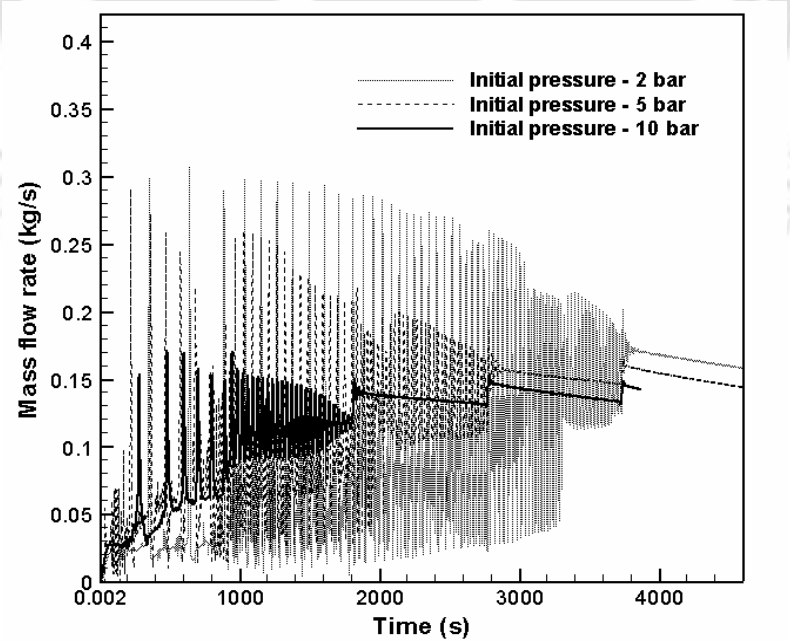

Figure 3.8. Transients observed for various initial pressures of NCTF.

TH-831_05610306

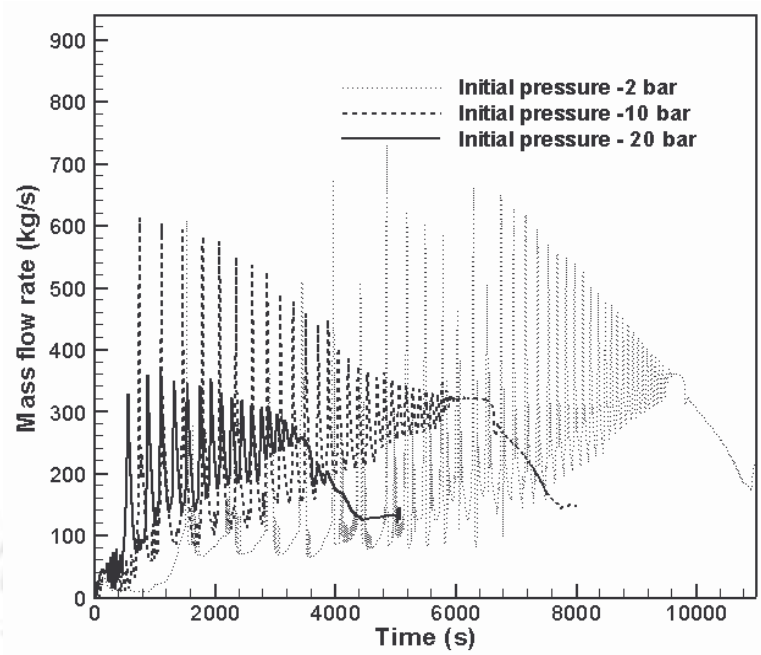

Figure 3.9. Transients observed for various initial pressure of the prototype.

Comparing the results obtained for the two models for the same initial pressures, it is observed that the time taken for the instabilities to die out in the NCBWR model is about two to three times longer than that in the NCTF model. This is as expected because NCTF was designed for a time scale that is half that of the prototype.

Simulations were done in order to observe the effect of inlet and outlet loss coefficient in the model and the prototype. The flow signatures during the inception of flow instabilities are shown in Fig. 3.10. It is observed that the amplitude of oscillation reduces as the inlet loss coefficient is increased. It is further inferred that the duration of flashing instability in the prototype is twice that in the test facility, which is as expected based on the time scale ratio for which NCTF was designed. Figure 3.11 illustrates that the amplitude of flashing oscillations decreases as we increase the outlet loss coefficient. The outlet loss coefficient is located in the near horizontal tail pipe leading to the vertical riser and hence acts as an inlet resistance to the riser section where flashing occurs.

TH-831_05610306

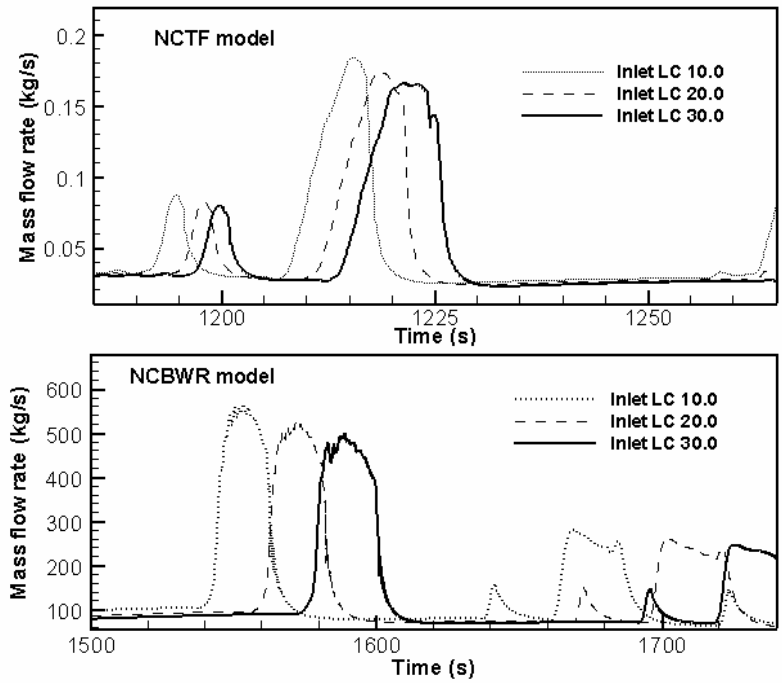

Figure 3.10. Transients observed for various inlet loss coefficients.

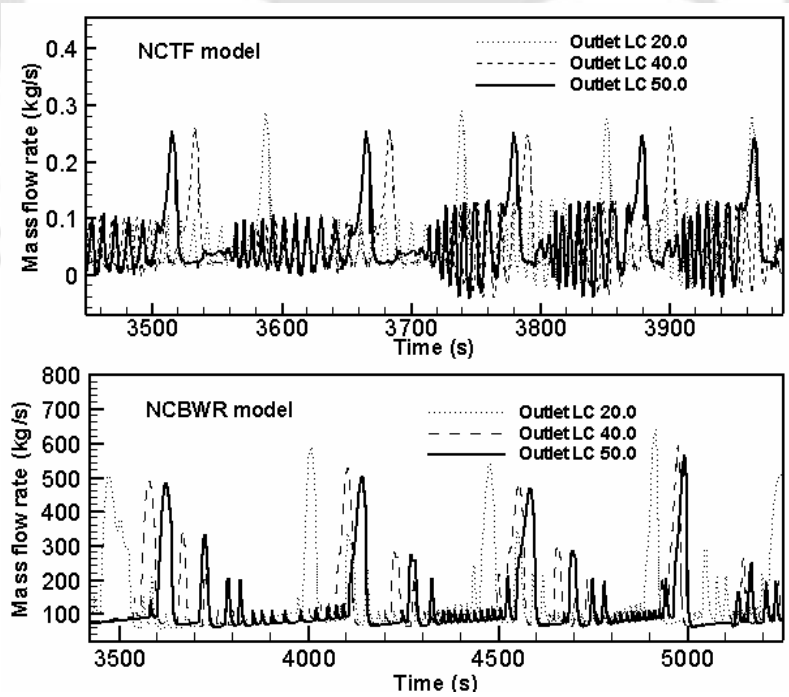

Figure 3.11. Transients observed for various outlet loss coefficients.

TH-831_05610306

For higher values of outlet loss coefficient, the average flow is brought to a lower value and the flow is seen to get reversed in the NCTF model. In general, both RELAP5 models show similar trends of parametric effects and the amplitude ratio is fairly close to the mass flow rate ratio expected between the test facility and the prototype

3.7. Summary

Numerical models of NCTF and NCBWR have been developed with RELAP5 code along with nodal sensitivity studies and verified with experimental results.

- In order to decide the number of nodes in the core (or heater) and the riser sections, nodal sensitivity studies are carried out for the RELAP5 models of the test facility and the prototype. The scheme with 8 core nodes and 16 riser nodes (8C 16R) for NCTF, and the scheme with 32 core nodes and 36 riser nodes (32C 36R) for NCBWR was selected.

- The RELAP5 model of NCTF has been validated for its steady state as well as transient predictions with the help of experimental observations. Though RELAP5 slightly overpredicts the frequency and amplitude of oscillations, it is evident that RELAP5 model is capable of predicting the nature of phenomena based oscillations at low-pressure low-power conditions during startup.

- As a verification process, the transient predictions and parametric trends (effect of pressure and flow restrictions) obtained by the NCBWR model have been compared with those of the NCTF model. Numerical predictions of the mass flow rate and the duration of flashing instabilities are also found to be as expected based on the scaling ratios for which NCTF was designed.

TH-831_05610306

Chapter 4

Analysis of Startup Oscillations

4.1. Introduction

Flow oscillations due to geysering and flashing are very common during startup conditions. The co-existence of both geysering and flashing instabilities and the mutual dependency between the two was reported by Jiang et al. (2000). Similar kind of flow oscillations are observed in the natural circulation test facility (NCTF), where the flow oscillates with a few pulses of lower amplitude followed by a higher amplitude pulse. In the absence of additional system parameters (void fraction, quality, etc.) along with the measured flow signal, one cannot clearly distinguish and understand the mechanism behind such signatures. In such case, it appears that the lower amplitude oscillations are due to geysering and the higher amplitude oscillations are due to flashing, by relating with the findings of Jiang et al. (2000) (Fig. 2.6). Whether these low and high amplitude oscillations are actually due to geysering, flashing or a kind of density wave instability is to be confirmed and classified. This can be done when a verified numerical model is in place, which can give additional system parameters that can be used to analyze and understand the mechanism of flow instabilities. In such a pursuit, RELAP5 simulations of both NCTF and NCBWR are used for the analysis and interpretation.

Different views on the structural nature (periodic, quasi-periodic and chaotic) of the transients were discussed (Section 2.2.1). In this context, it is desirable to study the dynamic characteristics of the flow transients during startup of NCTF and NCBWR, by using methods of nonlinear time series analysis. The computation of power spectral density, Lyapunov exponents and Poincaré sections helps in understanding the structural behavior of flow signals observed in natural circulation boiling systems.

TH-831_05610306

The current chapter is focused on the analysis of flow oscillations observed during experimental and numerical studies under low-pressure low-power startup conditions. Section 4.2 interprets and classifies these transients by comparing and relating with already reported facts in open literature. The flow transients simulated for the prototype are compared with the flow transients observed in the model (NCTF). Further, using the methods of nonlinear time series analysis, the structural nature of these oscillations is studied in Section 4.3.

4.2. Analysis of Startup Oscillations

Flow oscillations were observed during the startup of NCTF, as shown in Fig. 3.6. Along with the flow signal, the data did not include void fraction or quality measurements. However, the development of the RELAP5 model has given us the advantage in predicting many system parameters that could help us in getting an insight of the phenomenon behind such flow oscillations. The fact whether the observed low and higher amplitude oscillations are actually due to geysering, flashing or a kind of density wave instability is to be confirmed and classified. The similarity between the startup transients observed in NCTF and the prototype is examined. The numerical results obtained through the RELAP5 models of both NCTF and NCBWR are used for the analysis and interpretation. It is to be noted that, while attempting to analyze flow oscillations characterized by strong voiding in the heater section, the assumption of constant power will not hold good and the effect of neutronic feedback should also be included, while developing a realistic reactor model.

4.2.1. Flow instabilities in NCTF

Using RELAP5 simulation, the void fraction data at the exit of the heater and riser sections are recorded and plotted along with the mass flow rate (Fig. 4.1 and 4.2). Fig. 4.1 shows the appearance of void pulses at the heater exit during the lower amplitude flow oscillation and no heater void during the higher amplitude flow oscillation. But, void pulses appear at the riser exit during the higher amplitude flow oscillation as shown in Fig. 4.2. It is inferred that the low amplitude oscillations are caused due to the void pulses generated in the heater section and the high amplitude oscillations are

TH-831_05610306

caused due to void pulses generated as a result of flashing in the adiabatic riser section. The alternating trend of oscillation seen here is very similar to the findings reported by Jiang et al. (2000) in their experimental setup where it was concluded that the low amplitude oscillations

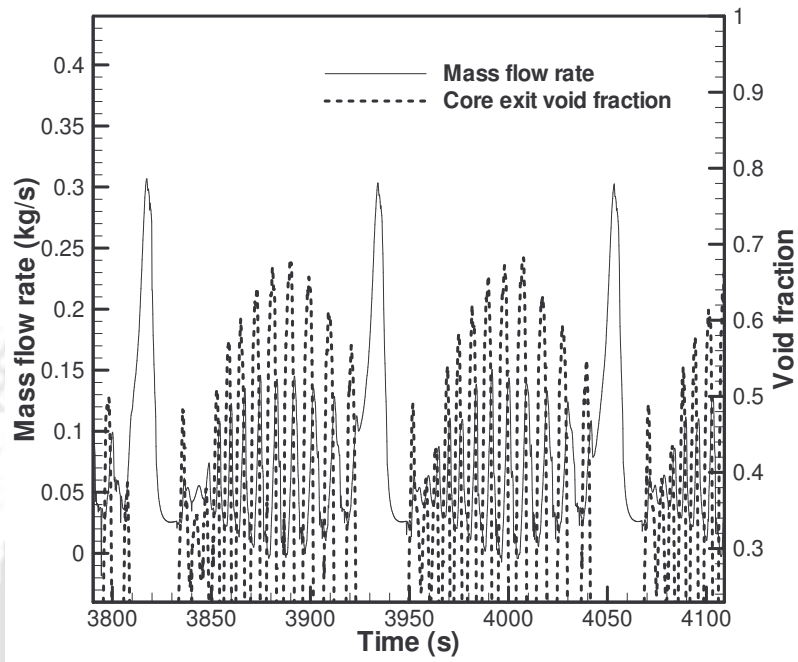

Figure 4.1. Mass flow rate and heater exit void fraction in NCTF simulation.

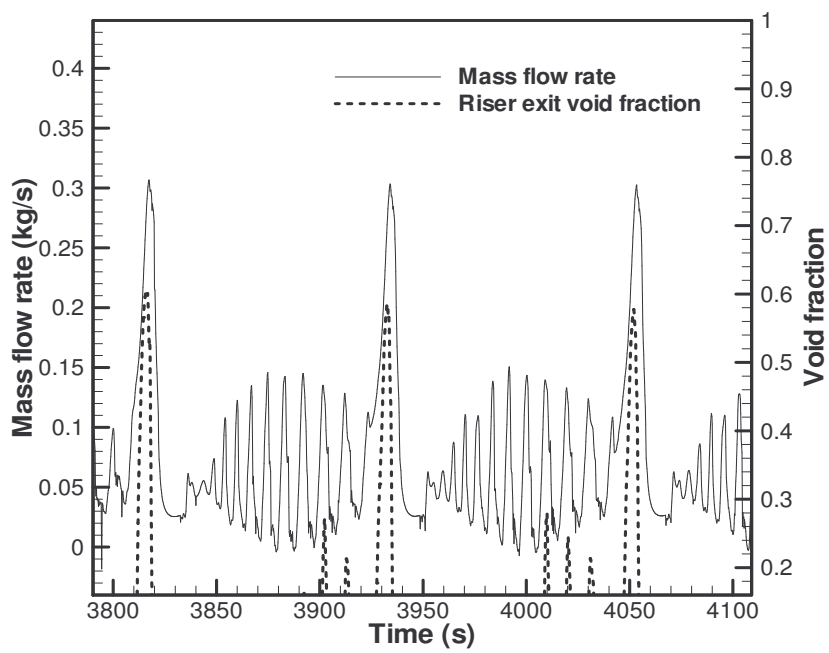

Figure 4.2. Mass flow rate and riser exit void fraction in NCTF simulation.

TH-831_05610306

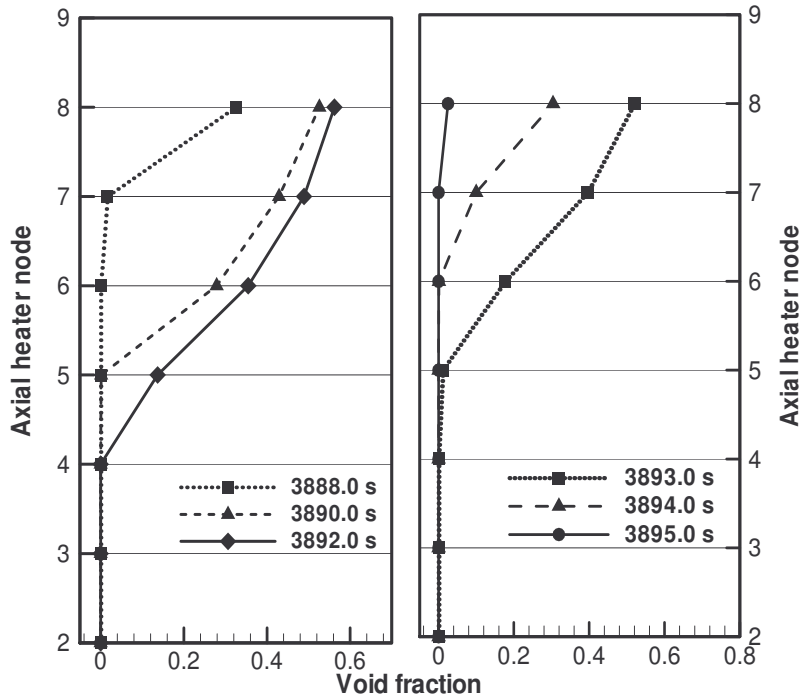

Figure 4.3. Core void fraction study for one geysering cycle.

were due to the phenomenon of geysering. In the case of NCTF, the same phenomenon of geysering may be the reason for the low amplitude flow oscillations but it can also be caused due to density wave instability. Hence, it has to be confirmed.

To understand the cause behind such instability due to core void generation and also to verify with the findings reported by Aritomi et al. (1993), an analysis is tried by using the void fraction data obtained by RELAP5 simulation. This is done by plotting the void fraction of each axial heater node at different instant of a chosen low amplitude flow pulse. A single flow pulse of duration 3888.0 to 3895.0 second (Fig. 4.1) caused by void generation in the heater section is considered. The oscillation begins at 3888.0 second and attains the maximum amplitude at 3892.0 second and dies at 3895.0 second. The void fraction at each axial heater node at every second is plotted as shown in the Fig. 4.3. As per the definition of geysering by Aritomi et al. (1993), the void generated in the core has to condense in the lower part of the riser. In such case, the reduction in void should initiate from the top of the heater (node 8), meaning that the void fraction

TH-831_05610306

at node 8 should be less than the void fraction at node 7 at any instant during the downward trend of the flow (3892.0–3895.0 s). However, it is inferred from Fig. 4.3 that the void fraction in the top heater node (node 8) is always higher than the lower node at any point of time. At 3895.0 second, the oscillation has almost died and the void fraction in all the heater nodes is zero except for the top core node. This conveys that the condensation is not initiated from the top of the heater. Hence, the reason for the suppression of oscillation could be the subcooled fluid entering the heater section. Thus, the small amplitude oscillation observed here are not condensation induced geysering instability and the instability may be termed as a Type-I density wave oscillation.

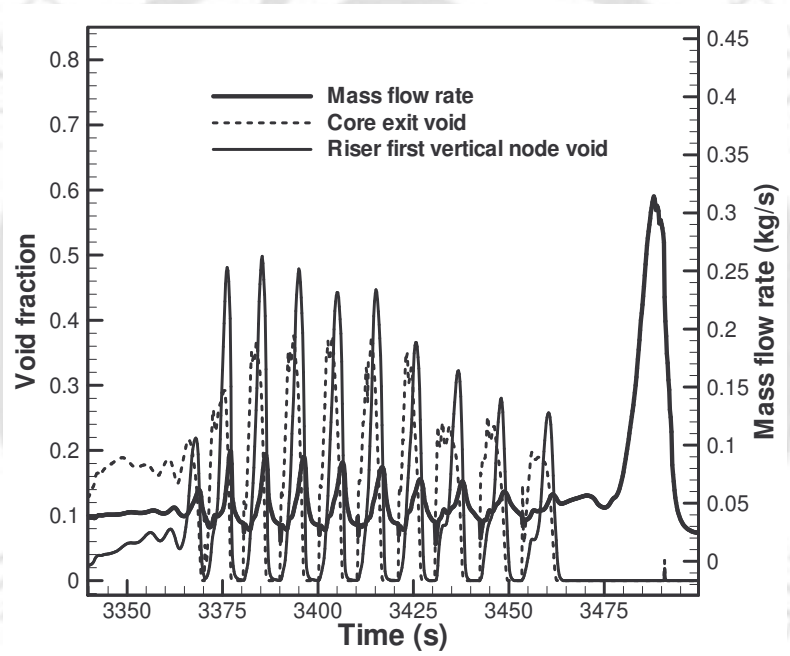

Figure 4.4. Core exit and riser inlet void fraction along with mass flow rate during NCTF simulation.

Another fact can be seen in Fig. 4.4, were additional void is generated in the lower part of the riser. When looking at the geometry of the NCTF loop, the heater section is followed by a small vertical riser section, followed by a long horizontal pipe and then by the long vertical riser. From Fig. 4.4, though it is clear that the small amplitude oscillations are due to void generation in heater, there is additional void generation corresponding to the vapor packets that move from the heater section into the adiabatic

TH-831_05610306

section. This enhancement in void fraction could be due to flashing in the small vertical section and change in slip ratio between the liquid and vapor phases. The void fraction at the lower riser is very well below the value of void in the heater section and increases only after pulses of void start to appear in the heater. Due to the sudden movement of the heater void, the liquid in the lower part of the riser is likely to experience an increase in temperature, resulting in additional void generation due to flashing. Thus, the small amplitude oscillation observed here can be termed as a kind of density wave instability but assisted by flashing as well.

4.2.2. Flow instabilities in NCBWR

Numerical tests for the startup of the prototype were carried out using its RELAP5 model. As expected, flow oscillations were observed at low-pressure, low-power conditions. The temporal traces during a startup test are shown in Fig. 4.5. From the numerical simulations (Section 3.6) it was observed that the time scale and flow ratios

between the model and the prototype are very close to the designed values. When further looked into, it was observed that there is a difference in the nature of startup oscillation for similar startup conditions. The flow does not seem to oscillate with two distinct lower and higher amplitudes as observed in NCTF startup simulations. There is no void generation in the core region almost throughout until the initial transients die out (Fig. 4.5). Fig. 4.6 shows that the higher amplitude oscillations are clearly a result of void generation in the riser (adiabatic) section termed as flashing. Based on the length scale ratio, the length of the riser pipes in the prototype will be 4 times that of the model. Hence, the effect of flashing is more pronounced due to the large variation of saturation temperature, leading to an enhancement of the natural circulation flow rate. As a result, more subcooled liquid is rushed into the core region, limiting the generation of void in the core region and the occurrence of low amplitude oscillation. A similar flow observation, with only flashing-induced oscillations was reported by Bagul et al. (2008) through their startup experiments conducted in the integral test loop (ITL) and the same was predicted by its RELAP5 model. It is to be noted that ITL is a scaled down facility of the prototype (pressure tube type reactor), but having a length scale of

TH-831_05610306

1:1. It is also not necessary that the flow in the scaled down test facility will always oscillate with two different amplitudes. It is possible that the flows is only characterized by flashing, and without core boiling, especially under high subcooling and reverse flow conditions under parallel-channel setup. Such condition are discussed later in Section 5.4.1 This indicates that the scaling criteria for a natural circulation system are likely to be quite complicated especially when the exact nature of the transients is to be predicted.

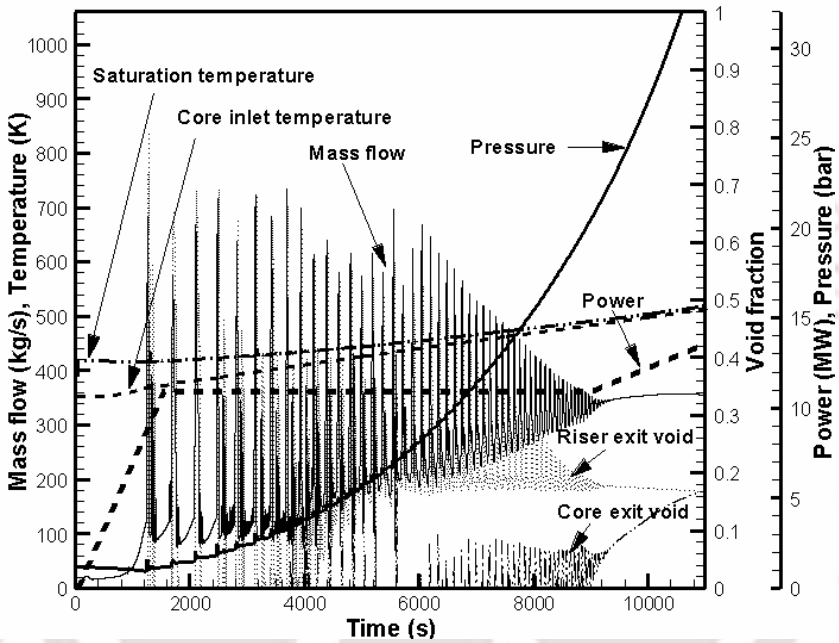

Figure 4.5. Startup simulation of the prototype using RELAP5.

4.3. Time Series Analysis

Time series analysis accounts for the fact that data points taken over time may have an internal structure (such as autocorrelation, trend or seasonal variation) that should be accounted for. In this section, the time series data obtained from experimental and numerical observations of NCTF and NCBWR is analyzed to identify the structural nature of the transients. The power spectral density (PSD) is computed by using a fast Fourier transform (FFT) algorithm (Parker and Chua, 1989). The nonlinear time series analysis (TISEAN) package (Hegger et al., 1999) is used for the computation of Lyapunov exponent and Poincaré section of the observed and computed flow data.

TH-831_05610306

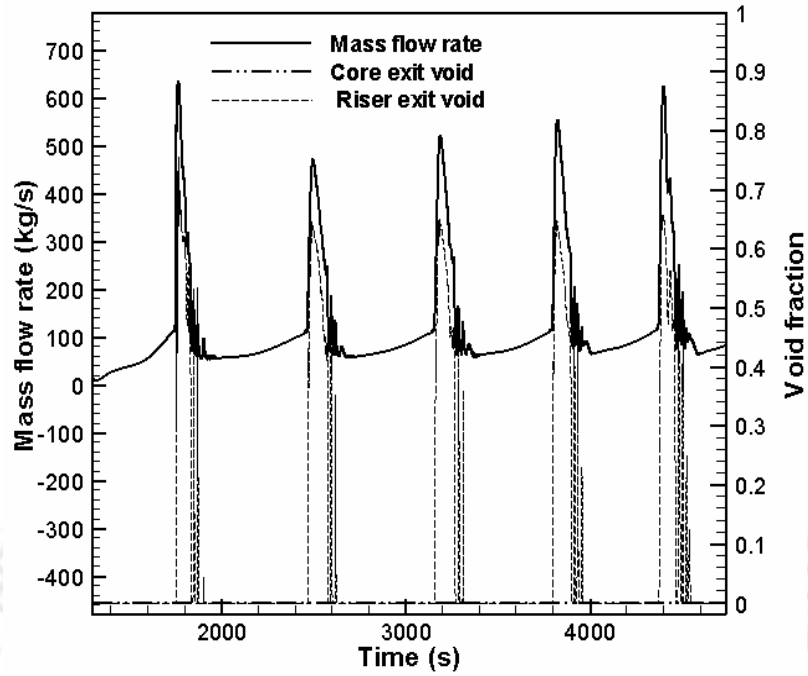

Figure 4.6. Mass flow rate and void fraction in NCBWR simulation.

4.3.1. Power spectrum analysis

The understanding gained about a dynamical system using the time-domain techniques can be significantly enhanced by extending the investigation to the frequency domain. It often yields surprisingly valuable information. The time evolution of a dynamical system can be represented by the time series of its dynamical variables sampled at regular intervals. If we represent the time series of a particular dynamical variable by

$$Y^{(k)} \; ; \qquad k = 0, 1, \ldots, N-1 \tag{4.1}$$

Then the discrete Fourier transform of the N points $Y^{(k)}$ is given by

$$Y^{(l)} = \sum_{k=0}^{N-1} Y^{(k)} e^{\frac{2\pi jkl}{N}} \tag{4.2}$$

Where, j = √-1. For a real time series, we need to consider only l = 0, 1,..., N/2. The transformation (Eq. 4.2) can be carried out efficiently by using a fast Fourier transform (FFT) algorithm (Press et al., 1993). For this purpose, the number of points N in the

TH-831_05610306

time series (Eq. 4.2) must be a power of 2. The periodogram estimate of the power spectral density (PSD) at (N/2 +1) frequencies f_l is then defined as

$$\begin{aligned} PSD(0) \equiv PSD(f_0) &= \left|\hat{X}^{(0)}\right|^2 \\ PSD(f_l) &= 2\left|\hat{X}^{(l)}\right|^2, \quad l = 1, 2, \ldots\ldots, (N/2 - 1) \\ PSD(f_c) \equiv PSD(f_{N/2}) &= \left|\hat{X}^{(N/2)}\right|^2 \end{aligned} \tag{4.3}$$

where

$f_l = \dfrac{l}{N\Delta\tau}$, $l = 0, 1, \ldots\ldots, N/2$

$\Delta\tau$ = sampling interval for the time series (Eq. 4.1), and

$f_c = \dfrac{1}{2\Delta\tau}$, the Nyquist frequency.

While data filtering or smoothing of the spectral estimates, careful attention must be paid to aliasing and frequency resolution. All the spectral power that lies outside the Nyquist frequency range is aliased (falsely translated or folded back) into that range by discrete sampling. Thus the sampling interval $\Delta\tau$ must be such that the higher frequency harmonics beyond $f_c = ½\Delta\tau$ are negligible. If f_* *denotes* a characteristic fundamental frequency associated with the time series, then $\Delta\tau$ is selected such that

$\dfrac{f_c}{f_*} = L$ is a large number, say between 8 to 64.

The time series data of the mass flow rate signal monitored during experimental and numerical simulation (Fig 3.6) is checked for its spectral density using fast Fourier transform (FFT) algorithm (Parker and Chua, 1989). A power spectrum containing sharp pulses at discrete frequencies indicates periodic oscillations while a continuous power spectrum indicates a chaotic or a quasiperiodic orbit. The experimental data that are analyzed here were recorded with a sampling interval of 0.5 second and hence the numerical time series data is also obtained for the same sampling time. The possibility of aliasing is also checked. For the considered mass flow rate signal, the value of L is greater than 10 and hence the chosen $\Delta\tau$ does not pose any problem of aliasing. Fig. 4.7 illustrates the chaotic nature of the measured mass flow rate signals from both experiment and RELAP5 simulation, where the spectrum maintains a band thought out the frequency range showing no well defined dominant frequency. The flow signals

TH-831_05610306

measured in the NCBWR startup simulation are also chaotic in nature as show by the spectral density in Fig. 4.8.

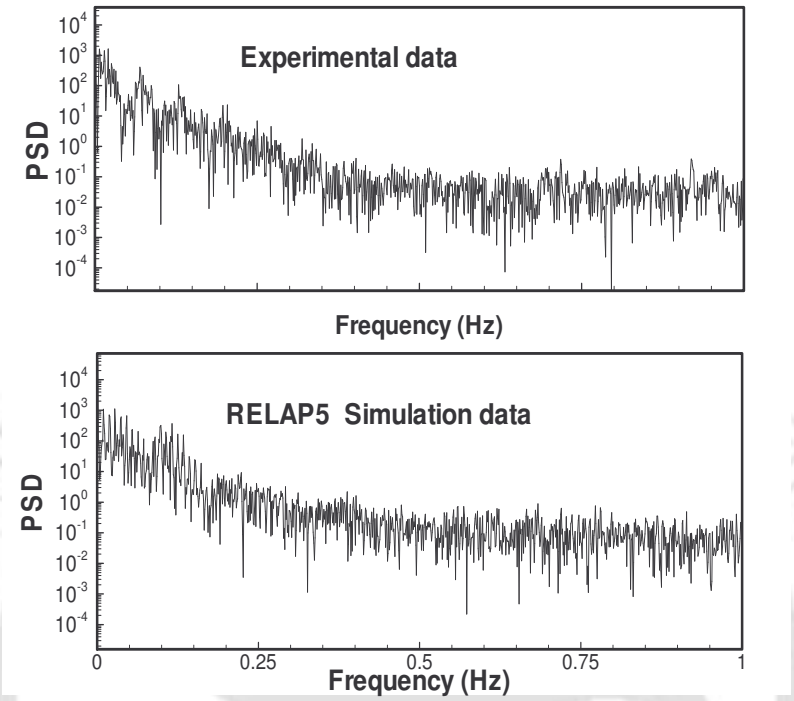

Figure 4.7. Fourier power spectrum for flow oscillations in NCTF.

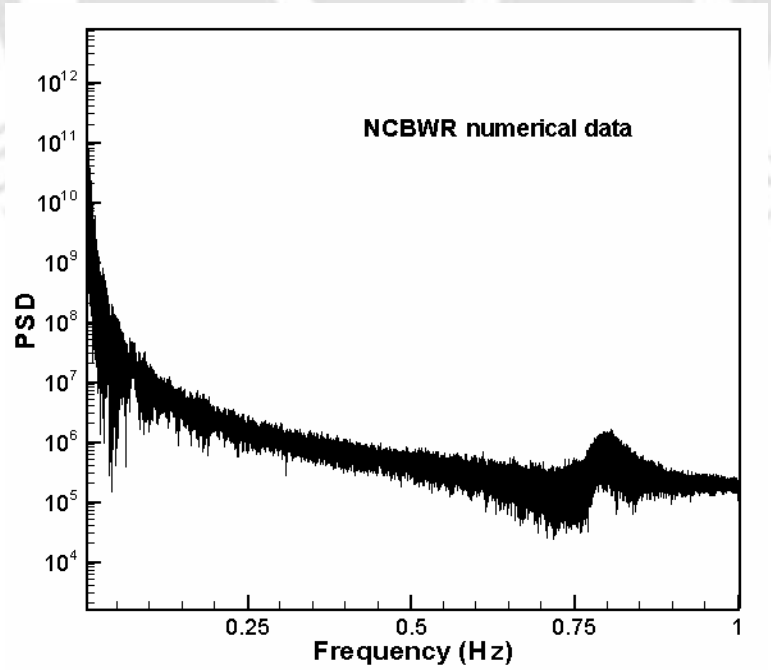

Figure 4.8. Fourier power spectrum for flow oscillations in NCBWR.

TH-831_05610306

4.3.2. Poincaré Section

Further time series analysis is carried out using the TISEAN package. The phase space diagrams of a dynamical system of order n can be simplified by introducing an (n-1)-dimensional surface of sections in the phase space. Hence, instead of studying a complete trajectory, one monitors only the points of its intersection with this surface. This reduces the study of continuous time dynamical systems (flows) to the study of reduced-order discrete-time systems (maps). As the trajectory crosses the surface from one side to the other of a hyper-surface, the set of points of intersection with the hyper-surface is referred to as the Poincaré section. Mapping an intersection point onto the subsequent intersection point is referred to as Poincaré map. Poincaré section of a periodic orbit consists of finite number of points, while that of a chaotic or a quasiperiodic orbit contains infinite number of points.

Poincaré maps were computed by using the TISEAN package. The program *pioncare* constructs a sequence vectors from a data set if one specifies the hyper plane and the embedding parameters. The intersection of the trajectory with the Poincaré plane is computed by a third order interpolation. Figure 4.9 shows the Poincaré section for a chosen embedding dimension (m=5) and delay (d=3). The points on the section are scattered and do not indicate a periodic or a quasiperiodic orbit, showing the character of a chaotic system. The placement of Poincaré surface is important for the usefulness of the result. An optimum location of the surface can be selected by maximizing both the variance of the resulting data and the number of intersection points. The number of intersections at the optimized surface position for the NCTF experimental (Fig. 4.9a), NCTF numerical (Fig. 4.9b) and NCBWR (Fig. 4.9c) data are 254, 267 and 68, respectively. The difference in the scatter of intersections seen between NCTF experimental (Fig. 4.9a) and numerical (Fig. 4.9b) data is due to slight over prediction of mass flow rate and frequency by the RELAP5 model, which was inferred while comparing the experimental and numerical predictions (Section 3.5). This uncertainty in the numerical model is aggravated due to the chaotic nature of oscillations, hence the state of the system becomes unpredictable and only the chaotic nature of oscillations can be inferred. The character and the number of intersections observed for the NCBWR data is found to be different, owing to difference in the nature of startup

TH-831_05610306

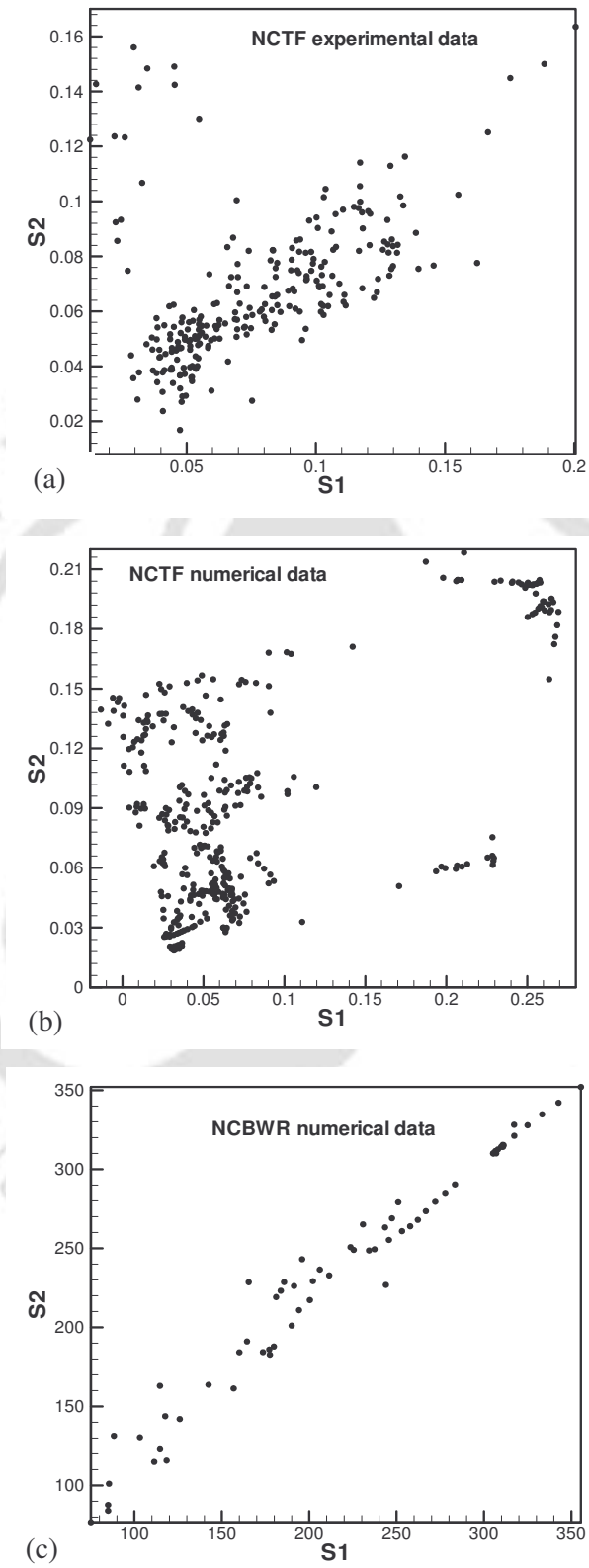

Figure 4.9. Poincaré section for flow oscillations (using TISEAN).

TH-831_05610306

oscillations observed in the model and the prototype, where, the flow in the model oscillates with both large and small amplitude oscillation, whereas in the prototype, only large amplitude flashing oscillations are observed (as discussed in Section 4.2.2).

4.3.3. Lyapunov exponent

Aperiodicity (chaoticity) observed in any system, for certain parameter range, results from the exponential divergence of initially close points on the limit set (asymptotic orbit). The rate of this divergence is characterized by Lyapunov exponents. In the present work, the Lyapunov exponents were computed using the *layp_r* algorithm available in the TISEAN package, which is based on the Rosenstein algorithm (Rosenstein et al., 1993). The phase space reconstruction of the attractor dynamics from a single time series is done using the method of delays as discussed by Wolf et al. (1985). In principle, when using the delay coordinates to reconstruct an attractor, an embedding of the original attractor is obtained for a sufficiently large (m) and almost any choice of time delay (d). However, in practice accurate estimation of Lyapunov exponent requires a careful choice of these two parameters. The implementation of any algorithms can be tested with several dynamical systems (Henon, Lorenz, and Rossler) to get a first hand knowledge in choosing the parameter involved in the evaluation of Lyapunov exponent. Since we have no prior knowledge over the dimension of the dynamical system under study (NCTF and NCBWR), we evaluate the Lyapunov exponent for different embedding dimensions. The flow data obtained from the startup test of NCTF and NCBWR is studied for the exponential divergence of the attractor for different embedding dimension and reconstruction delay time. The average of divergence versus time is plotted in Fig. 4.10 and is found to increase exponentially. This confirms the chaotic nature of the flow oscillations, as diagnosed in Sections 4.3.1 and 4.3.2. It can be observed that the slope of the curve is steep at the initial region that actually defines the largest Lyapunov exponent and later the curve saturates at longer time as the system is bounded in a phase space. Figures 4.10a-c show the effect of embedding dimension on the prediction of Lyapunov exponent. The algorithm works well for a range of embedding dimension (m). Increasing the reconstruction delay time (d) more than what is required increases the level of contamination of the data as shown in Figs. 4.10d-f.

TH-831_05610306

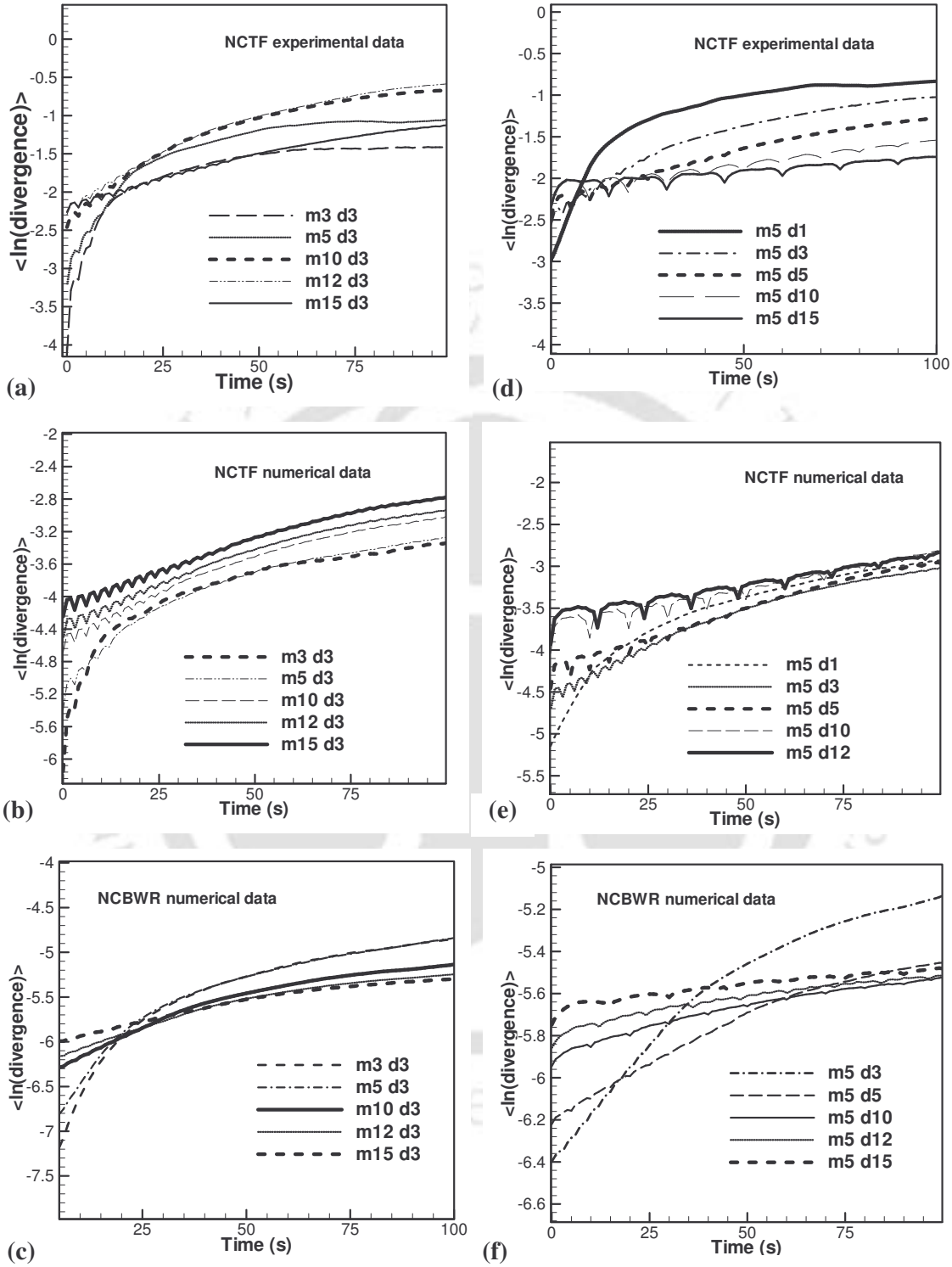

Figure 4.10. Lyapunov exponent for flow oscillations (using TISEAN). (a, b, c) effect of embedding dimension. (d, e, f) effect of reconstruction delay.

TH-831_05610306

4.4. Summary

The numerical results obtained through the RELAP5 models of both NCTF and NCBWR are used for the analysis and interpretation. In the NCTF model, the flow oscillates with a few pulses of lower amplitude followed by a higher amplitude flashing pulse.

- The flow oscillations seen in the NCTF model have resulted due to alternating void generation at two different parts of a vertical channel, namely, the heater and riser sections.

- The small amplitude oscillations are due to void generation in the heater region, and there is additional void generation corresponding to the vapor packets that move from the heater section into the adiabatic section. These oscillations are not condensation induced geysering instabilities, but a density wave instability supported by flashing.

- The similarity between the nature of startup transients observed in the NCTF and the prototype is examined. The effect of flashing is more pronounced in the prototype due to the large variation of saturation temperature, as the length scale is 4 times that of the model.

- The power spectral density (PSD), computed using a fast Fourier transform (FFT) algorithm conveys that the observed startup transients are chaotic in nature. This aperiodicity is further confirmed by the computation of Lyapunov exponent and Poincaré section using the nonlinear time series analysis (TISEAN) package.

TH-831_05610306

TH-831_05610306

Chapter 5

Startup Oscillations in Parallel-Channel Systems

5.1. Introduction

The past findings reported in literature on instabilities under low-pressure low-power startup conditions are a result of research focused on the development of single channel vessel type NCBWR like ESBWR. In these studies the nature of transients is mostly explained through single channel systems. Largely, the motivation behind the previous double-channel works (Section 2.2.5) was to simulate the flow inside the parallel tubes of the reactor cores and heat exchangers. The current study assumes importance in simulating a multi-channel pressure tube type reactor, having tubes with adiabatic section (riser) running up to 25 m height. Due to the strong variation of saturation temperature along the length, flashing is expected in the adiabatic section during the startup of the reactor.

The objective here is to investigate the existence of in-phase and out-of-phase Type-I instabilities that could occur during startup of parallel-channel systems. The details of the parallel-channel RELAP5 model are discussed in Section 5.3. The observations under similar and different boundary conditions (power and flow restriction) in the channels are discussed along with a comparison in flow behaviour observed in a test facility and its prototype (Section 5.4).

5.2. Description of Parallel-Channel Systems

It is intended to study the behaviour of a parallel-channel reactor under a low-pressure low-power startup condition. The boiling water reactor (BWR) under study is a vertical, natural circulation cooled, pressure tube type reactor (Sinha and Kakodkar, 2006). The

TH-831_05610306

major dimensions and components of the primary heat transport (PHT) system are as given in Fig. 5.1. A brief description of the prototype design and passive safety features is presented in Appendix C. The PHT loop consists of 452 coolant channels (core and riser) connected to 4 steam drums. For the current study, a numerical model comprising a system of two identical parallel loops, each consisting of a core, a riser and a common downcomer, is considered. Each of the loops represents 56 channels, and both loops together represent one-fourth of the total channels of the prototype. All the 56 channels are averaged into a single equivalent channel assuming that all the channels get the same power. The flow area of a single equivalent channel is equal to the flow area of 56 channels. The hydraulic diameter of the equivalent channel is equal to the hydraulic diameter of a single-channel in the prototype. The details of the scaled system, considered for the parallel-channel study, are from the natural circulation test facility (NCTF). The schematic, the model-to-prototype scaling ratio, and the major dimensions of a single loop of the test facility are as mentioned in Chapter 3.

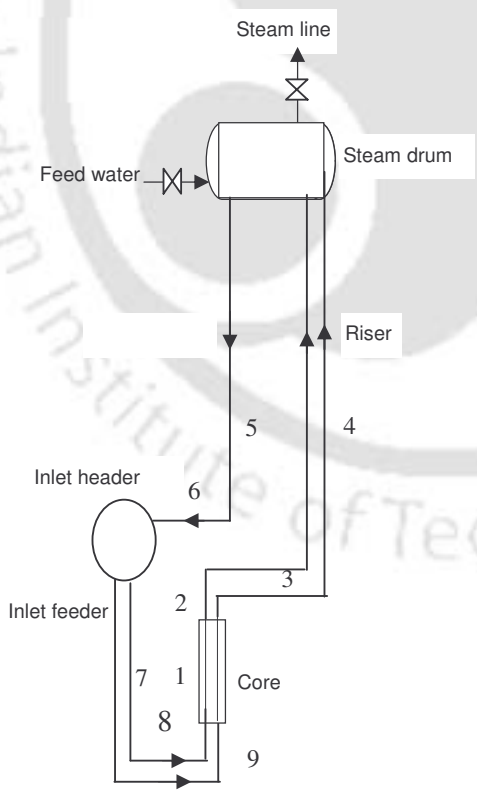

Link No.	*Single channel flow area (m^2)*	*Length (m)*	*Change in elevation (m)*
1	0.00485	3.5	3.5
2	0.00325	3.8	3.8
3	0.00325	23.6	0.0
4	0.0017	25.5	25.5
5	0.00231	26.8	-26.8
6	0.00231	6.33	0.0
7	0.00742	10.62	-10.62
8	0.00742	7.11	0.0
9	0.00273	4.89	4.89

Figure 5.1. Schematic and major dimensions of PHT loop.

TH-831_05610306

5.3. Numerical Model

Numerical model for the parallel-channel systems described above is developed with RELAP5. This parallel-channel RELAP5 model is an extension of a single-channel model developed and validated with experimental results (Chapter 3). The details of the RELAP5 nodalization scheme and the simulation procedure followed for predicting the startup transients in a parallel-channel reactor are discussed in this section.

5.3.1. Nodalization scheme for RELAP5 simulation

The PHT loop described in Section 5.2 is nodalized in RELAP5 as shown in Fig. 5.2. The core and the riser sections are modeled as pipe components, each divided into 32 and 36 control volumes for NCBWR, and 8 and 16 control volumes for the test facility, respectively. The choice of nodal size is based on the nodal sensitivity study done for the single-channel model (Section 3.4.2). A simple *separator* model is used for modeling the steam drum, and the downcomer is modeled as a *pipe* component.

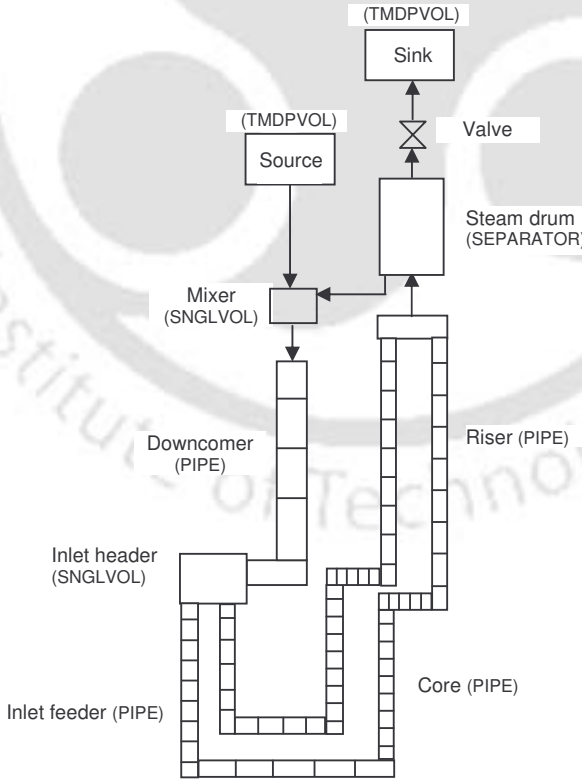

Figure 5.2. RELAP5 nodalization scheme for PHT loop.

TH-831_05610306

In order to facilitate the connection of both the parallel riser pipes to the steam drum, a *branch* component having an area equal to the sum of those riser pipes is used. The lower part of the steam drum is modeled as a mixer using a *single volume* component. A *trip valve* is used for modeling the steam control valve. A *time dependent junction* between the source and the mixer facilitates the control of feed water supply, which is equal to the mass flow rate of steam exit from the drum to sink. The heater elements are modeled as *heat structure*. The length of each axial heat structure node is consistent with the length of the hydrodynamic component. To account for the effect of thermal capacitance, heat structures are applied for all the components of the loop.

5.4. Results and Discussion

The existence of in-phase and out-of-phase flashing instabilities during the startup of parallel-channel systems were investigated. Simulations were carried out under equal and unequal initial flow and power boundary conditions between the channels. The behavior of flow oscillations for different values of flow resistance between the two channels is studied. The nature of flow transients under double channel power input conditions are investigated. Cases with equal and unequal power boundary conditions between channels are studied as discussed in this section.

5.4.1. Single-channel power input

Startup simulation, under single channel power input conditions for test facility is carried out using a constant power boundary condition (2% and 5% of full power). The initial conditions of the loop and prototype being set as mentioned in Section 3.2. The system parameters under single channel power input conditions for the test facility is shown in Fig. 5.3.

Fig. 5.3a shows the mass flow rate measured at the inlet of channels and downcomer exit, when 2% of full power is applied to channel-1. From the heated channel (Channel-1) mass flow rate, it is observed that the flow oscillates with pulses large amplitude,

TH-831_05610306

and in the other unheated channel (Channel-2), it is found to be in the opposite direction with Channel-1. In the downcomer, the oscillations are corresponding to the flow fluctuations in Channel-1 and the flow rate is the summation of Channel-1 and Channel-2. From Fig 5.3b, it is observed that the flow oscillates with both small and large amplitude pulses, when 5% of full power is applied to Channel-1. It can be inferred (Fig 5.3a) that at very low power conditions in a parallel-channel system, the small amplitude oscillations, which are due to boiling in the heater section are absent, and the flow oscillated only due to flashing. This is due to the flow reversal in the unheated channel (Channel-2), which causes more subcooled fluid to flow in to the heater section of channel-1 through the common inlet header, and thus does not allows boiling to happen in the heater section.

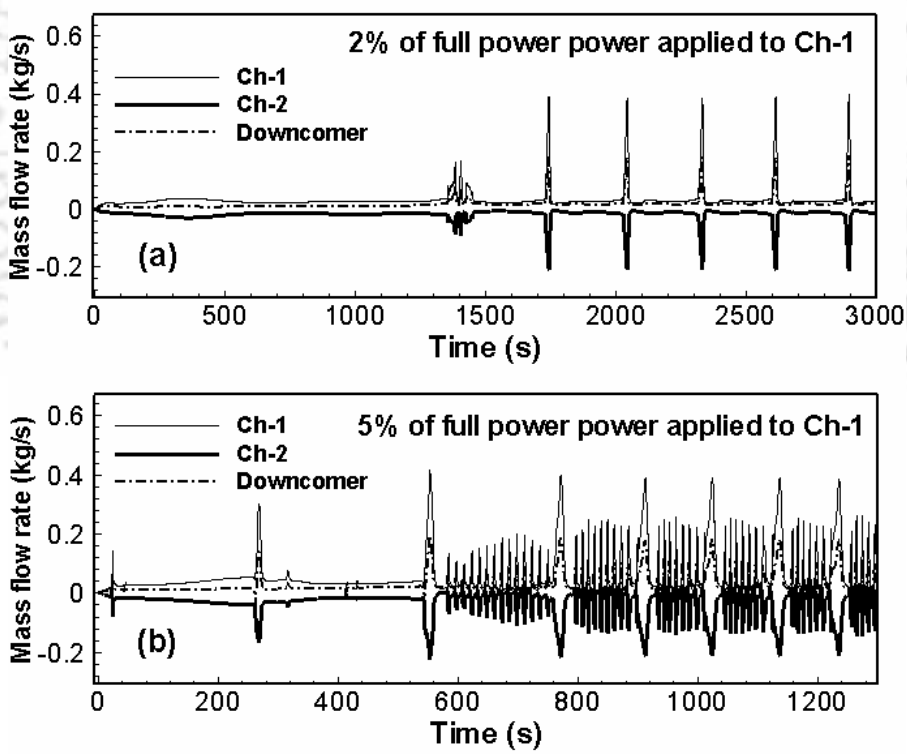

Figure 5.3. Prediction for single channel power input in test facility

TH-831_05610306

5.4.2. Double-channel power input

The nature of flow transients under double-channel power input conditions are investigated. Cases with equal and unequal power boundary conditions between channels are studied, as discussed in this section.

Channels with equal power:

Simulations were carried out using a constant power (5% of full power) with the initial conditions set at 80ºC. Figure 5.4 shows the flow behavior during startup simulations of both model and prototype under equal power boundary conditions. In model, the flow is characterized by pulses which are out-of-phase between Channel-1 and Channel-2, and flow reversal is predicted in both the channels with equal magnitude (Fig. 5.4a). It can be inferred that the flow in both the channels is in-phase, until it reaches the peak of the first pulse and from there on develops a phase difference. Earlier, the persistence of out-of-phase oscillations even under equal power condition between channels was reported through experimental studies by Subki et al. (2003) and Chen et al. (1999). Similar observation is reported by Jain et al. (2009) in their experiments conducted in a natural circulation parallel-channel model, and also characterized such oscillations as mixed mode oscillation. Figure 5.4b shows that the flow in NCBWR is characterized by flashing pulses which are in-phase between Channel-1 and Channel-2, with no flow reversal. Hence, there is a difference between the nature of flow oscillations predicted in model and prototype, in the context of in-phase and out-of-phase behaviour. In general, the major cause for the different nature of startup oscillations in the model and prototype can be attributed to the reduced height of the test facility considered. Hence, the choice of major scaling parameters (height, pressure, etc) for a natural circulation system is likely to be complex, especially when the facility has to simulate the exact transient phenomenon occurring right from startup to operating conditions.

TH-831_05610306

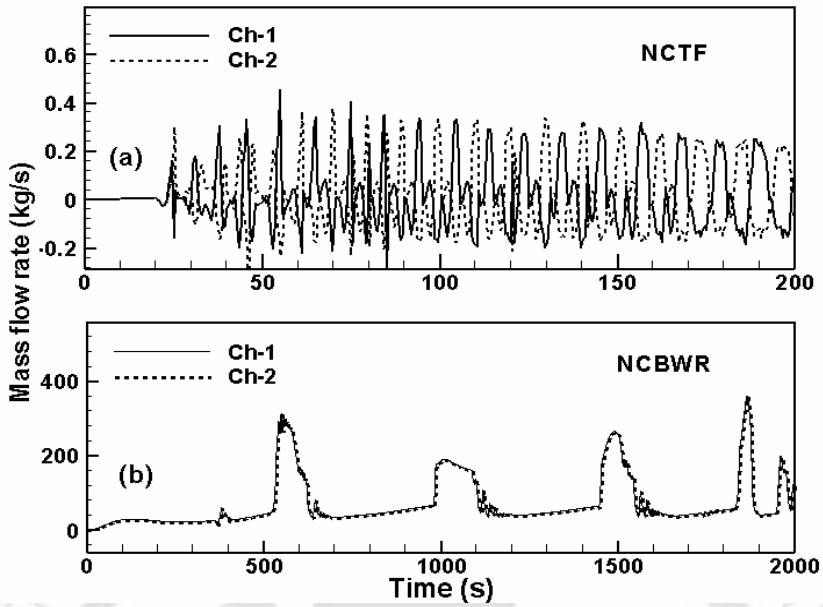

Figure 5.4. Prediction for double channel power input with equal power

Channels with unequal power:

Simulations were carried out for a power difference of 10% and 50% between channels. The observations made under such different power boundary conditions in model and NCBWR are presented in this section.

Figure 5.5 shows the flow behavior, predicted when Channel-1 of model is supplied with 4 kW and channel-2 with 3.6 kW, i.e. 10% power difference between channels. The flow oscillations in the channels are found to be in out-of-phase, with the flow pulses in Channel-2 lagging behind. Figure 5.6 shows the flow behavior, predicted when Channel-1 of the model is supplied with 4 kW and channel-2 with 2 kW, i.e. 50% power difference. Although the usual trend of out-of-phase behaviour is predicted during the initial flow oscillations, it should be noted that, after the occurrence of first flashing pulse (at 225 s) in channel-1, the flow in channel-2 gets reversed and remains to flow in the negative direction for a longer period (until 1500 s). This is due to the fact that the rate of increase in temperature of liquid in channel-2 is comparatively low, causing a delay in vapor generation. In addition to that, the liquid in channel-2 is not allowed to gain enough heat for vapor generation as there is flow reversal caused by the oscillations in channel-1.

TH-831_05610306

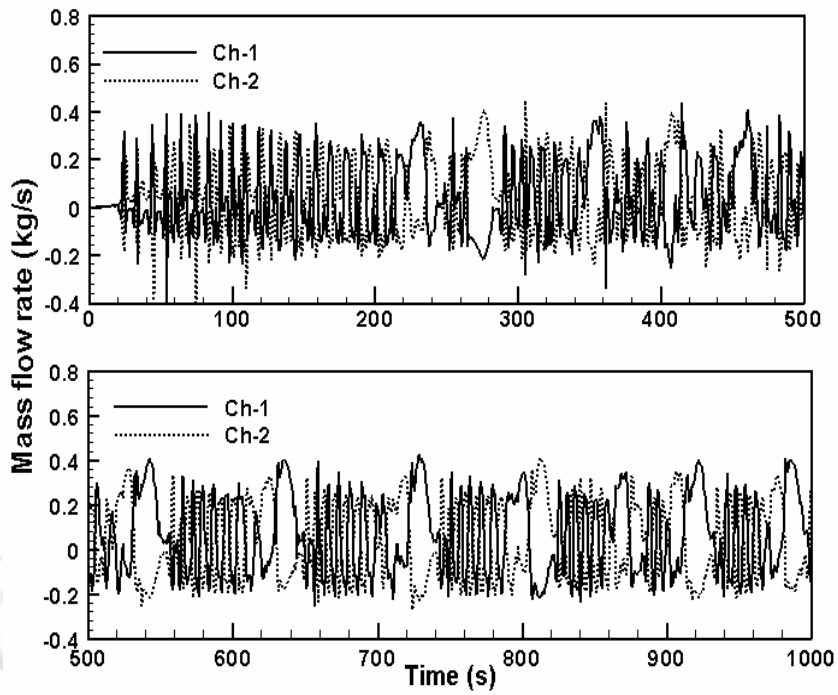

Figure 5.5. Core inlet flow rate for 10% power difference between channels in NCTF

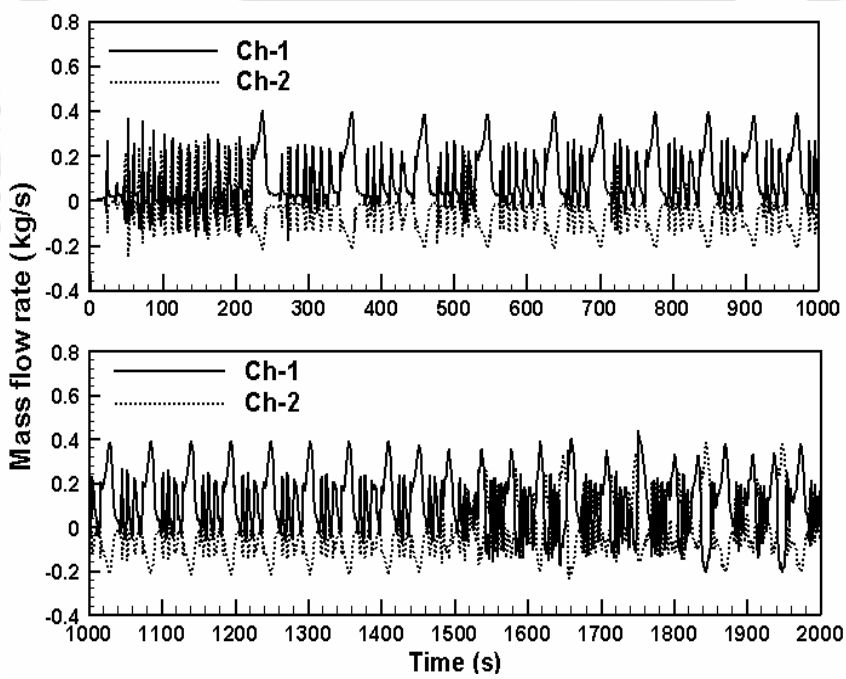

Figure 5.6. Core inlet flow rate for 50% power difference between channels in NCTF

TH-831_05610306

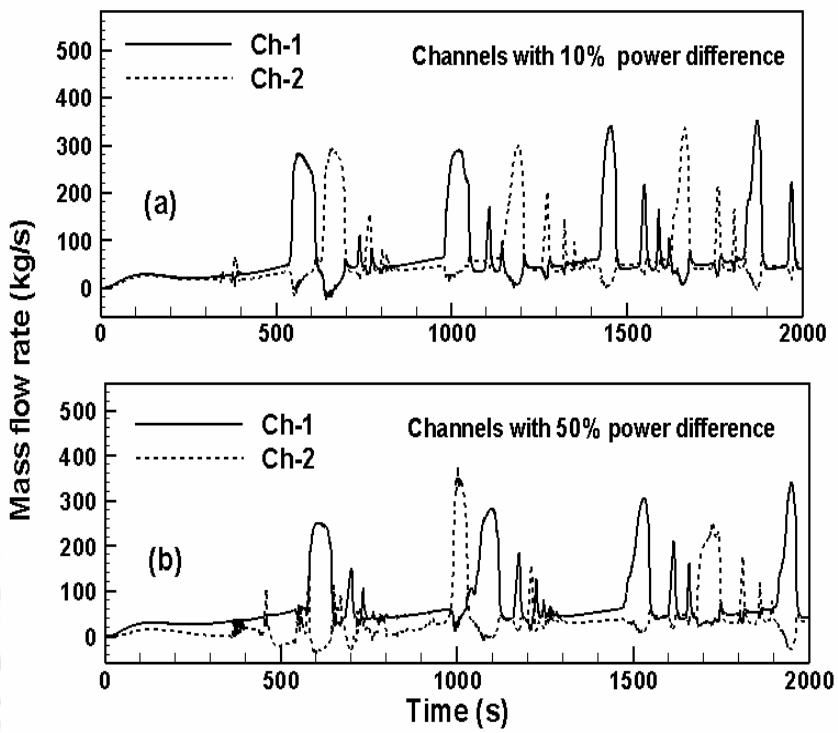

Figure 5.7. Core inlet flow rate for 10% and 50% power difference between channels in NCBWR

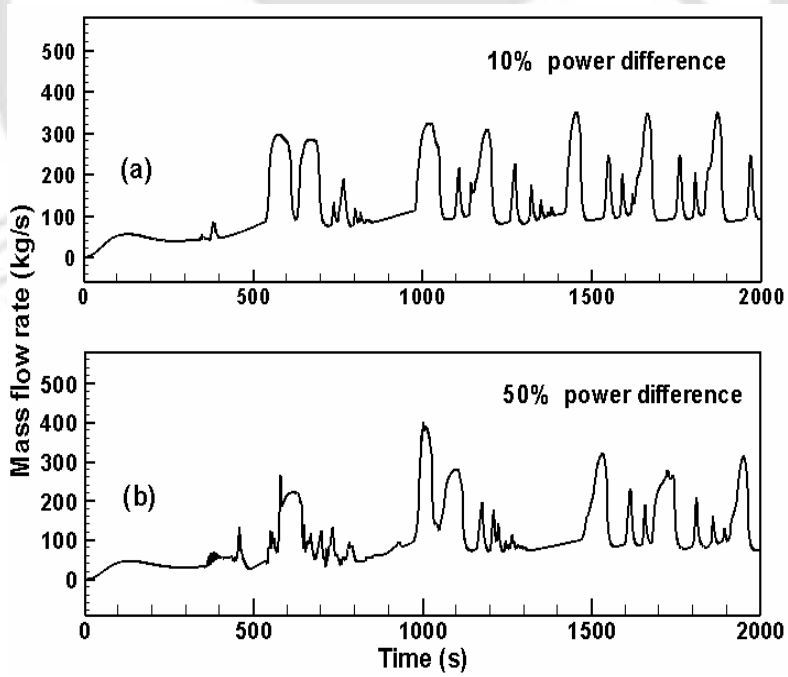

Figure 5.8. Downcomer flow rate for 10% and 50% power difference between channels in NCBWR

TH-831_05610306

Figure 5.7 shows the flow behavior predicted in NCBWR, when Channel-1 is supplied with 10% and 50% power difference between channels. Under 10% power difference (Fig. 5.7a), the flow oscillation in Channel-2 is out-of-phase with Channel-1, however, the trend of the flashing pulses in both the channels are identical. In case of 50% power difference, the flow oscillation in Channel-2 is out-of-phase with Channel-1, with the first flashing pulse lagging behind approximately 400s and the lag continues to increase with time for subsequent peaks. The trend of the flashing pulses in both channels is not identical either (Fig. 5.7b). Channel-2 experiences flow in reverse direction even at a stable flow condition during the initial stage of startup. This is due to lack of vapor generation owing to a relatively very low power supplied to channel-2. In common, both the cases (10% and 50% difference) show intermittent flow reversal, which is not observed under equal power condition. Flow reversal in this context refers to change in flow direction in one channel when there is a sudden surge in flow in the other channel due to flashing. The flow oscillations in the downcomer section are as shown in Fig. 5.8. Due to out-of-phase character of the flashing pulses in the channels, the number of flow pulses in the downcomer is doubled when compared to equal power condition where the flow is in-phase.

5.4.3. Effect of loss coefficients

In the present study, the effect of flow resistance on Type-I oscillation is explored by starting the system with the two channels having different flow restrictions, introduced at core inlet, core exit/riser inlet, and riser exit of the channels. For the simulation, the flow resistance is increased in only one channel (channel-1), leaving the other channel with normal loss coefficient values. The effect of flow resistance and the effect due to unequal resistances in the channels are presented in Figure 5.9 (NCTF) and Figure 5.10 (NCBWR).

The flow instability observed in the model is a result of void generation in both core and riser sections, as reported earlier (Section 4.2.1). It was found that the instability caused by core void generation is signified by low-amplitude high-frequency oscillations, and the riser void generation (flashing) results in high-amplitude low-frequency oscillation. Hence, flow resistance applied at different sections would have a

TH-831_05610306

corresponding effect on the instability arising from the respective section of the channel. Figure 5.9a shows the effect of inlet resistance on the flow in channel-1. It can be seen that the amplitude of channel-1 oscillation is reduced comparatively and the effect is only on the low-amplitude high-frequency oscillations as it is a core phenomenon. Additional flow resistance at the core exit is found to have a destabilizing effect on the system resulting in an increase in amplitude of oscillations in channel-1 (Fig. 5.9b). It is known from literature that, in general, inlet resistance has a stabilizing effect and outlet resistance destabilizes the system. In case of riser exit resistance, it is expected to destabilize the system by influencing the flashing instability which is a riser phenomenon. This effect can be seen in Fig. 5.9c, as there is repeated appearance of high amplitude flashing pulse in channel-1 due to the additional resistance to flow at the riser exit.

In the NCBWR simulations, it is relatively straightforward to analyze the effect of loss coefficients, as the instability is only due to flashing in the riser and there is no core void generation. It is inferred from Fig. 5.10a that the amplitude of flow oscillations in channel-1 is considerably reduced compared to channel-2, due to the presence of additional loss coefficient at channel-1 core inlet. When the loss coefficient is in place at the riser inlet (Fig. 5.10b), there is a similar effect on the amplitude of oscillations and only differs in the context of time lag between flashing pulse. In general perception, the riser inlet resistance can be taken as core exit resistance which has a destabilizing effect on the system. However, in this case, vapor generation (flashing) is predicted only in the riser section and hence the resistance at the core outlet acts as an inlet resistance to riser section, resulting in reduction of the amplitude of flow oscillation. In case of an increased resistance at the exit of the riser, there is no significant difference in the amplitude of the pulses but, the trend of phase lag i.e. flashing in channel-2 precede channel-1 (Fig. 5.10c) unlike the effect seen under core inlet and riser inlet restriction. Thus, the presence of additional loss coefficient in one channel results in out-of-phase flow oscillation in a parallel-channel NCBWR.

TH-831_05610306

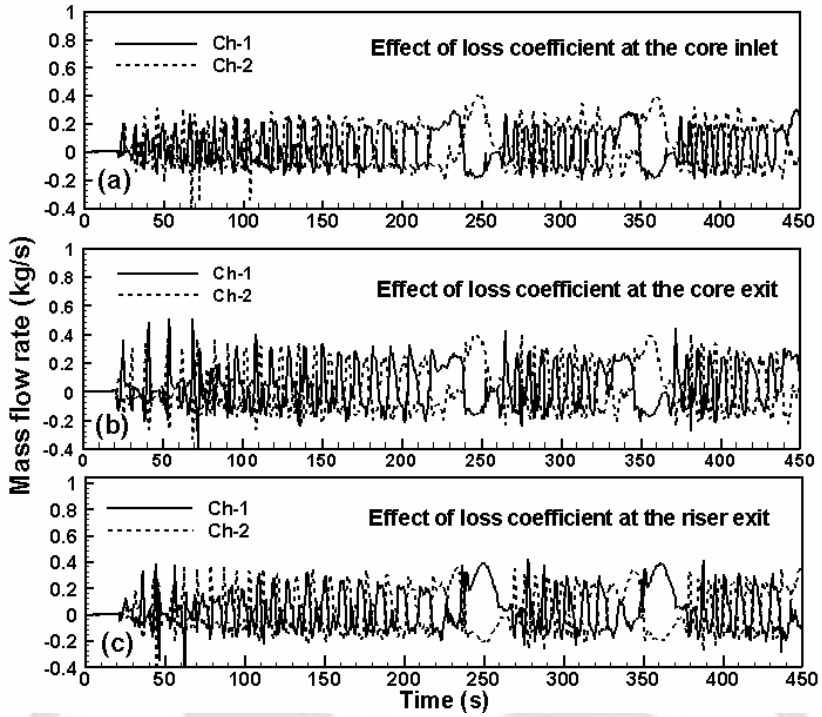

Figure 5.9. Effect of loss coefficient on startup oscillations in double-channel model

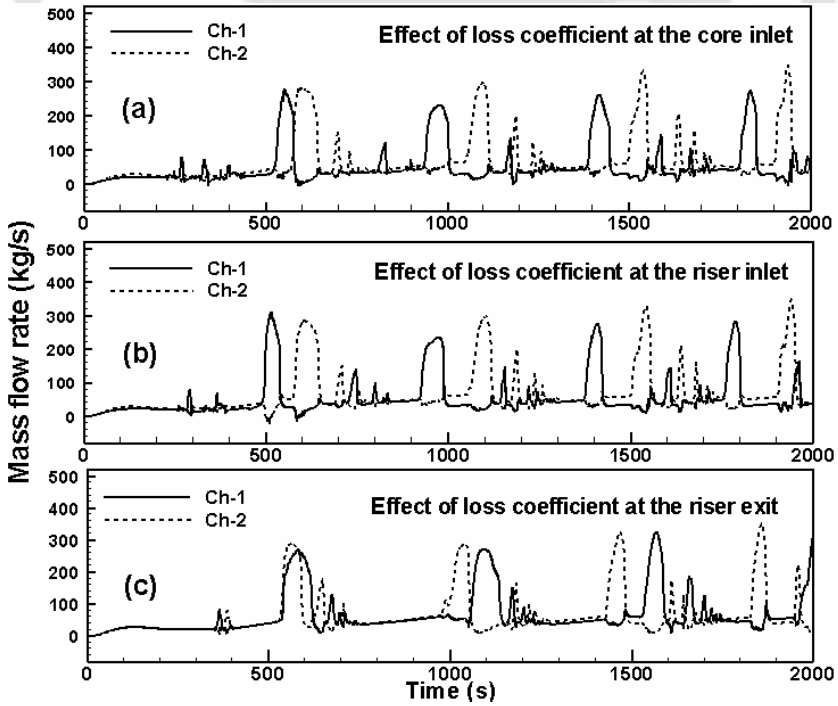

Figure 5.10. Effect of loss coefficient on startup oscillations in double-channel

NCBWR

TH-831_05610306

5.5. Summary and Conclusions

Numerical models of parallel-channel pressure tube type natural circulation boiling water systems have been developed using RELAP5/MOD3.4. Simulations have been done to predict the startup flow transients in parallel-channel systems with difference in power and flow restriction between channels.

- For identical startup conditions in channels, it is inferred that the nature of flow oscillation predicted in scaled model and the prototype is not similar, in the context of in-phase and out-of-phase behaviour. In the prototype model, the flow behavior in both the channels is characterized by flashing pulses which are in-phase. Whereas in the scaled model, even for identical conditions, there exists a phase difference between flow oscillations in channels.
- Under non-identical conditions in channels, the simulations for both model and the prototype show similar trend, i.e. the flow oscillations in the channels are out-of-phase.
- In condition like difference in channel power, flow reversal is predicted in one channel when there is a sudden surge in flow due to flashing in the other channel.
- The amplitude of flow oscillations are considerably reduced due to the presence of additional loss coefficient at the core and riser inlet. Presence of additional loss coefficient in one channel results in out-of-phase flow oscillation in a parallel-channel NCBWR.

In-phase oscillations would lead to high amplitude flow pluses in the downcomer as the flow in the downcomer is the sum of the flow in the parallel channels, and the time period would be equal to that of a flashing pulse. In case of out-of-phase oscillation the frequency of downcomer flow oscillations will be higher but the amplitude will be lower. It would be desirable to investigate the effect of in-phase and out-of-phase oscillations on flow-induced vibrations and material fatigue.

TH-831_05610306

TH-831_05610306

Chapter 6

Power Ramping Procedure for NCBWR

6.1. Introduction

As mentioned in Section 2.4, a normal power ramping (startup) procedure can be divided into four distinct phases: Phase I - Single-phase core heat up, Phase II - Net vapor generation in core, Phase III - Saturated chimney, and Phase IV - Power ascension to full power. The nature of transition through Phase II and Phase III is important, where the instabilities like geysering (in Phase II) and flashing (in Phase III) are highly dominant. In dealing with Phase II and Phase III, an initial pressure above 20 bar is found to be critical, and different methodologies can be adopted in raising the system pressure to the desired level. From the very few proposed startup procedures reported in literature (Section 2.4), it appears that the methods suggested for initial pressurization needs a major auxiliary system or modifications in design. A procedure by creating a steam cushion in the system and allowing flashing to occur only above the riser exit with no void generation in the core or riser sections was proposed (Manera, 2003). However, the procedure was developed for the startup of a vessel type NCBWR, and it would be very difficult to avoid flashing in the riser tubes of a pressure tube type NCBWR having a long riser (about 25 m). For such a system, a different method of startup is to be conceptualized and analyzed. A suitable heat-up rate is an important part of a power ramping procedure. Rohatgi et al. (1997) have done studies on a wide range of reactor heat-up rates, and suggested a suitable scheme for the SBWR design. It was also demonstrated that, a heat-up scheme with coupled void fraction distribution and power could destabilize the transients during startup, and the flow oscillations are amplified by inclusion of void-reactivity feedback (Kuran, 2006).

The objective here is to identify a suitable heat-up rate, focusing on a minimal void generation in the core region and faster reactor pressurization, and also to examine the

TH-831_05610306

feasibility of a complete single-phase startup (Section 6.3). In Section 6.4, a startup procedure is conceptualized and proposed whereby the unstable two-phase region is completely avoided. The method to take the system to the operating condition without encountering flow oscillations is numerically simulated.

6.2. Numerical Experiments on Reactor Heat-up Rate

The verified RELAP5 model of a single-channel NCBWR (Chapter 3) is used for the simulation of startup. Before startup, the steam dome pressure is kept at a very low-pressure (55 kPa) and the coolant in the entire loop is kept at an initial temperature of 80ºC (which is the saturation temperature at 55 kPa). The steam control valve remains closed during the single-phase natural circulation, keeping no contact between the system and the sink. Simulations are done for different heat-up rate, using the same initial conditions. The mass flow rate, pressure, and temperature reported in the subsequent sections shall be presumed as predicted at the inlet of the core, if not otherwise mentioned.

6.2.1. An initial startup test

The first startup test is carried out using a constant power of 2 MW with the initial conditions of the reactor being set as mentioned above. Fig. 6.1 shows the temporal traces of the system parameters observed during the startup test using RELAP5. It is observed that the system experiences an increase in pressure and coolant temperature. The flow in the reactor is in a single-phase natural circulation mode as there is void generation neither in the core nor in the riser until 10000 s. Later, void pulses (due to flashing) starts to appear at the exit of the riser section when the temperature of liquid reaches it local saturation temperature due to the strong variation in hydrostatic head along the tall vertical riser (25 m). As a result, the system flow sets up to an oscillatory mode. It is inferred that, the reactor moves from a stable single phase region (<10000s) to an unstable two-phase region, and stays for a very longer period in an unstable state, even up to 50000 s, without entering into the stable two-phase region. Hence, the ways and means for crossing the unstable two-phase region in a shorter duration has to be looked at.

TH-831_05610306

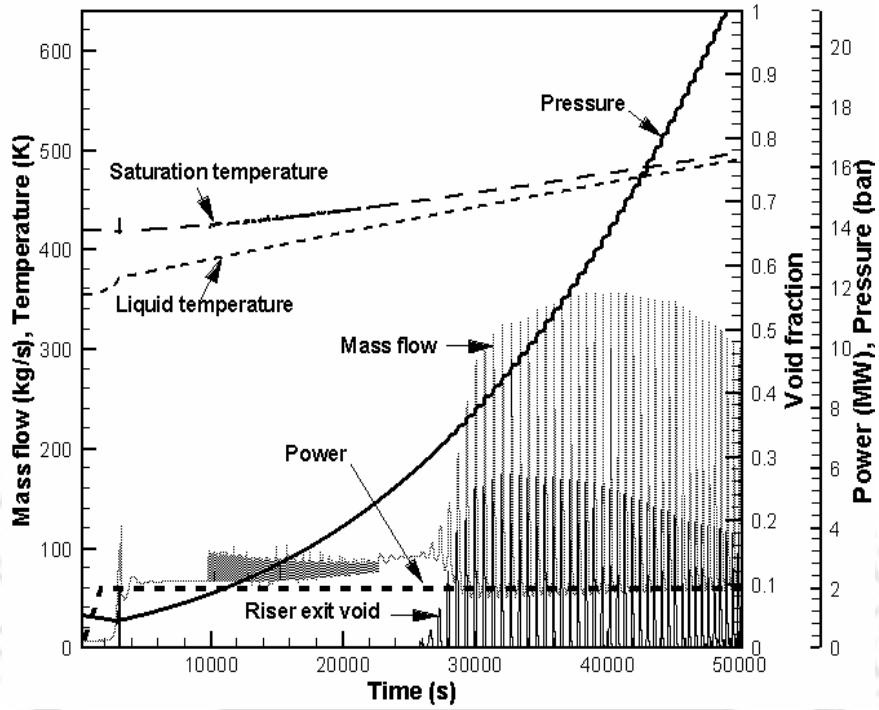

Figure 6.1. System parameters during startup with constant 2 MW power input.

6.2.2. Simulations for various heat-up rates

The flow oscillations seen in Fig. 6.1 are a result of flashing instabilities in the riser section which is strongly dependent on the system pressure and it is a general consensus that they disappear at higher pressure (20 to 25 bar). To help suppress these oscillations, an increased rate of pressurization is essential which implies an increase in steam generation rate and that in-turn is dependent on reactor heat-up rate. To decide on the heat-up rate, a number of numerical experiments were carried out, focusing on a minimal void generation in the core region and faster reactor pressurization. The issue of void generation in the core assumes importance, as the coolant flow rate is very low during the initial stages of startup especially during the oscillatory mode and may entertain CHF related problems at low-pressure conditions in a vertically heated core.

Numerical experiments with various heat-up rate are grouped into three different schemes namely Case-1, Case-2 and Case-3 as show in Fig. 6.2. Each reactor heat-up

TH-831_05610306

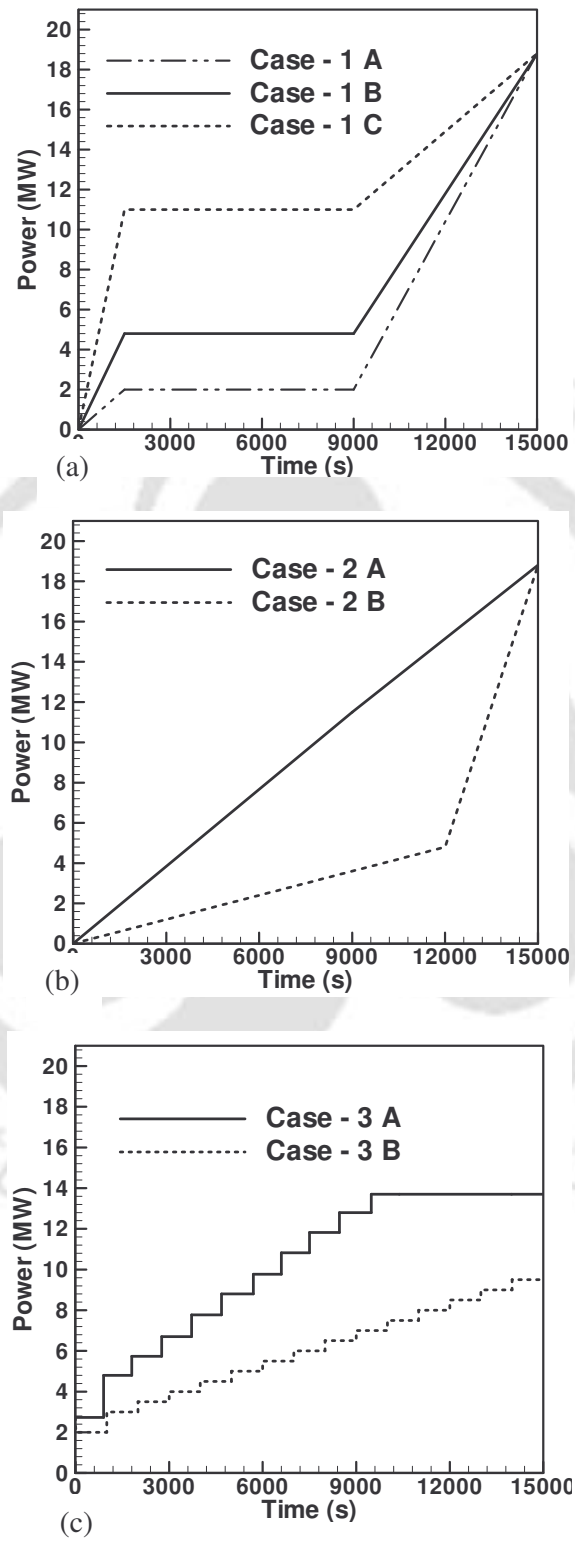

Figure 6.2. Heat-up rate for the startup of NCBWR.

TH-831_05610306

schemes (1A, 1B and 1C) under Case-1 consist of an initial linear ramp followed by a constant power input for the most part and then a linear increase. Power input through Case-2A and 2B are of linear increasing nature. In both Case-1 and Case-2, it is intended to reach 8% of full power (230 MW) in 15000 s (4 hr 10 min). For startup simulations under Case-3, power input is applied in steps where 1 MW per step is applied in Case-3A and 0.5 MW per step in Case-3B. The effect of axial peaking factor is also taken into account. It is found that there is no significant effect due to the different power profiles (top, mid and bottom peaked), as the oscillations are not core phenomena and are rather caused by void flashing in the adiabatic riser section. Hence, a flat power profile is adopted for the startup simulations.

Startup simulation – Case 1:

Case-1 consists of three different heat-up schemes as shown in Fig. 6.2a. The temporal traces of system parameters during startup under Case-1A are shown in Fig. 6.3. It is observed that only after 9000 s there is notable increase in temperature and pressure of the reactor. Later the flow stets up to an oscillating mode and pressurization rate increase as steam is produced due to flashing. A steep surge in power results in generation of high amplitude void pulses in the core region (13000s) under oscillating flow condition and at pressure as low as 4 bar. The reactor enters the stable two-phase region at around 4.5 hrs of operation.

During the startup test under Case-1B, the two-phase oscillating condition starts at 2000 s and remains up to 14000 s until the system enters into a stable two-phase region (Fig. 6.4). The oscillations seen in Fig. 6.4 are mainly due to flashing in the riser section, and void generation in the core starts only when the flow has shifted to a higher level and at around 7 bar pressure. The period of each flashing oscillation is comparatively larger than that observed during the startup test under Case-1A.

TH-831_05610306

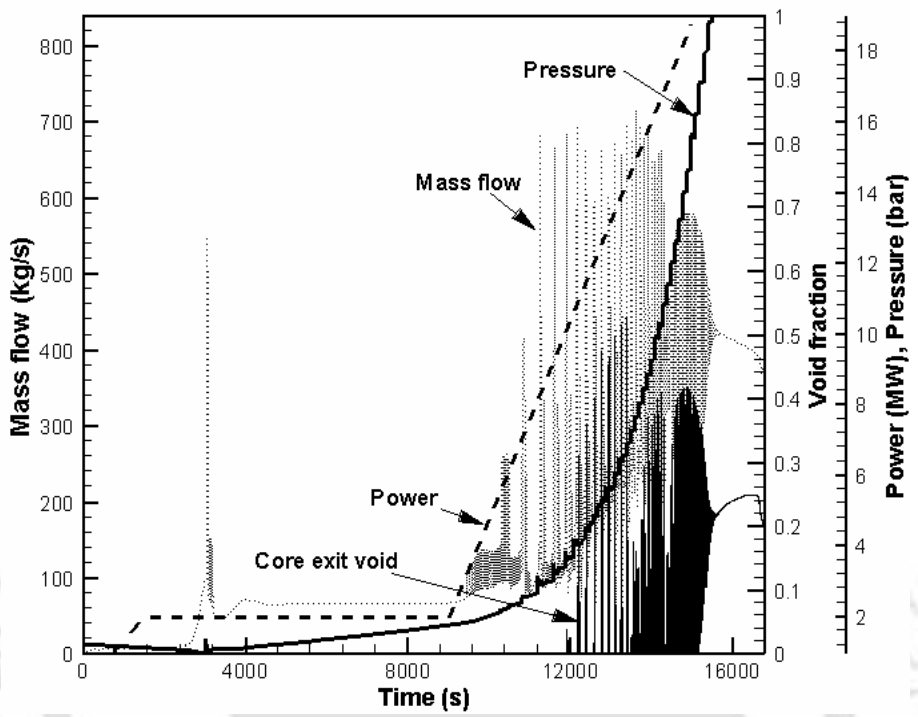

Figure 6.3. System parameters during startup (Case-1A).

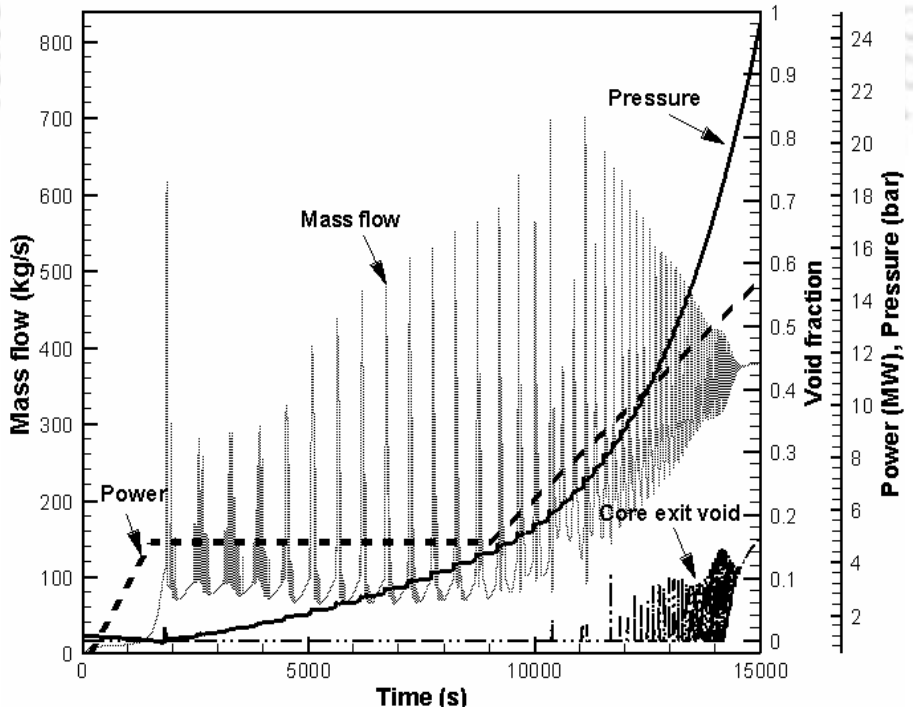

Figure 6.4. System parameters during startup (Case-1B).

TH-831_05610306

In Case-1C, the constant power applied is 5% (11.5 MW) of full power, which is higher than in Case-1B (2 %). The system is found to cross the unstable two-phase region in a much shorter duration as can be seen in Fig. 6.5. However, even during the constant heat-up phase, high amplitude void pulses are observed and are undesirable as the reactor is still in a low-pressure oscillating flow condition. The flashing induced instabilities are found to occur at higher frequency when compared with Case-1B. At higher power level, the average flow will be comparatively high, leading to faster propagation of enthalpy perturbation resulting in a shorter duration of oscillation and higher frequency of occurrence. The fact that these flashing induced instabilities are suppressed at a rector pressure around 20 bar can also be inferred from the startup test under Case-1B and 1C (Figs. 6.4 and 6.5).

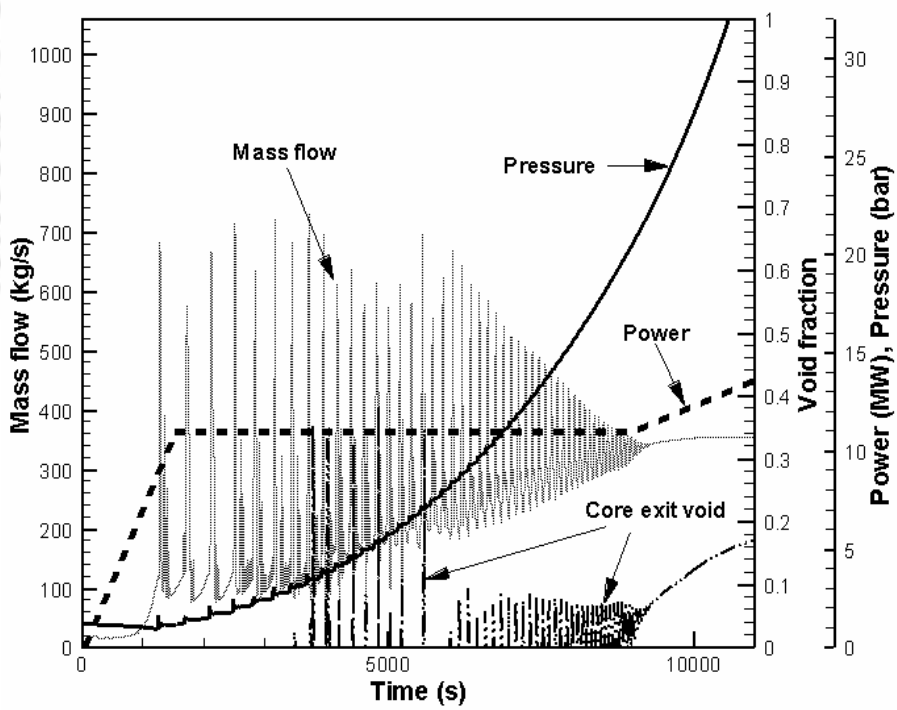

Figure 6.5. System parameters during startup (Case-1C).

TH-831_05610306

Startup simulation – Case 2:

The power ramps in Case-2 consist of linear heat-up rate as shown in Fig. 6.2b. During the startup test under Case-2A, the pressurization is considerably fast and the system enters the stable two-phase condition at approximately 12000 s. The value of maximum void fraction at the exit of the core ranges from 0.15 to 0.2 except for a few peaks of void fraction having a maximum value of 0.5 as shown in Fig. 6.6. When the scheme Case-2B is used as power boundary condition, the value of void peaks found in the core section is greater than 0.45 at a very low flow and pressure level (Fig. 6.7). Since the rate of pressurization was very slow during the initial stage, the system is not able to cross the two- phase oscillating region in a considerable time. Under the Case-2 power boundary condition, the system is found to generate more void in the core section especially in Case-2B.

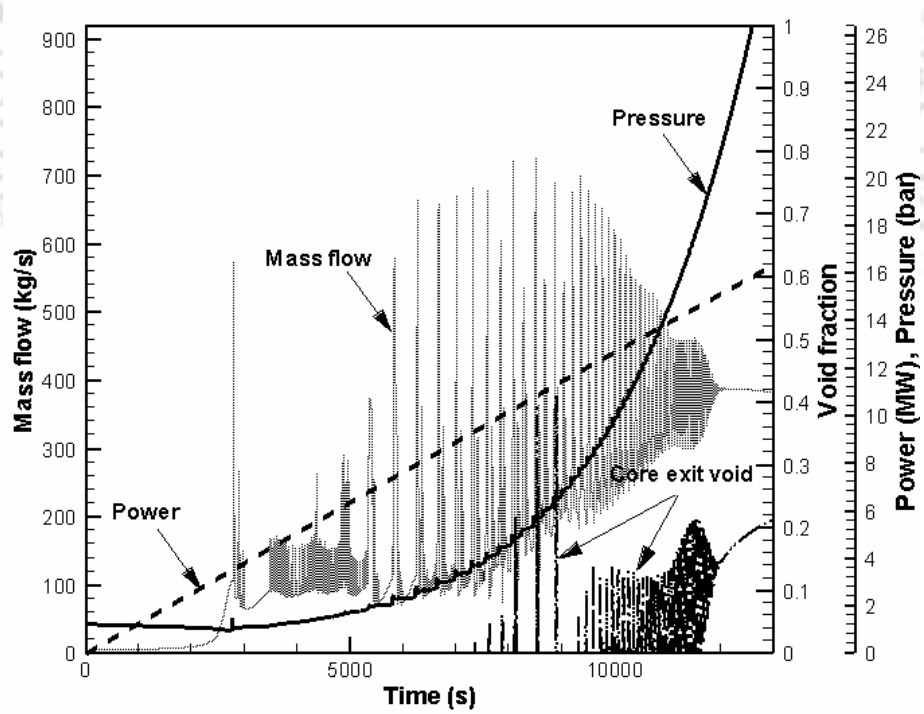

Figure 6.6. System parameters during startup (Case-2A).

TH-831_05610306

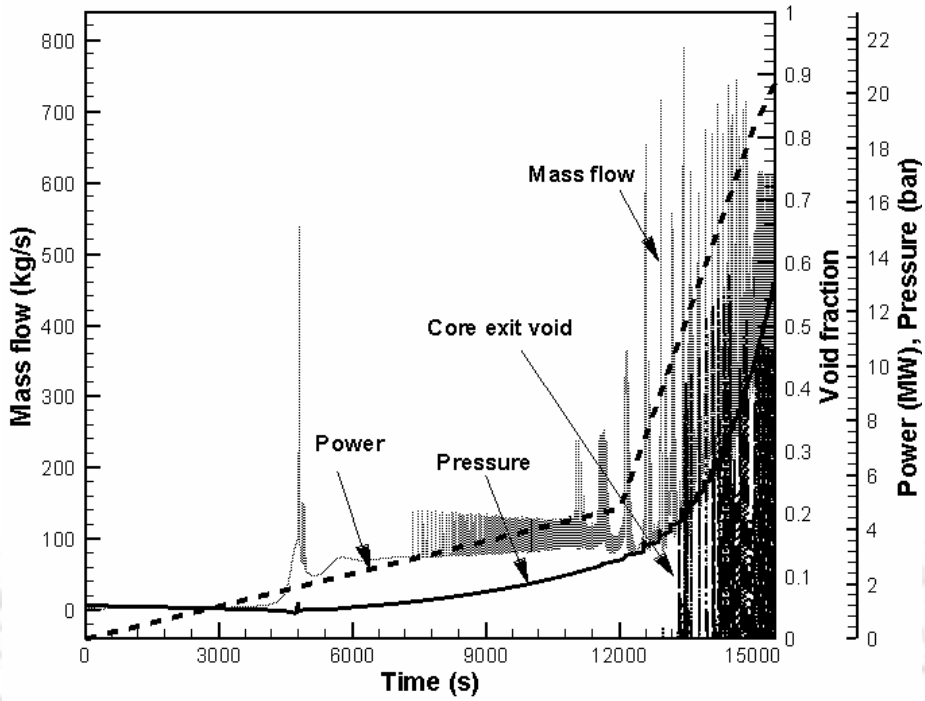

Figure 6.7. System parameters during startup (Case-2B).

Startup simulation – Case 3:

In a third Case, a series of step inputs (Fig. 6.2c) of power is used for the startup of the reactor. In Case-3A, 1 MW is applied at every step input and the reactor is found to enter the unstable two-phase region at 1500 s and step into the stable two-phase region at around 10000 s as shown in Fig. 6.8. As the temperature of the coolant is fast approaching its saturation temperature at core inlet, void peaks starts to appear in the core exit at 6000 s and this is even when the flow in the loop is at a very low level. The void peaks are found to be intermittent, although it cannot be attributed to the step increase in power. In another case (3B), where only 0.5 MW is applied at ever step inputs, the void generation in the core region in found to be very minimum as shown in Fig. 6.9. The system is expected to enter in to the stable two-phase region at around little later than 15000 s. From both Figs. 6.8 and 6.9, it is observed that the flashing induced instabilities are suppressed at 20 bar pressure.

TH-831_05610306

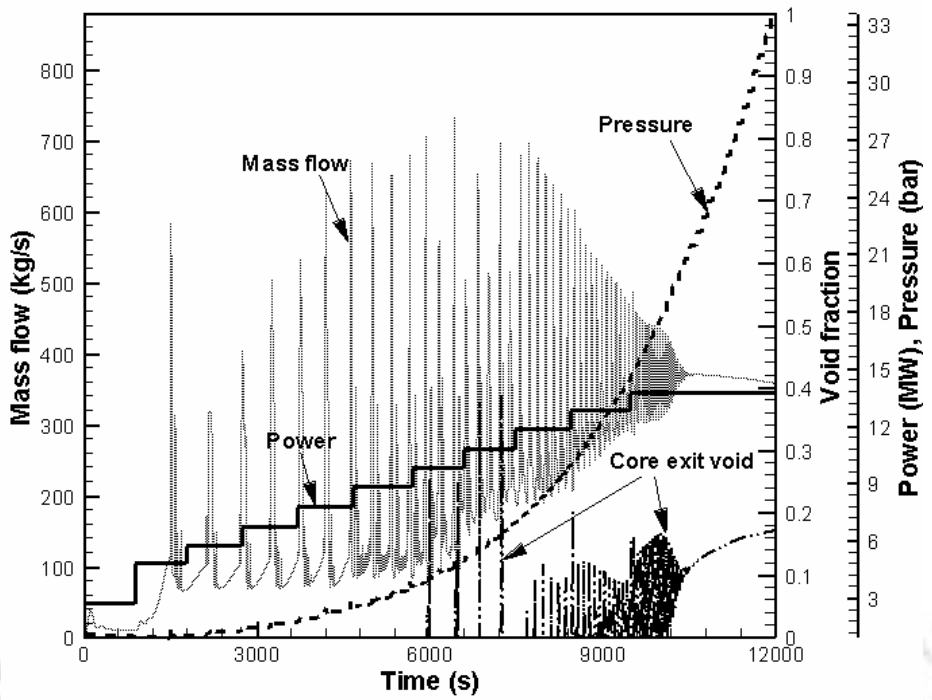

Figure 6.8. System parameters during startup (Case-3A).

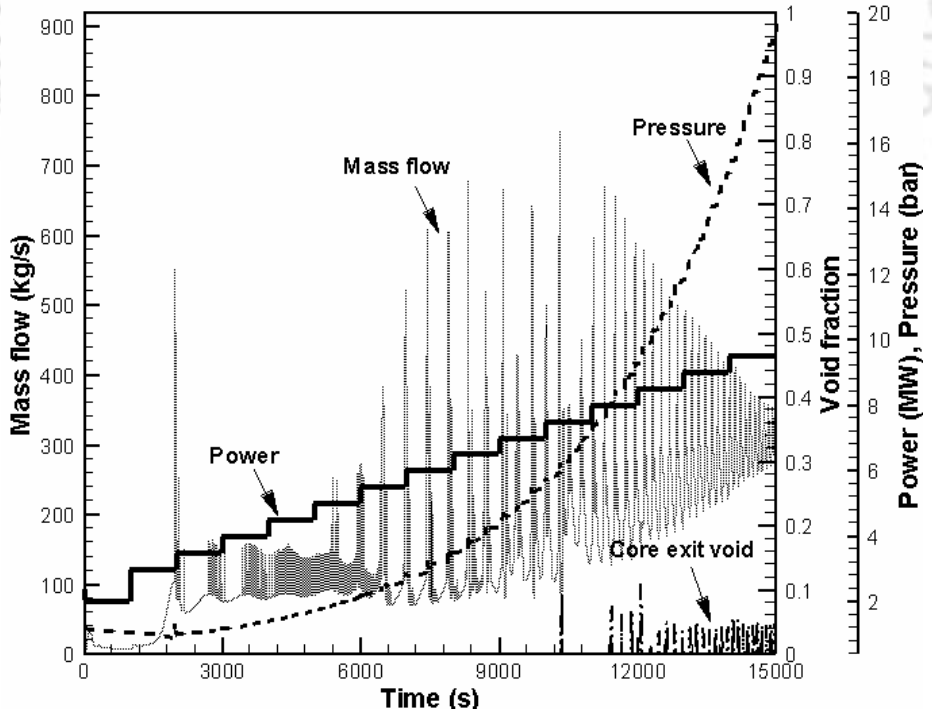

Figure 6.9. System parameters during startup (Case-3B).

TH-831_05610306

From the numerical studies, two suitable heat-up schemes, namely Case-1B and Case-3B can be chosen for the startup of the NCBWR. This is by the criterion of low core void generation and a reasonably fast rate of pressurization. The intensity of flow oscillation under these cases is also relatively less. The time period between two flashing oscillations in Case-1B and Case-3B is found to be approximately 7.5 min and 9 min respectively.

6.3. Startup of NCBWR under Single-Phase Condition

The feasibility of a complete single-phase startup is also to be examined. To maintain the system in a single-phase condition all through the pressurization process, it requires control over the coolant temperature in the PHT loop. As inferred from the startup test discussed in the previous section, the major source of flow instability is the phenomenon of flashing in the riser section. To avoid flashing, it is essential not to allow the coolant to reach its local saturation condition in the tall riser section and hence the subcooling at the core inlet has to be higher than 20 K, especially at low-pressures. In ensuring such a high subcooling, an additional cooling system is required in the form of heat exchanger. In the RELAP5 simulation, the heat exchanger is modeled by employing a heat structure to the lower part of downcomer with the boundary condition corresponding to the cooling water. As there is enough subcooling in the system during the initial stage owing to the coolant initial conditions, the heat exchanger is made active only after 0.5 hrs of operation.

The system parameters observed during the single-phase startup test are shown in Fig. 6.10. It is observed that the flow in the system is steady and there is an increase in system pressure under single-phase heat-up. However, the rate of pressurization is very low resulting in a gain of only 7 bar even after 13 hrs of operation. Hence, taking the reactor to the required pressure level through single-phase pressurization may not be considered due to the time factor and the requirement of an additional heat exchanger (only for the startup) that involve modifications in the design of the PHT and other related components

TH-831_05610306

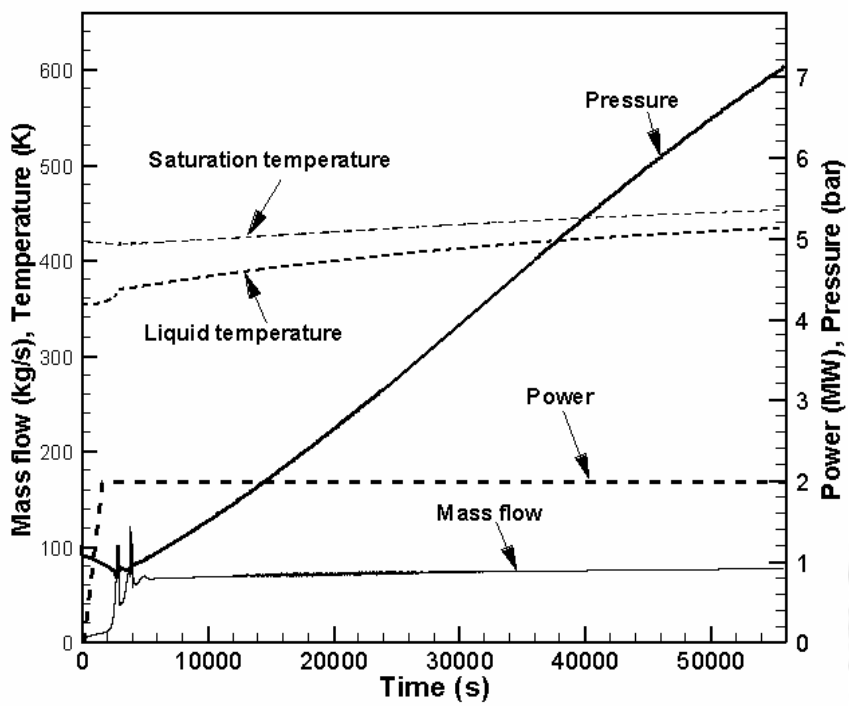

Figure 6.10. System parameters during single-phase startup.

6.4. Conceptualization of a New Startup Procedure

In the previous section it was concluded that, using a suitable heat-up rate, the reactor can be pressurized to the desired operating conditions without considerable void generation in the core, in a reasonable time. Although flashing is prominent and helps in steam production, the amplitude of flow oscillations induced by flashing is the event of concern. These oscillations may result in structural vibration and fatigue of other related components. This is a serious concern especially when there are hundred of parallel-channels involved, as in the case of the pressure tube type NCBWR studied here. Hence it is essential to either quantify the extent of applicability of the heat-up rate involving a two-phase unstable region in parallel-channel model or to devise a startup procedure; thereby the unstable two-phase region can be completely eliminated. In view of the later, a startup procedure is conceptualized and the method to take the system to the operating condition without encountering flow oscillations is numerically examined.

TH-831_05610306

As discussed in the introduction and also observed in the current study, the startup instabilities disappear at a pressure around 20 bar. If the reactor is started from an initial pressure above this condition, the singe-phase system can be directly taken into the stable two-phase region. It is feasible to obtain a higher initial system pressure by having a full drum level and hydro pressurizing through pump up to the desired limit. In a later stage, the drum level can be brought to normal by bleeding the excess coolant through sequential operation of valves. Over pressurization due to thermal expansion of liquid in the initial stage of operation can be estimated (based on material properties), and can be controlled by the activation of relief valves set at lower limits. For example, for a steel container of typical dimensions, the increase in pressure due to thermal expansion of liquid will be around 2 bar per degree raise in temperature of the liquid. The startup procedure conceptualized for the NCBWR is as follows.

1. The PHT loop is completely filled with water and hydro pressured to 20 bar. The initial coolant temperature is kept at 80ºC and the PHT loop is isolated by closing the main steam line valve.
2. The reactor is started with a very low-power of 0.5 MW.
3. As the system pressure raises to 25 bar the first bleeding valve is made active and remain working with an upper and lower pressure limit of 25 and 23 bar respectively. The valve will remain closed once the drum level drops below a prefixed level (level-1). The power input may be raised to a marginal level (2% of full power) at 5000 s.
4. When the system pressure reaches 30 bar, the second bleeding valve is operated until the drum level drops below level-2.
5. It is essential to have a good rate of increase in coolant temperature and hence the power is further increased to 11.5 MW (5% of full power) at 15000 s.
6. The drum level is further brought down by operating the third and fourth bleeding valve in series and all the valves remain closed once normal drum level is achieved.
7. A 5% of full power is maintained until the system pressure reaches the normal operating condition.

TH-831_05610306

6.4.1. RELAP5 simulation procedure

The above mentioned procedure is numerically tested using the RELAP5 model of NCBWR. Few additional RELAP5 components are added to the RELAP5 model discussed in Section 3.4.1. The bleeding valves are modeled as trip valves operated using RELAP5 trip logics which essentially simulate the operation of a relief valve. The trip valves are connected between the lower part of drum (point of bleed) and sink. To facilitate the positioning of bleeding valves and drum level assessment, the steam drum is modeled as a pipe component. The nodalization scheme including the bleeding valves is shown in Fig. 6.11. The other aspects of nodalization scheme are very similar to that as discussed in Section 3.4.1.

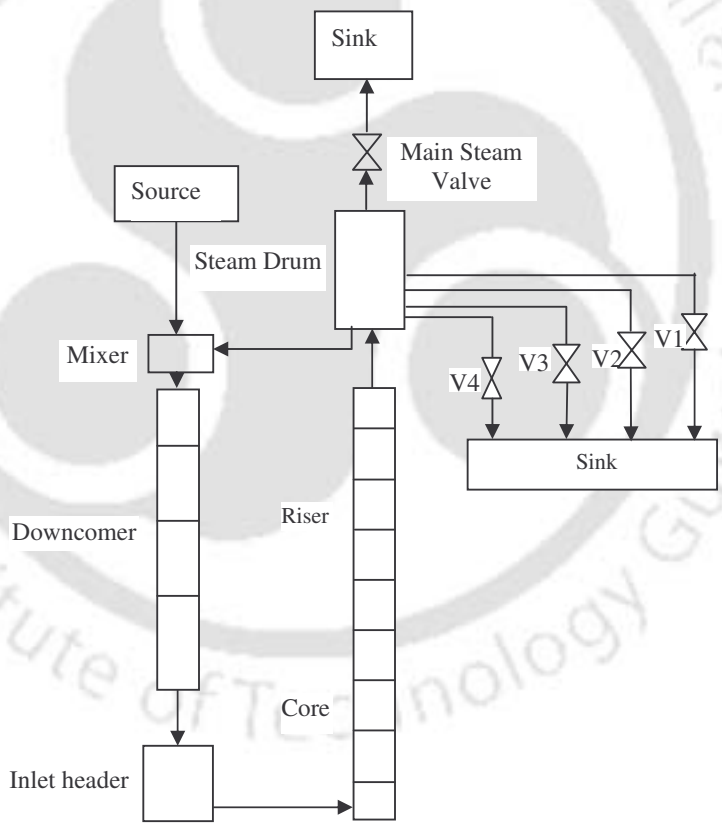

Figure 6.11. RELAP5 nodalization scheme for startup.

TH-831_05610306

6.4.2. Numerical demonstration of startup procedure

The PHT loop is filled with water and the initial pressure and temperature are 20 bar and 80ºC, respectively. The loop is isolated by closing the main steam line valve. The reactor is started with a very low-power of 0.5 MW. As the system pressure rises to 25 bar, the first bleeding valve, having an upper and lower pressure limit of 25 and 23 bar, is made active. The valve will remain closed once the drum level drops below a prefixed level (level-1). The second bleeding valve is operated when the system pressure reaches 30 bar and remains active until the drum level drops below level-2. A normal drum level is achieved by operating the third and fourth bleeding valve in series and there-after all the valves remain closed. To maintain a good rate of increase in coolant temperature, the power input is raised to 4.6 MW (2% of full power) at 5000 s and 5% of full power is maintained from 15000s, till the system pressure reaches the normal operation condition. The temporal traces of the system parameters are shown in Fig. 6.12.

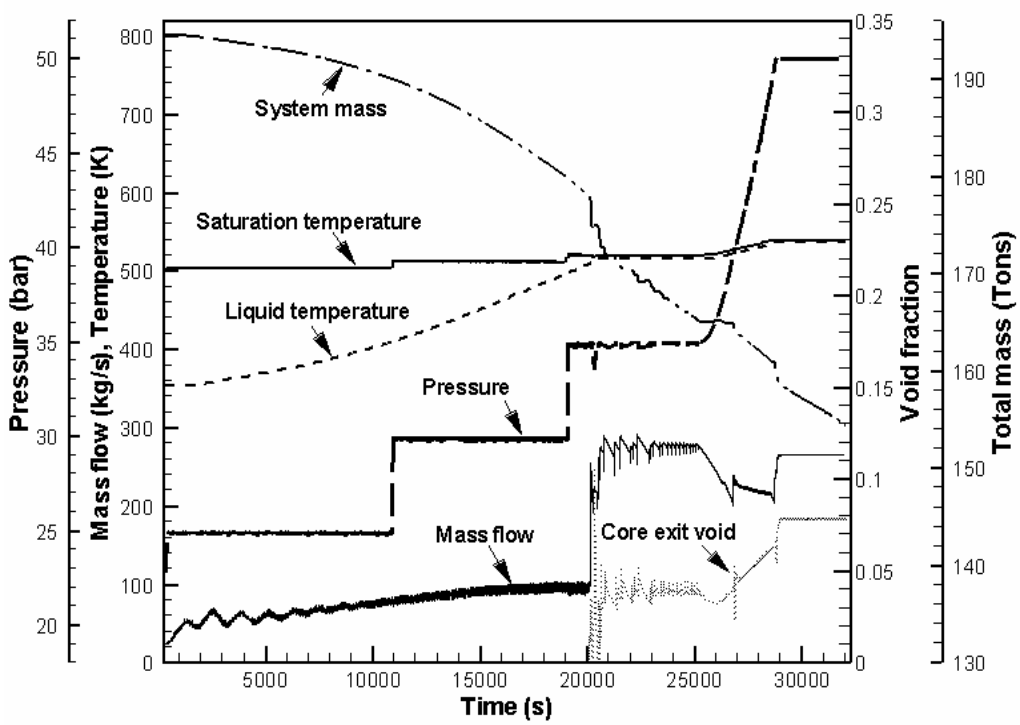

Figure 6.12. System parameters during startup.

TH-831_05610306

It is observed that the system transfers itself from a stable single-phase condition to a stable two-phase operating condition at around 16000s without encountering any unstable region. The flow is found to shift to a higher level once net vapor generation starts in the core region (20000s). The drum level is also brought to normal as expected. In spite of a very high subcooled initial condition, the coolant temperature reaches it saturation in a reasonable time and the system is smoothly taken to the stable two-phase operating condition in approximately 7 hrs.

6.4.3. Point of bleed

The operation of bleeding valves is an integral part of the startup procedure proposed and simulated above. The point of bleed, i.e. the location of valve in the loop should be on the single-phase side, and it is located in the bottom half of the steam drum for the procedure demonstrated here. However, the excess coolant can also be bled from other sections of the systems, for example, inlet header. Simulations are done to identify the effect of bleeding through inlet header by placing valves 3 and 4 at the inlet header, while valves 1 and 2 remain in the steam drum. The flow transients observed are presented through Fig. 6.13. It is inferred that, once valve 3 located at the inlet header is operational, the flow starts to oscillate with large pulses in both forward and reverse directions. The sudden release of coolant through the valve opening causes perturbation in the liquid flow at the inlet header and the instability further extends to the inlet of the heater channel. Thus, the bleeding at inlet header results in flow transients and is not a good option. Another example shows the effect of point of bleed, in which valves 3 and 4 are located at the very bottom of the steam drum. It is observed that there is a sudden loss in pressure level at 18000s and 23000s (Fig. 6.14). This drop in pressure is due to the presence of void at the drum bottom for the respective time period, which escapes through the bleeding valves along with the liquid. Hence, it is also essential to place the valves in the steam drum at a height where single-phase condition is ensured.

TH-831_05610306

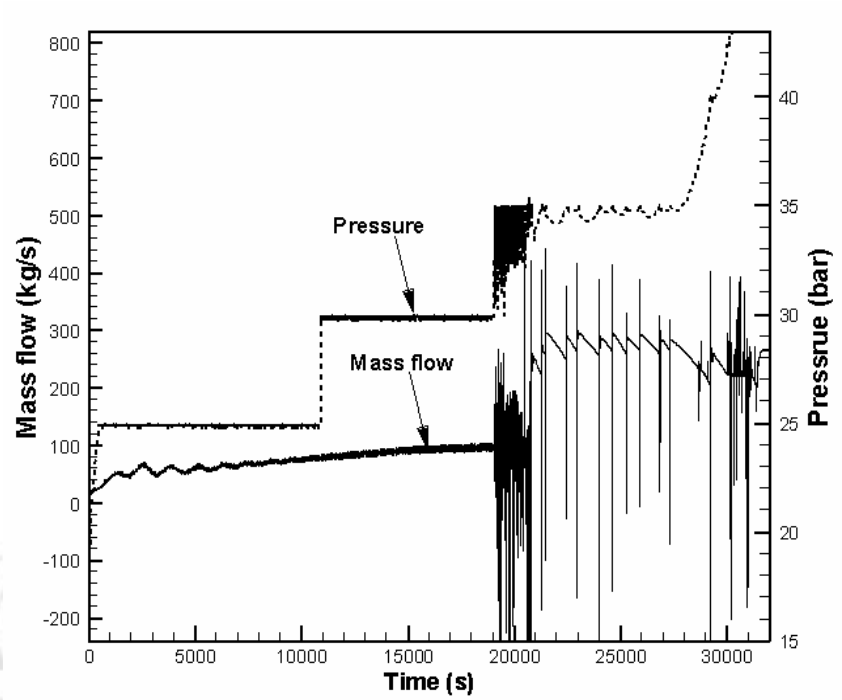

Figure 6.13. System parameters during startup simulation with bleeding at inlet header.

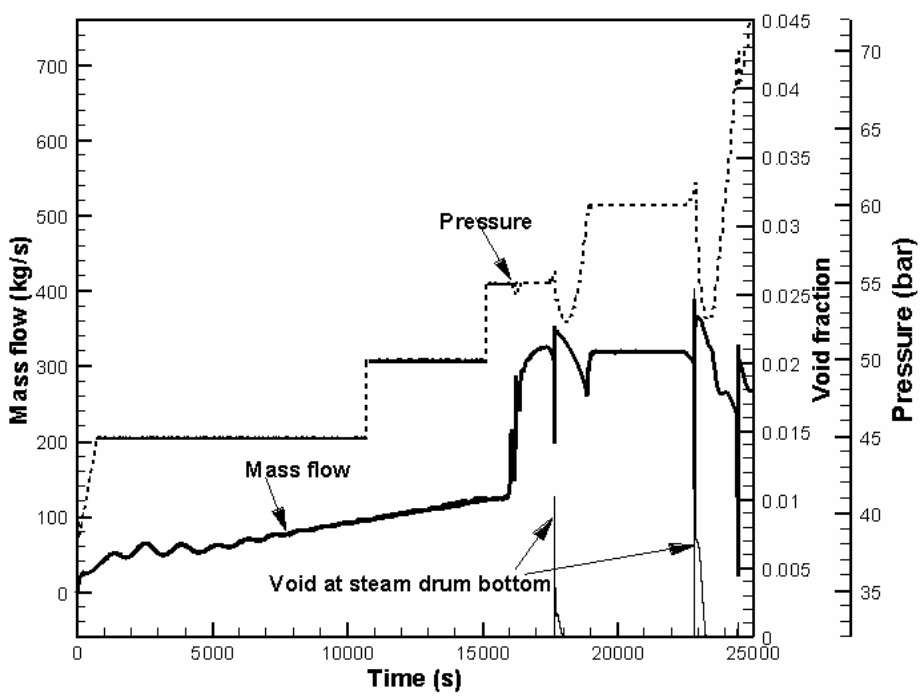

Figure 6.14. System parameters during startup simulation with bleeding at steam drum bottom.

TH-831_05610306

6.5. Summary

Thermal-hydraulic system code RELAP5 has been used to model and simulate the startup of an NCBWR. Numerical experiments with various heat-up rates have been carried out and the feasibility of a complete single-phase startup has been examined. A new startup method is conceptualized and demonstrated numerically.

- Two heat-up schemes, namely Case-1B and Case-3B are found to be best suited for the startup of the NCBWR. This is by considering a low core void generation and a reasonably fast rate of pressurization, although flashing in the riser section is unavoidable. It is also clearly evident that certain heat-up rates cannot be adopted.

- A complete single-phase startup is found not attractive, considering the time factor and the requirement of an additional heat exchanger (used only during the startup) that involve modifications in the design of the PHT loop and other related components.

- A startup procedure is conceptualized, whereby the unstable two-phase region is completely avoided and the method to take the system to the operating condition without encountering flow oscillations (due to flashing) is numerically demonstrated.

- The bleeding at the inlet header results in high amplitude flow oscillations, and is not a good option. It is also essential to place the bleeding valves in the steam drum at a height where single-phase condition is always ensured.

TH-831_05610306

Chapter 7

Ascension to Full Power

7.1. Introduction

A startup procedure, as mentioned earlier, can be divided into four distinct phases: Phase I, Phase II, Phase III and Phase IV. The significance of Phase II and Phase III during a reactor startup has been well understood and a new method of startup, that can address the Type-I oscillations has been proposed in Chapter 6. It is equally important to look into the Phase-IV (Ascension to Full Power) of startup, especially in devising an effective startup procedure for test facilities. During startup, as the system pressure crosses the Type-I region and enters the stable region (Phase IV), the power is further increased so as to take the system to the normal operating pressure. The fact that the thermodynamic state of the system is continuously changing while there is a raise in pressure, puts the system in an unknown territory, especially due to the lack in knowledge about the current Type-II boundary. For such reasons, the normal practice is to maintain a very low-power so as to avoid the system from entering into an unstable region and experience Type-II oscillations. This results in a very low rate of increase in pressure, making the daily startup of the test facility a fickle and a time consuming process. In addressing this issue, it is very essential to have an idea of the Type-II boundary (at the instantaneous pressure), and if the boundary can be tracked, then the power can also be ramped accordingly with assurance that the power applied is well below the Type-II boundary throughout the process of pressure rising.

A power ramping procedure based on this concept, which aims at a safe and faster pressurization of the system is devised with the help of RELAP5 and demonstrated on the test facility. The developed RELAP5 model of the test facility is used to predict the power at Type-II boundary at any instantaneous condition of the system. The Chapter also deals with the scalability of this powering procedure to the prototype NCBWR.

TH-831_05610306

7.2. Power Ramping Procedure for the Test Facility

A power ramping procedure for the test facility is conceptualized and demonstrated experimentally. The conceptualized procedure for the test facility is as follows.

1. The initial fluid temperature is kept at 80°C and the primary loop is isolated from the condensor by closing the steam and condensate return valve.
2. The system is started with a low-power (1-2 % of full power).
3. The power is increased by a small amount (2.0 % of full power) every 10 min.
4. Step 3 is repeated until the startup oscillations die out.
5. The power is increased to 75 % of the Type-II boundary of the current system pressure and core inlet subcooling.
6. Step 5 is repeated every 4-5 minutes until the system gets pressurized to the operating pressure.

The power at the Type-II boundary in step 5 is given by a power law fit which is obtained from the data set generated through RELAP5 simulations.

7.3. Prediction of Stability Boundary using RELAP5 Model

The data set for defining the Type-II boundary was generated by doing RELAP5 simulations for a number of combinations of pressures (8 to 45 bar) and inlet subcoolings (5 to 20°C). For each combination the power was increased gradually, starting from a moderate value and the maximum power for stable operation was identified, above which the system becomes unstable. A power law expression was fitted for power as a function of pressure and inlet subcooling using a nonlinear regression fit. The expression obtained is as follows.

$$Q = 5.10\, p^{0.400}\, T_{sub}^{\;0.304} \qquad (7.1)$$

TH-831_05610306

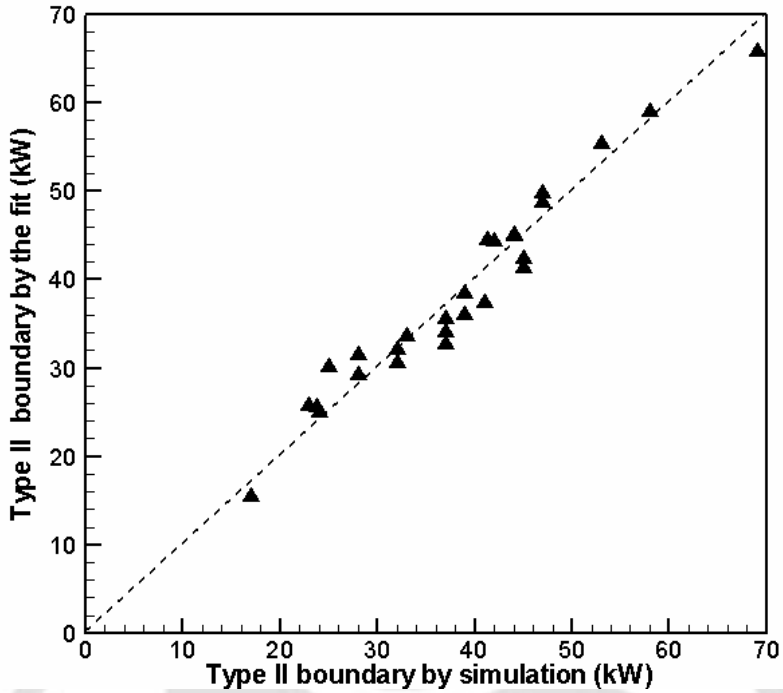

Figure 7.1. Comparison of Type-II boundaries obtained by power law fit and RELAP5.

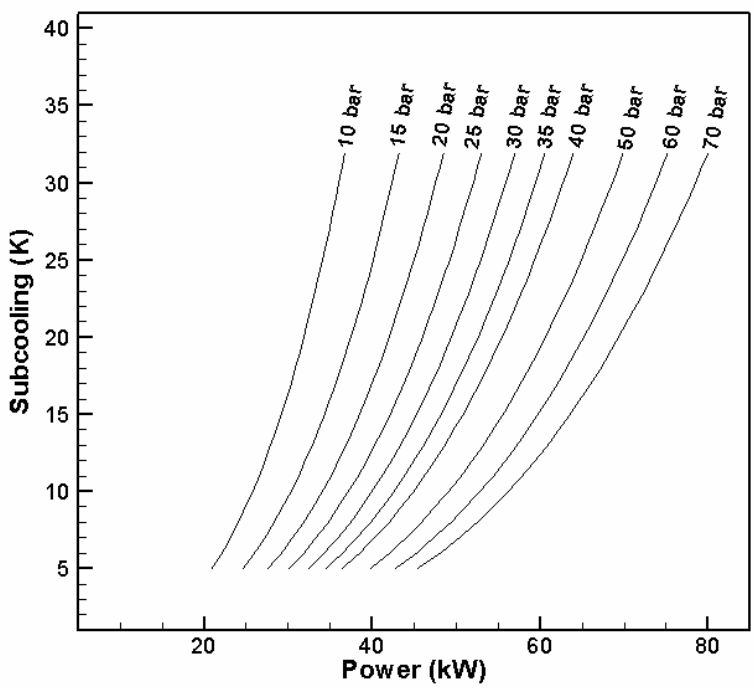

Figure 7.2. Type-II boundary prediction by RELAP5.

TH-831_05610306

where, Q (kW), p (bar) and T_{sub}(K) are the power, pressure and inlet subcooling respectively. A comparison of the power at the Type-II boundary obtained by Eq. 7.1 with that obtained by the RELAP5 simulations is shown in Fig. 7.1. Using this equation the Type-II boundary at various pressures was obtained and plotted as shown in Fig. 7.2. Based on this, the powering procedure given above was devised and implemented in the experiment. The transients during startup were observed. It is to be noted that the Type-II boundary is not independent of geometry as repotted in previous studies (Durga Prasad, 2008; Durga Prasad and Pandey, 2008), where stability boundary and parametric effects for systems with different geometry were carried out and compared. Hence, the correlation given by equation 7.1 will be geometry dependent and the procedure can only be adopted but a new empirical correlation will have to be obtained for any particular system under study.

7.4. Experimental Demonstration of Power Ramping Procedure

The power ramping procedure which was proposed in Section 7.2 was demonstrated in the test facility. The initial fluid temperature was kept at 80°C and the primary loop was isolated from the condensor by closing the steam and condensate return valve. The system was started with a low-power (1.5 kW) and then the power was increased in a step of 2 kW for every 10 min until the system crossed the initial transients. Once the flow became steady, an input power corresponding to the power at the Type-II boundary for the current system pressure was obtained using the above mentioned fit. Keeping a margin of safety, 75 % of the obtained power was applied and this process was repeated for every 5 minute until the system reached the operating pressure. Figure 7.3 shows the temporal traces during the start up pressurization. It can be noted that there are two major regions of operation in the power ramping procedure used here: the initial region until the transients stop (step3) and the later region till the desired system pressure is reached (step 5). The focus of the proposed power ramping procedure is largely on the later region, where RELAP5 predictions are used in deciding the power ramp. Thus, a considerable saving in the time required for raising the system pressure to the operating condition is achieved, as can be seen in Fig. 7.4.

TH-831_05610306

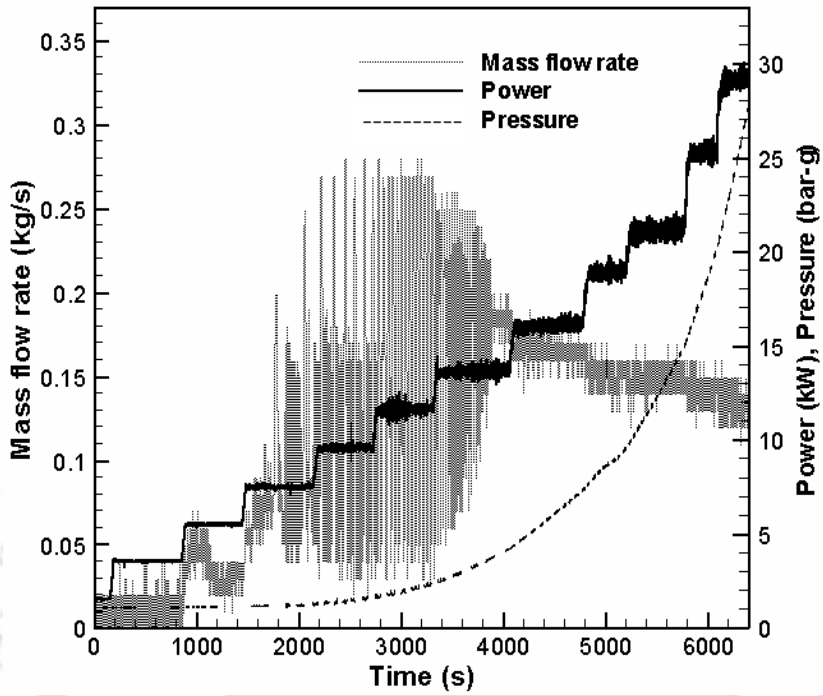

Figure 7.3. System parameters during startup experiment in NCTF.

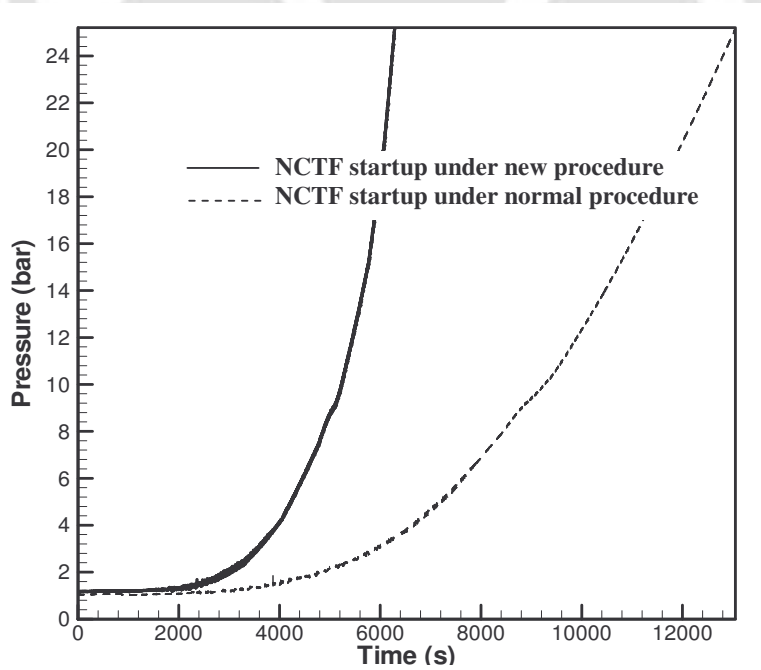

Figure 7.4. Comparison of system pressure rise in the NCTF experiment under different startup procedures.

TH-831_05610306

7.5. Scale-up for NCBWR

Based on the power ramping procedure conceptualized for the test facility and demonstrated experimentally, the power ramping procedure is scaled up for the prototype and tested numerically. Similar to the procedure for the test facility, the power in the prototype is to be increased in steps, where the time intervals and the sizes of the steps are according to the time scale ratio and the power scale ratio (Table 3.1), respectively. This procedure is numerically simulated and the results are presented in Fig 7.5. As observed in the experimental demonstration for the test facility (Section 7.4), there are two major regions of operation in the power ramping. The numerical simulation for the prototype (Fig. 7.5) shows that there are no instabilities in the later region even though the power is increased in larger steps compared to the initial region. It is also seen that the average flow and amplitude of oscillations are as expected according to the model to prototype scaling ratio. At a stable condition, say immediately after the transients die, the system flow rate for NCTF and the prototype is approximately 0.15 kg/s and 395.0 kg/s. Hence the actual model to prototype flow ratio is also expected to be very close to the designed value.

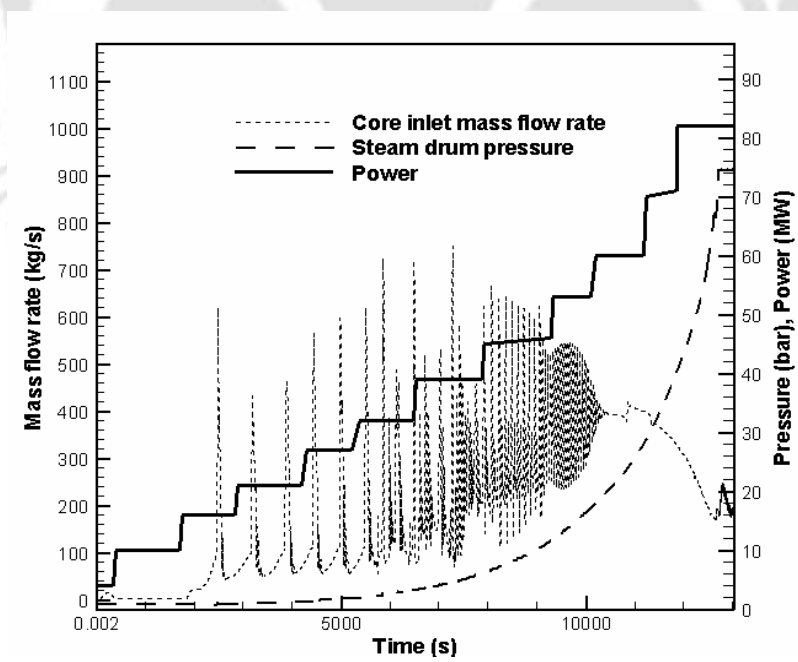

Figure 7.5. System parameters during startup simulation for the prototype using RELAP5.

TH-831_05610306

7.6. Summary

- A powering procedure for the full power ascension of NCTF has been conceptualized with the help of its RELAP5 model and demonstrated experimentally, which results in saving considerable amount of time in raising the system pressure to the desired operating condition.

- The method of power ramping for ascension to full power is also scaled up for the prototype and tested numerically with its RELAP5 model.

- The significance of this procedure is that, the experiment is guided online by the predictions obtained by the numerical model, and the procedure can be a very effective method for startup of test facilities.

- Based on the requirement, this procedure can be used in combination with the method (to suppress Type-I instability) proposed in Chapter 6 to evolve a startup procedure that can address all the phases of the startup procedure.

TH-831_05610306

TH-831_05610306

Chapter 8
Conclusions

The events during startup of a natural circulation boiling system were addressed. Numerical prediction of startup instabilities like flashing and low-pressure density wave oscillation was done using system code RELAP5 along with experimental validation. Startup transients in both single and double channel systems were analyzed. Startup procedures addressing different stages of startup were conceptualized and demonstrated.

Numerical models of NCTF and NCBWR were developed with RELAP5 code along with nodal sensitivity studies, and verified with experimental results. From the nodal sensitivity studies, it is inferred that a very course mesh size would lead to wrong predictions of the flashing behaviour and an optimum nodal size is very essential for predicting the transient in a natural circulation boiling system. The ability of RELAP5 to predict low-pressure transients especially flashing instability was verified with experimental results of NCTF. As a verification process for the numerical model of the prototype, transient predictions and parametric trends (effect of pressure and flow restrictions) obtained by the NCBWR model were compared with those of the NCTF model and found to be in good agreement.

In getting an insight of the phenomena behind the low-pressure low-power transients, the numerical results obtained through the RELAP5 models of both NCTF and NCBWR were used for the analysis and interpretation. The flow oscillations observed during experimental and numerical studies were analyzed and classified. In the NCTF model, the flow oscillates with a few pulses of lower amplitude followed by a higher amplitude flashing pulse. The small amplitude oscillations are due to void generation in the heater region, and these oscillations are not condensation induced geysering instabilities, but a density wave instability supported by flashing. Comparing the nature

TH-831_05610306

of startup transients observed in the test facility and the prototype, a different kind of startup oscillations was found in the prototype, where only flashing exists. This difference in nature of oscillations is due to the dominance of flashing, as the phenomenon is more pronounced when the height scale is increased (4 times), and there is a strong variation of saturation temperature along the riser at low-pressures. The power spectral density (PSD), computed using a fast Fourier transform (FFT) algorithm conveyed that the observed startup transients are chaotic in nature. The aperiodicity was further confirmed by the computation of Lyapunov exponent and Poincaré section.

The existence of in-phase and out-of-phase flashing instabilities in the parallel-channel systems (prototype and scaled model) was investigated through the parallel-channel RELAP5 model extended from the single-channel model. Simulations were done under equal and unequal power boundary conditions and flow restrictions in the channels. For identical startup conditions, it was inferred that the nature of flow oscillation observed in scaled model and the prototype is not similar, in the context of in-phase and out-of-phase behaviour. In the prototype model, flow behavior in both the channels is characterized by flashing pulses which are in-phase, whereas in the scaled model, even for identical conditions, there exists a phase difference between channels. Unlike in equal power conditions, intermittent flow reversal was observed under unequal power condition. Flow reversal in this context refers to change in flow direction in one channel when there is a sudden surge in flow in the other channel due to flashing. Flow restriction at the core and riser inlet results in considerable reduction of flow amplitude. Presence of additional loss coefficient in one channel results in out-of-phase flow oscillation in a parallel-channel NCBWR. It would be desirable to carry out an experimental investigation through a parallel-channel system with similar geometrical configurations, and also assess the effect of in-phase and out-of-phase oscillations on flow-induced vibrations and material fatigue.

Power ramping procedures for different stages of startup were addressed. Focusing on the early phases (phase II and phase III) of startup, numerical experiments with various heat-up rates were carried out and the feasibility of a complete single-phase startup was examined. Considering a low core void generation and a reasonably fast rate of

TH-831_05610306

pressurization, suitable heat-up schemes are suggested. However, flashing in the riser section is unavoidable under such schemes. A complete single-phase startup is also found not attractive, considering the time factor and the requirement of additional auxillary systems. Further, a startup procedure completely bypassing the unstable two-phase region was conceptualized and numerically demonstrated. The consequence of the positioning of bleeding valves used in the startup procedure was also emphasized, and it is desirable to conduct experimental studies to demonstrate these effects.

The Phase-IV of startup, which assumes importance during the daily startup of any test facility, was also addressed. Here a powering procedure for the full power ascension was conceptualized and demonstrated experimentally. It involved numerical prediction of Type-II boundary, obtaining a power law expression and its implementation during startup of test facility. The exercise resulted in saving considerable amount of time in raising the system pressure to the desired operating condition, and obtaining a unique experience in integrating numerical predictions and experimentation.

TH-831_05610306

TH-831_05610306

Appendix A

Numerical Simulation for PUMA Facility

A.1. Simulation for Startup Transients in PUMA Facility

A numerical model of an experimental test facility (PUMA) was developed with RELAP5 (Lakshmanan and Pandey, 2007). Numerical simulations were done with this model and results were compared with experimental findings reported in literature. The oscillations in the core void fraction and the downcomer velocity obtained from numerical simulations were found to be similar to those in the experiment.

A.2. Results and Discussion

The RELAP5 simulation results are presented here and compared with the experimental results of PUMA startup (Kuran et al., 2006). Oscillations were observed in the core exit void fraction predicted with RELAP5 (Fig. A.1), which agrees with the experimental observations under the same conditions (Fig. A.2). The mean value of the predicted void fraction was close to, albeit somewhat higher than, the core exit void fraction measured during the experiment. Some intermittent excursions in the predicted void fraction were observed, which can be attributed to the condensation and vapor generation models employed in RELAP5. The chimney void fraction obtained from numerical simulations and experimental measurements is shown in Fig A.3 and Fig. A.4 respectively. The void fraction in the chimney inlet and exit was overpredicted in RELAP5 simulations.

TH-831_05610306

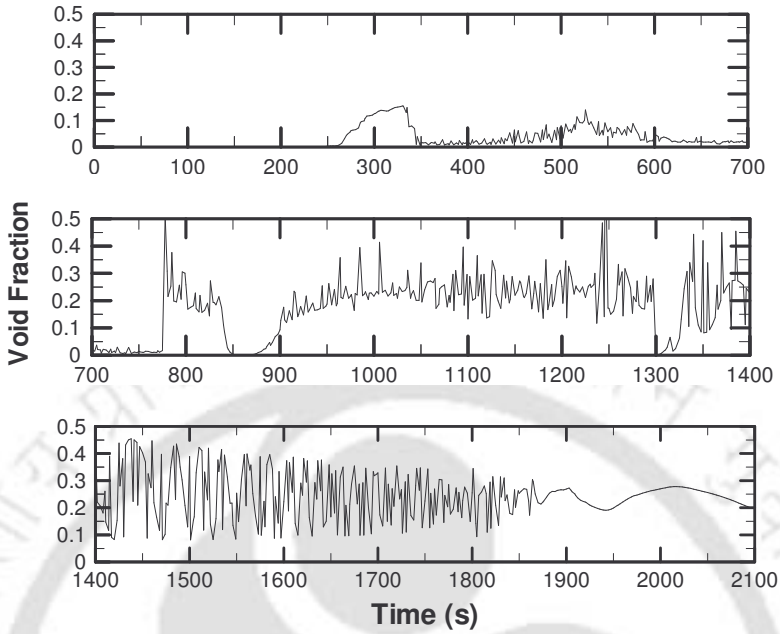

Figure A.1. Core exit void fraction prediction using RELAP5

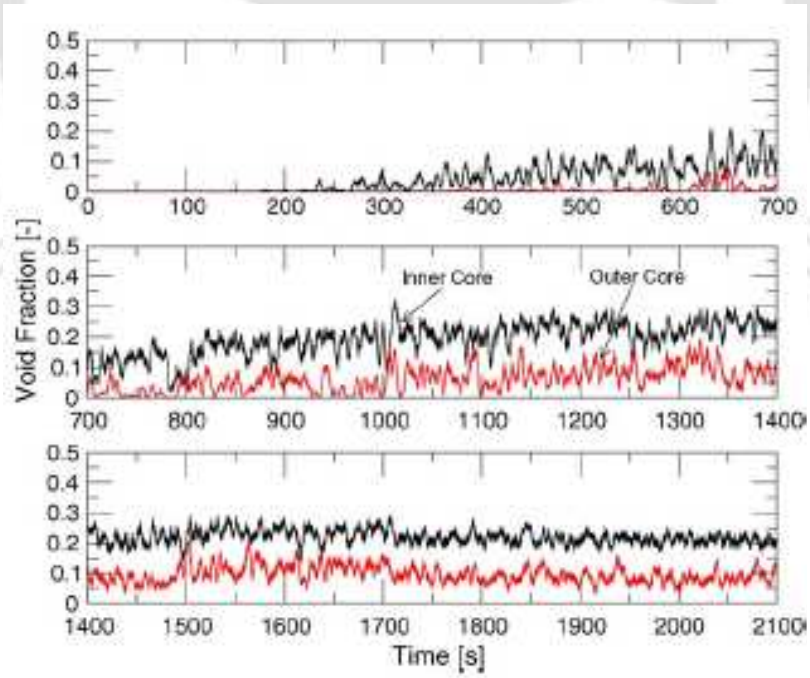

Figure A.2. Core exit void fraction observed in the experiment (Kuran et al., 2006).

TH-831_05610306

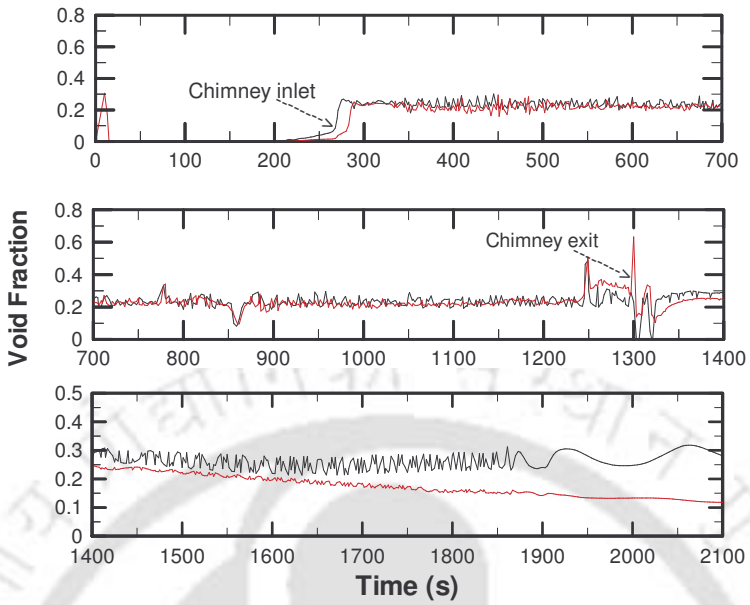

Figure A.3. Chimney void fraction prediction using RELAP5.

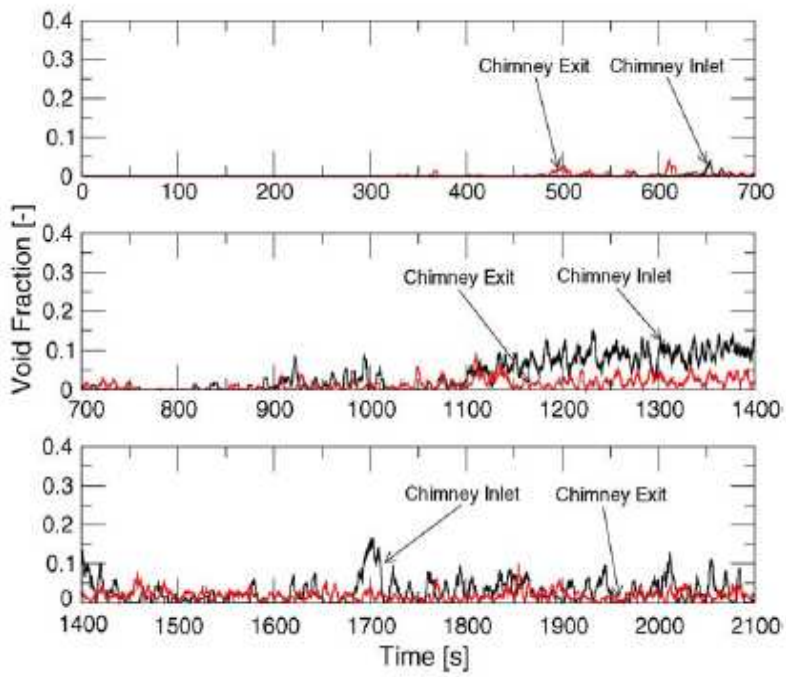

Figure A.4. Chimney void fraction observed in the experiment (Kuran et al., 2006).

TH-831_05610306

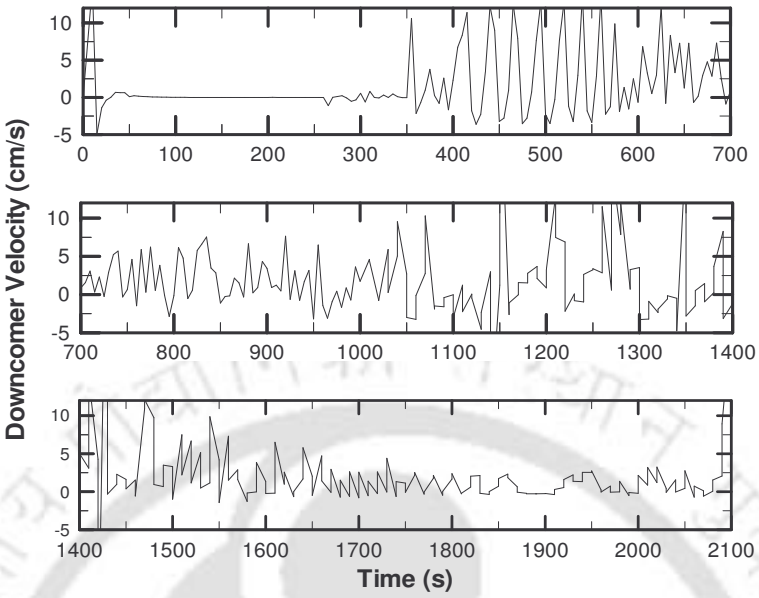

Figure A.5. Downcomer velocity prediction using RELAP5.

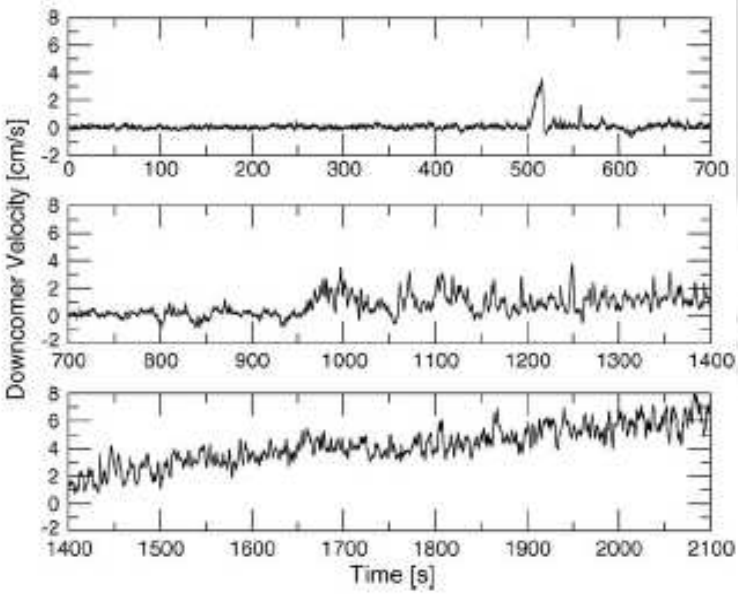

Figure A.6. Downcomer velocity transients observed in the experiment (Kuran et al., 2006).

TH-831_05610306

An increase in the height of the chimney would result in void generation (flashing) in the upper part of the chimney. Figures A.5 and A.6, respectively, show the flow velocity in the downcomer as predicted with RELAP5 and as measured during the startup test of PUMA facility. In both the figures, velocity fluctuations are small during the initial transients and become large with time. The amplitude of the predicted oscillations is high compared to the measured values. Flow reversal is observed due to the void generation (in the core) and its condensation in the lower part of riser, when the condensation rate is higher than the void generation rate. Although the trends predicted by numerical simulations are fairly matching, the need for further validation arises due to the non availability of key dimensions and quantitative experimental data in the literature.

TH-831_05610306

TH-831_05610306

Appendix B

Salient Features of NCTF

The Natural Circulation Test Facility (NCTF) designed and developed at IIT Bombay, is a four parallel channel facility with flexibility to operate in single channel, two channel and three channel modes. The details of the test facility discussed here are from (Iyer and Kandengal, 2003; Pradeep et al., 2010). The experimental facility is designed for a power of 295 kW and 70 bar pressure. The height of the loop above the core is 7.5 m and the heated length of the test sections are 0.875 m. All the components of the primary loop are made of SS316 (L) and were designed as per ASME Section-VIII and Division-I (2001). The NCTF consists of two loops with four risers connected to two drums. While one simulator with its riser, drum, downcomer and feeder represents one loop, the other loop with three simulators, three risers, one drum, one downcomer and three feeders represent the other three loops of the prototype. For the current study, the data is obtained from the single loop of the natural circulation system shown in Fig. B.1, which includes the details of the links and valves used for friction number estimation. The major components and features of the facility are briefly discussed here.

B.1. Heater Section and riser

The heater section of the facility is an annulus pipe (Fig. B.2) that simulates the core of the prototype. Energy is supplied to the channel of the fuel simulator through joule heating. The electrical resistance of the channel is such that the operating point is well within the limits of the power supply characteristics of the existing power source. The outer channel is be made of a standard pipe of 1¼ inch, Sch. 80 with outer diameter of 42.2 mm and inner diameter of 32.5 mm. For the heated length of 875 mm in the model, the outer channel diameter is machined to 38.46mm.

TH-831_05610306

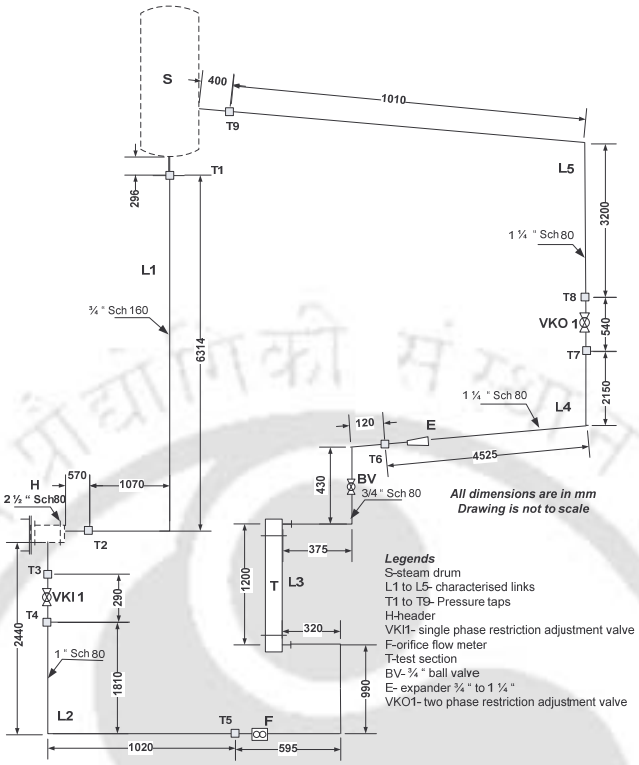

Figure B.1. Link details of NCTF loop (Pradeep et al., 2010)

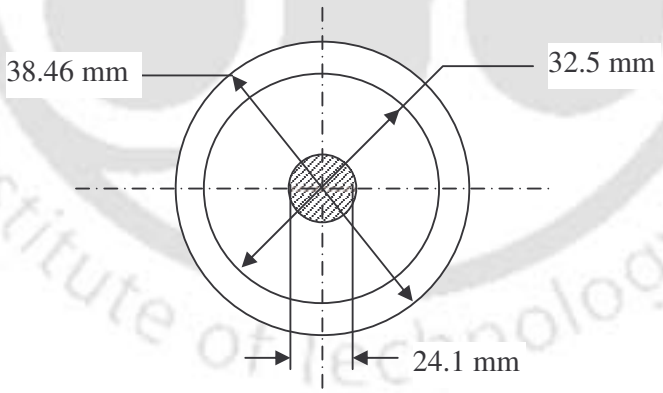

Figure B.2. Schematic configuration of the fuel simulator

The risers simulate the tail pipes of the prototype. This link connects the fuel simulator outlet to the steam separator, where one raiser in the single channel loop is to represent around 113 channels in the prototype.

TH-831_05610306

B.2. Steam Separator Drums

The test facility employs two steam drums of different sizes. The small drum simulates one drum of the prototype facility and the other bigger drum simulates the other three drum of the prototype combined together. For the current study only one loop and one drum will be operated (Fig. B.3). The liquid height in both the drums is the scaled dimensions of the prototype drum liquid height. An additional height of about 1.5 meters is provided for steam space above the liquid height to minimize the carry-over. Cylindrical baffles are provided in the drums to prevent steam being carried under into the downcomers. To maintain the liquid level in the drum, an over flow line with isolation valves is provided, which is connected to an auxiliary drum. To study the effect of liquid height, another overflow line is also provided at double the liquid height. The liquid volume in the model is scaled from the liquid volume of the prototype using the volume scale ratio as follows. Liquid volume of one channel drum is 0.01349m3.

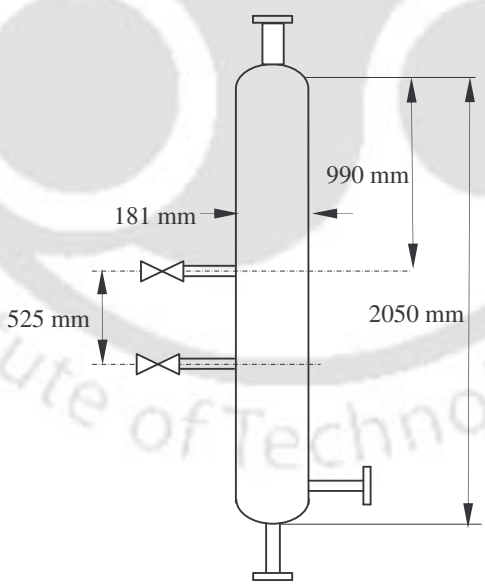

Figure B.3. Schematic of the stream drum

TH-831_05610306

B.3. Downcomer

The downcomer is the link, which connects the steam separator drum exit to the header. In prototype there are 16 downcomers which is connected to a ring header. These 16 downcomers are connected to four identical drums with four downcomers per drum. In the model test facility there are two separate downcomers that connect to the two steam drums to a common cylindrical header. The lengths of the downcomers for the model are determined by the length scale ratio and the diameter is based on the scaled flow area.

B.4. Header and feeders

The shape of the header of in the prototype is a circular ring with ring diameter of 17.5 m. In the model facility, a cylindrical shape is considered. The dimensions of the header for the model are determined by preserving the volume scale and the considered volume of header is 2.4 litres. Further, the diameter ratio of the header to downcomer diameter in the prototype is 2. In the model, the downcomer diameters for the ¾ loop and ¼ loop are different, and the total length of the header is partitioned into two compartments with ¼th and ¾th lengths for connecting to the steam drums simulating $1/4^{th}$ and $3/4^{th}$ of the prototype system. The feeders connect the header and the heater section. The 452 feeder lines in the prototype are simulated by a single feeder in $1/4^{th}$ loop of the model facility and by three feeders in the $3/4^{th}$ loop of the model test facility. The length and height of the feeders in the model are determined from the length scale, and the feeder line inside diameter is 26.45 mm.

B.5. Condenser

The condenser provided in the test facility is designed to operate over a wide range of power and pressure requirement. It is of shell and tube type, with steam condensing in shell side and coolant flowing through U tubes. The condenser couples the primary and secondary of the facility. The schematic of the secondary loop is shown in Fig. B.4. There are 47 U tubes, which are grouped into six manifolds, so that any desired number

TH-831_05610306

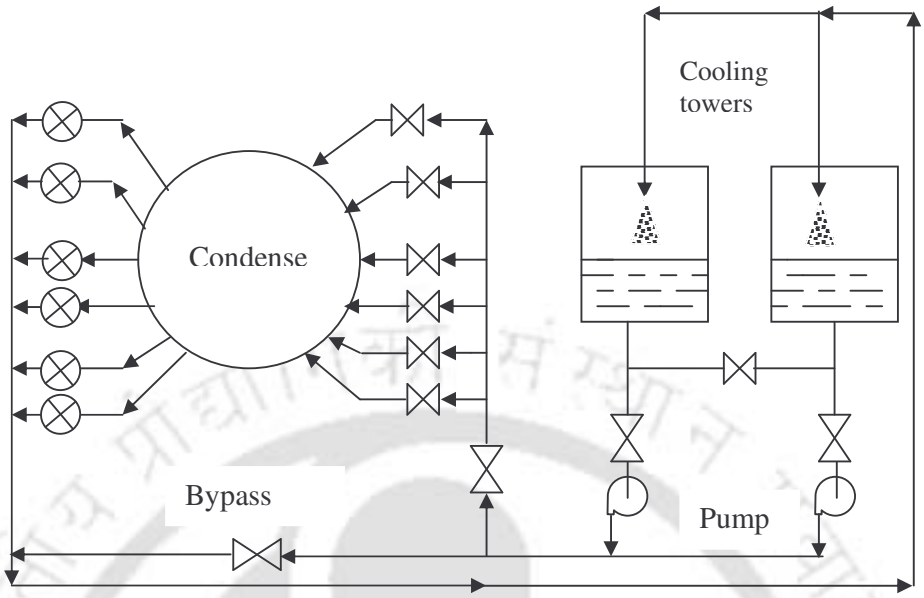

Figure B.4. Schematic of the secondary loop (Pradeep et al., 2010)

of tubes between one and forty-seven can be put in service. By varying the level of the condensate in the shell, and coolant flow rate, the system pressure and degree of subcooling can be adjusted from 0.2 m/s to 2 m/s. The condenser is equipped to handle the variable heat load, to anchor the system pressure at the desired level, and to provide the necessary sub cooling to the condensate.

Characterisation of NCTF Loop

The single-phase frictional pressure drop of the pipe and fittings in one channel of the primary flow loop were determined by characterizing the loop at two temperatures, one at 40°C and other at an elevated temperature of 80°C. The various links comprising of combination of pipes and fittings characterised are shown in Fig. B.1. Low pressure filling pump provided in the loop was used to carry out the characterisation. Uniform fluid temperature in all the links of the loop was ensured and temperature variation was within +/- 2°C . The differential pressure measured for various links are then corrected for the gravitational pressure drop and acceleration pressure drop to extract the total frictional pressure drop. 1. The friction numbers of the characterised links are presented in Fig. B.5, as a function of the Reynolds number. Characterisation at 40 ºC is

TH-831_05610306

represented by blue colour and characterisation at 80 ºC is represented by red colour. The Reynolds number indicated are based on the inner diameter of 1" Sch80 pipe where the orifice flow meter is mounted.

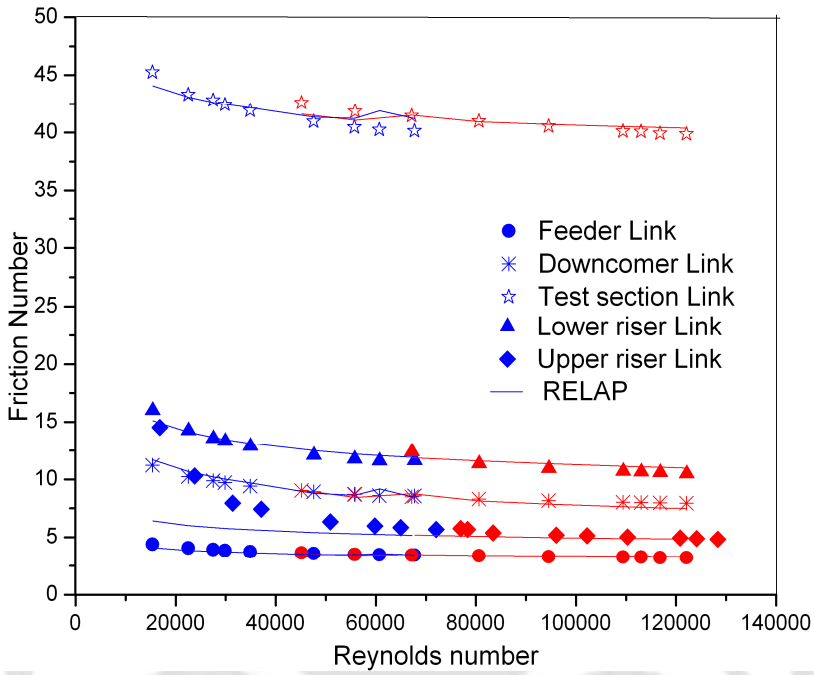

Figure B.5. Characterised friction numbers for various links (Pradeep et al., 2010)

TH-831_05610306

Appendix C

Design Features of the Prototype

C.1. Advanced Heavy Water Reactor

The details of the advanced heavy water reactor (AHWR) discussed in this section are from Sinha and Kakodkar (2006). The AHWR is a vertical pressure tube type reactor cooled by boiling light water under natural circulation. The fuel used is Thorium. This reactor works on direct cycle. The reactor is mainly heavy water moderated. One of the attractive features of this reactor is that the heat removal from the core takes place by natural circulation during start-up, power raising and accidental conditions in addition to the rated full power operating condition. This enhances passive safety by eliminating the recirculation pumps, which are normally present in conventional forced circulation boiling water reactors. The Primary cycle of the AHWR consists steam producing components core, riser, steam drum, downcomer and inlet header. These are coupled to the safety systems. The secondary cycle consists of High Pressure Turbine (HPT), Low pressure Turbine (LPT), moisture separator, bleed steam reheaters, condenser, pumps, moderator heat exchanger, and feed water heaters. The general arrangement of AHWR components is shown in Fig. C.1.

C.2. Major Design Features

The AHWR has been designed with advanced safety features like negative void reactivity coefficient and passive heat removal under all conditions. The negative void coefficient is achieved using Dysprosia as burnable absorber and reduction in moderator inventory by using inter-lattice void tubes in the fuel cluster. To obtain required natural circulation flow rate, the height of the riser is comparatively much larger than a forced circulation Boiling Water Reactor. The reactor design incorporates

TH-831_05610306

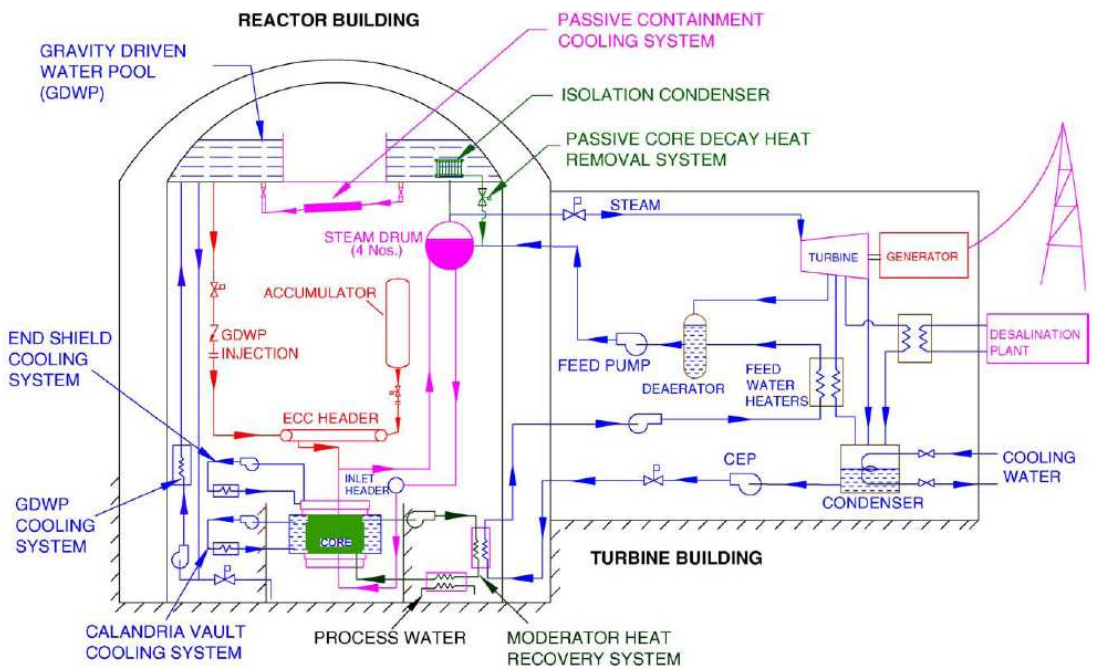

Figure C.1. Schematic arrangement of AHWR (Sinha and Kakodkar, 2006)

advanced technologies, together with several proven positive features of Indian Pressurized Heavy Water Reactors (PHWRs). These features include pressure tube type design, low-pressure moderator, on-power refuelling, diverse fast acting shutdown systems, and availability of a large low temperature heat sink around the reactor core. The AHWR design has adopted boiling light water in a direct cycle as the main cooling system. The AHWR incorporates several passive safety features. These include:

1. Core heat removal through natural circulation, direct injection of Emergency Core Coolant System (ECCS) water in fuel.
2. Passive systems for containment cooling and isolation, and
3. Availability of a large inventory of borated water in overhead Gravity Driven Water Pool (GDWP) to facilitate sustenance of core decay heat removal, Emergency Core Cooling System (ECCS) injection and containment cooling for three days without invoking any active systems.

TH-831_05610306

C.3. Reactor Physics Design

The reactor physics design is tuned for maximizing the use of Thorium based fuel, and achieving a slightly negative void coefficient of reactivity. The fulfillment of these requirements has been possible through the use of PuO_2 - ThO_2 *MOX* (mixed oxide fuel), and ThO_2-$U^{233}O_2$ *MOX* in different pins of the same fuel cluster, and the use of a heterogeneous moderator consisting of amorphous carbon in 80% and heavy water in 20% by volume. The AHWR has the flexibility to have on power as well as off-power fuel handling. The dimensional details of the core are given in Table C.1.

C.4. Heat Transport System

The Advanced Heavy Water Reactor (AHWR) is being designed with incorporation of many passive systems/elements to facilitate the fulfillment of safety functions e.g. reactor operation, reactor shutdown, residual heat removal, emergency core cooling,

Table C.1: Dimensional details of core (Sinha and Kakodkar, 2006)

Total no. of lattice locations	505
Number of fuel channels	452
Number of lattice locations for control rods	12
Number of lattice locations for shut-off rods	41
Lattice pitch (mm)	245
Active core height (m)	3.5
Calandria	
Inner diameter of the main shell (m)	7.4
Inner diameter of the sub-shell at each end (m)	6.8
Length (m)	5.3
Tube material	
Pressure tube	Zr2.5 Nb
Calandria tube	Zircaloy-4
Tube dimension	
Inner diameter/WT of Pressure tube (mm)	120/4
Outer diameter/WT of Calandria tube (mm)	168/2
Moderator purity (% of D_2O)	99.8
Moderator temperature (K)	353

TH-831_05610306

confinement of radioactivity etc. Primary circulation pumps are eliminated and the necessary flow rate is achieved by locating the steam drums at a suitable height above the center of the core, taking advantage of the reactor building height. The steam-water mixture from each coolant channel is led through 123 mm tail pipes to four steam drums, which are located with an elevation of 39 m with respect to inlet feeder (coolant channel bottom). The steam at a pressure of 7MPa is separated from the steam-water mixture in steam drums. The steam is led to turbine by two 400 mm pipes. The steam from the turbine is condensed and after purification of the condensate and preheating, it is pumped back to the steam drums and the feed water is mixed with the water separated from steam-water mixture at 285 ºC in the steam drums. The water level in the steam drum is a function of reactor power and is maintained at a set level during power operation. Orifices are provided at the entry to the coolant channels to improve the thermal hydraulic stability, and are sized to yield nearly uniform exit quality of steam in all the channels.

C.5. Fuel Cluster

The AHWR fuel cluster contains three rows of fuel pins surrounding a central displacer rod. The inner two rows contain thirty $(Th\text{-}U^{233})O_2$ fuel pins and the outer row contains twenty-four $(Th\text{-}Pu)O_2$ fuel pins. The cross sectional view of the fuel cluster is as shown in the Fig. C.2. The central rod contains Dysprosium in Zirconia matrix. The fuel also incorporates a water tube for the injection of Emergency Core Coolant System (ECCS) water directly on fuel pins during a postulated Loss of Coolant Accident (LOCA). A description of AHWR fuel assembly is listed in Table C.2.

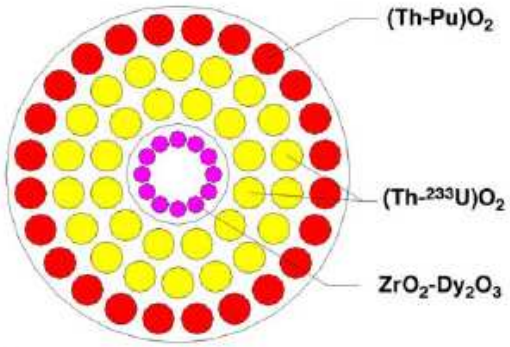

Figure C.2. Arrangement of fuel rods in a fuel cluster (Sinha and Kakodkar, 2006)

TH-831_05610306

Table C.2: Description of AHWR fuel assembly (Sinha and Kakodkar, 2006)

Parameter	***Value***
Number of fuel pins	54
Outer diameter (mm)	11.2
Density (g/cm3)	9.6
Fuel clad	
Material/thickness (mm)	Zircaloy-2/0.6
Fuel type/number of pins	
Inner ring	$(Th–^{233}U)O_2/12$
Middle ring	$(Th–^{233}U)O_2/18$
Outer ring	$(Th–Pu)O_2/24$
Fuel enrichment (wt%)	
Inner ring (^{233}U)	3.0
Middle ring (^{233}U)	3.75
Outer ring (Pu)	3.25 (average)
Upper half	2.5
Lower half	4.0
Central rod	
Tube o.d./thickness (mm)	36/2
Number of pins/capsule	12
Outer diameter of pin (mm)	6
Material/o.d. (mm)	$ZrO_2 + Dy_2O_3$
Dysprosium (wt%)	3.0
Average discharge burnup (MWd/t)	24,000
Average linear heat rating (kW/m)	10.6

C.6. Passive Safety Features of AHWR

One of the most important elements of the requirements stipulated for the next generation nuclear reactor is to incorporate passive safety features especially for the reactor core removal under all operational states, including accident conditions, as isolation and cooling of the containment in the event of an accident. AHWR has these features.

These features are as following:

1. During normal reactor operating conditions, removal of the heat by natural circulationnof light water coolant through the reactor core is achieved by locating steam drums at high elevation.

TH-831_05610306

2. During normal reactor shut down removal of the core decay heat in natural circulation mode is by means of steam condensation in isolation condensers. These isolation condensers are immersed in a large pool of water, called Gravity Driven Water Pool (GDWP).
3. In case of Loss of Coolant Accident (LOCA), removal of the reactor core decay heat and flooding the core, without operator intervention for a period of three days, is achieved by means of ECCS accumulators and GDWP. Subsequent to submergence of the under water, the core is cooled in a long-term re-circulation mode.
4. Isolation of the reactor building ventilation system is achieved through water seal, established due to pressure rise in the containment following LOCA and also removal of the containment heat by Passive Containment Coolers (PCCs) with GDWP serving as a heat sink.
5. A double containment is provided to minimize ground level releases of radioactivity.

TH-831_05610306

References

Aguirre, C., Caruge, D., Castrillo, F., Dominicus, G., Geutjes, A.J., Saldob, V., van der Hagen, T.H.J.J., Hennig, D., Huggenberger, M., Ketelaar, K.C.J., Manera, A., Munoz-Cobo, J.L., Prasser, H.-M., Rohde, U., Royer, E., Yadigaroglu, G., 2005. Natural circulation and stability performance of BWRs (NACUSP). Nucl. Eng. Des. 235, 401–409.

Aritomi, M., Chiang, J.H., Nakahashi, T., Watarum, M., Mori, M., 1992. Fundamental study on thermo-hydraulics during start-up in natural circulation boiling water reactors (I). J. Nucl. Sci. Technol. 29 (7), 631–641.

Aritomi, M., Chiang, J.H., Mori, M., 1993. Geysering in parallel boiling channels. Nucl. Eng. Des. 141, 111–121.

Auban, O., Paladino, D., Zboray, R., 2004. Experimental investigation of natural circulation flow behaviour under low-power/low-pressure conditions in large-scale PANDA facility. Nucl. Technol. 148, 294–311.

Bagul, R.K., Pilkhwal, D.S., Vijayan, P.K., Saha, D., 2008. Investigations to arrive at a stable start-up procedure for AHWR. In: Proceedings of ASME International Conference on Nucl. Engineering, Orlando, FL, USA, ICONE16-48165.

Boure, J.A., Bergles, A.E., Tong, L.S., 1973. Review of two phase flow instability. Nucl. Eng. Des. 25, 165–192.

Chaxton, K. T., Collier, J. G., Ward., J. A., 1972. H.T.F.S. correlation for two-phase pressure drop and void fraction in tubes. AERE-R7162.

Chatoorgoon, V., 1986. SPORTS – A simple non-linear thermal hydraulic stability code. Nucl. Eng. Des. 93, 51-67.

Chen, W.L., Wang, S.B., Chung, C.R., Twu, S.S., Pan, C., 1999. Two-phase flow instability in a double-channel natural circulation loop with equal or unequal heating powers. In: Proc. International Conference on Nuclear Engineering, Tokyo, Japan, ICONE-7141.

Cheng, H. S., Khan, H. J., Rohatgi, U. S., 1998. Simulation of SBWR startup transients and stability. Brookhaven National Laboratory, BNL-65535.

Cheung, Y.K., Rao, A.S, 2000. Startup simulation of a natural circulation plant – ESBWR. In Proc: 8th Int. Conf. on Nucl. Eng. ICONE-8, April 2-6, Baltimore, MD, USA.

TH-831_05610306

Chisholm, D., 1967. A theoretical basis for the Lockhart-Martinelli correlation for two-phase flow. Int. J. Heat Mass Transfer 10, 1767-1778.

Chiang, J.H., Aritomi, M., Inoue, R., Mori, M., 1994. Thermo-hydraulics during startup in natural circulation boiling water reactors. Nucl. Eng. Des. 146, 241–252.

Curtis, A.R., Reid. J.K., 1971. FORTRAN subroutines for the solution of sparse sets of linear equations. Atomic Energy Research Establishment, Harwell, AERE-R6844.

D'Auria, F., Debrecin, N., Galassi, G.M., Galeazzi, S., 1993. Application of Relap5/Mod3 to the evaluation of loss of feedwater in test facilities and in nuclear plants. Nucl. Eng. Des. 141, 409–428

Dilla, E.M., Yeoh, G.H., Tu, J.Y., 2006. Flow instability prediction in low-pressure subcooled boiling flows using computational fluid dynamic codes. Anziam J. 46 (E), C1336–C1352.

Durga Prasad, G.V., Pandey, M., Kalra, M.S., 2007. Review of research on flow instabilities in natural circulation boiling systems. Prog. Nucl. Energy 49, 429–451.

Durga Prasad, G.V., Pandey, M., 2008. Stability analysis and nonlinear dynamics of natural circulation boiling water reactors. Nucl. Eng. Des. 238, 229–240.

Durga Prasad, G.V., Pandey, M., Pradhan, S.K., Gupta, S.K., 2008. Study of flow instabilities in a double channel natural circulation boiling system. Nucl. Eng. Des. 238, 1750–1761.

Ferng, Y.M., Lee, C.H., 1994. Numerical simulation of natural circulation experiments conducted at IIST facility. Nucl. Eng. Des. 148, 119-128.

Fukuda, K., Kobori, T., 1979. Classification of two-phase flow instability by density wave oscillation model. J. Nucl. Sci. Technol. 16 (2), 95–108.

Furuya, M., Inada, F., Van der Hagen, T.H.J.J., 2005. Flashing-induced density wave oscillations in a natural circulation BWR-mechanism of instability and stability map. Nucl. Eng. Des. 235, 1557–1569.

Furuya, M., 2006. Experimental and analytical modeling of natural circulation and forced circulation BWRs – thermal-hydraulic, core-wide, and regional stability phenomena. Doctoral dissertation. Delft University of Technology.

Hari, S., Hassan, Y.A., 2002. Improvement of the subcooled boiling model for low-pressure conditions in thermal-hydraulic codes. Nucl. Eng. Des. 216, 139–152.

Hegger, R., Kantz, H., Schreiber, T., 1999. Practical implementation of nonlinear time series methods: the TISEAN package. Chaos 9, 413–435.

TH-831_05610306

Inada, F., Furuya, M., Yasuo, A., 2000. Thermo-hydraulic instability of boiling natural circulation loop induced by flashing (analytical approach). Nucl. Eng. Des. 200, 187-199.

Ishii, M., Revankar, S.T., Dowlati, R., Bertodano, M.L., Babelli, I., Wang, W., Pokharna, H., Ransom, V.H., Viskanta, R., Wilmarth, T., Han, J.T., 1996. Scientific design of Purdue University Multi-Dimensional Integral Test Assembly (PUMA) for GE SBWR. Tech. Rep. NUREG/CR-6309. U.S. Nuclear Regulatory Commission.

Iyer, K.N., Kadengal, A., 2003. Scaling of natural circulation boiling systems. In: Proceedings of ASME Heat Transfer Conference, Las Vegas, Nevada, USA, HT2003–47568.

Jain, V., Nayak, A.K., Vijayan, P.K., Saha, D., Sinha, R.K., 2009. Experimental investigation on the flow instability behaviour of a multi-channel boiling natural circulation loop at low-pressures, In: Proc. International Topical Meeting on Nuclear Reactor Thermal Hydraulics (NURETH-13), Kanazawa, Japan.

Jiang, S.Y., Yao, M.H., Bo.F J.H., Wu, S.R., 1995. Experimental simulation study on start-up of the 5MWnuclear heating reactor. Nucl. Eng. Des. 158, 111–123.

Jiang, S.Y., Wu, X.X., Zhang, Y.J., 2000. Experimental study of two-phase flow oscillation n natural circulation loop. Nucl. Sci. Eng. 135, 177–189.

Kaliatka, A., Uspuras, E., 2000. Benckmark analysis of main circulation pump trip events at the Ignalina NPP using RELAP5 code. Nucl. Engg. Des. 202, 109–118.

Kaliatka, A., Uspuras, E., 2002. Thermal-hydraulic analysis of accidents leading to local coolant flow decrease in the main circulation circuit of RBMK-1500. Nucl. Engg. Des. 217, 91–101.

Koncar, B., Mavko, B., 2003. Modeling of low pressure subcooled flow boiling using RELAP5 code. Nucl. Eng. Des. 220, 255–273.

Kruijf, W.J.M., de Ketelaar, K.C.J., Avakian, G., Gubernatis, P., Caruge, D., Manera, A., Van der Hagen, T.H.J.J., Yadigaroglu, G., Dominicus, G., Rohde, U., Prasser, H.-M., Castrillo, F., Huggenberger, M., Hennig, D., Munoz-Cobo, J.L., Aguirre, C., 2003. Planned experimental studies on natural-circulation and stability performance of boiling water reactors in four experimental facilities and first results (NACUSP). Nucl. Eng. Des. 221, 241–250.

Kuran, S., Xu, Y., Sun, X., Cheng, L., Yoon, H.J., Revankar, S.T., Ishii, M., Wang, W., 2006. Startup transient simulation for natural circulation boiling water reactors in PUMA facility. Nucl. Eng. Des. 236 (22), 2365–2375.

Kuran, 2006. Modeling and simulation if coupled flow/power behavior in low pressure natural circulation systems. Doctoral dissertation, Purdue University.

TH-831_05610306

Lakshmanan, S.P., Pandey, M., 2007. Numerical simulation of startup transients in a natural circulation boiling system. In: Proceedings of 12th International Topical Meeting on Nuclear Reactor Thermal Hydraulics (NURETH-12), Pittsburgh, PA, USA, Log No. 95.

Lee, J. D., Pan, C., 2005. Non linear analysis for a double-channel two-phase natural circulation loop under low-pressure conditions. Annals of Nuclear Energy 32, 299–329.

Lockhart, R. W., Martinelli, R. C., 1949. Proposed Correlation of Data for Isothermal Two-Phase, Two-Component Flow in Pipes. Chem. Eng. Progress. 45 (1), 39-48.

Manera, A., 2003. Experimental and analytical investigations on flashing-induced instabilities in natural circulation two-phase systems. Doctoral dissertation. Delft University of Technology.

Manera, A., 2005. A startup procedure for natural circulation boiling water reactors. In: Proceedings of the 11th International Topical Meeting on Nuclear Reactor Thermal Hydraulics (NURETH-11), Avignon, France, Log No. 80.

Manera, A., van der Hagen, T.H.J.J., 2003. Stability of natural-circulation-cooled boiling water reactors during start-up: experimental results. Nucl. Technol. 143, 77–88.

Manera, A., Rohde, U., Prasser, H.-M., van der Hagen, T.H.J.J., 2005. Modelling of flashing induced instabilities in the start-up phase of natural circulation BWRs using the two-phase flow code FLOCAL. Nucl. Eng. Des. 235, 1517-1535.

Marcel, C.P., 2007. Experimental and numerical stability investigations on natural circulation boiling water reactos. Doctoral dissertation. Delft University of Technology.

Pan, C., Wang, S.B., Hsieh, C.C., Lee, J.D., Chen, W.L., Jong, C.R., Twu, S.S., 1999. Using a natural circulation loop to investigate the relevant thermal hydraulic phenomena in an ABWR. TPC Project Report.

Paniagua, J.,Rothagi,U.S., Prasad, V., 1999. Modeling of thermal hydraulic instabilities in single heated channel loop during startup transients. Nucl. Eng. Des. 193, 207–226.

Parker, T.S., Chua, L.O., 1989. Practical Numerical Algorithms for Chaotic Systems. Springer-Verlag.

Pradeep, K.P., Khardekar, A., Iyer, K.N., 2010. Experimental and numerical investigations on two phase natural circulation test facility. In: Proceedings of 20th National and 9th International ISHMT-ASME Heat and Mass Transfer Conference, Mumbai, India.

TH-831_05610306

Press, W. H., Teukolsky, S. A., Wetterling, W.T., Flannery, B.P., 1993. Numerical Recipes in C. Cambridge University Press.

RELAP5/SCDAP, Development Team, 1997. SCDAP/RELAP5/MOD3.2 Code Manual Volume I: SCDAP/RELAP5 interface theory. NUREG/CR-6150-Rev 1.

RELAP5 Team, 2001. RELAP5/MOD3.3 Code manual volume I: Code structure, system models, and solution methods. NUREG/CR-5535/Rev 1-vol I.

RELAP5 Team, 2001. RELAP5/MOD3.3 Code manual volume IV: Models and correlations. NUREG/CR-5535/Rev 1- vol IV.

Rohatgi, U. S., Cheng, H. S., Khan, H. J., Wulff, W., 1997. Preliminary phenomena identification and ranking tables (PIRT) for SBWR start-up stability. Brookhaven National Laboratory, BNL-NUREG-52504.

Rosenstein, M.T., Collins, J.J., De Luca, C.J., 1993. A practical method for calculating largest Lyapunov exponents from small data sets. Physica D 65, 117–134.

Shieh, A.S., Ransom, V.H., Krishnamurthy, R., 1994. RELAP5/MOD3.0 code manual volume 6: Validation of numerical techniques in RELAP5/MOD3.0.

Sinha, R.K., Kakodkar, A., 2006. Design and development of AHWR-the Indian thorium fuelled innovative nuclear reactor. Nucl. Eng. Des. 236, 683– 700.

Subki, M.H., Aritomi, M.,Watanabe, N., Kikura, H., Iwamura, T., 2003. Transport mechanism of thermohydraulic instability in natural circulation boiling water reactors during startup. J. Nucl. Sci. Technol. 40 (11), 918–931.

Taylor, D., 1984. TRAC-BD1/MOD1: An Advanced Best Estimate Computer Program for Boiling Water Reactor Transient Analysis, Volume I: Model Description, Idaho National Engineering Laboratory, NUREG/CR-3633, EGG-2294.

Tiselj, I., Cerne, G., 2000. Some comments on the behaviour of RELAP5 numerical scheme at very small time step. Nucl. Sci. Eng. 134, 306–311.

Tu, J.Y., Yeoh, G.H., 2002. On numerical modeling of low-pressure subcooled boiling flows. Int. J. Heat Mass Transfer 45, 1197–1209.

Urbonas, R., Uspuras, E., Kaliatka, A., 2003. State-of-the-art computer code RELAP5 validation with RBMK-related separate phenomena data. Nucl. Eng. Des. 225, 65–81.

van Bragt, D. D. B., van der Hagen, T. H. J. J., 1998a. Stability of natural circulation boiling water reactors: PartI: Desciption stability model and theoretical analysis in terms of dimensionless groups. Nucl. Technol. 121.

TH-831_05610306

van Bragt, D.D.B., de Kruijf, W.J.M., Manera, A., van der Hagen, T.H.J.J., van Dam, H., 2002. Analytical modeling of flashing-induced instabilities in a natural circulation cooled boiling water reactor. Nucl. Eng. Des. 215, 87-98.

Wang, D. Z., 1993. The design characteristics and construction experiences of 5 MWt nuclear heating rector. Nucl. Eng. Des. 143, 19-24.

Wang, S.B., Wu, J.Y., Pan, C., Lin, W.K., 1994. Thermal-hydraulic oscillations in a low pressure two-phase natural circulation loop at lowpressures and high inlet subcoolings. In: 4th Int. Tropical Meet. Nuclear Thermal Hydraulics Operations and Safety, Taipei, Taiwan, Paper 53-C.

Wolf, A., Swift, J.B., Swinney, H.L., Vastano, J.A., 1985. Determining Lyapunov exponents from a time series. Physica 16 D, 285–317.

Weaver, W. L., Shumway, R. W., Singer, G.L., Rouhani, S.Z., 1986. TRAC-BF1 Manual: Extensions to TRAC-BD1/MOD1, Idaho National Engineering Laboratory. NUREG/CR-4391, EGG-2417.

Wu, C.Y., Wang, S.B., Chin, Pan, 1996. Chaotic oscillations in a lowpressure two-phase natural circulation loop under low power and high inlet subcooling conditions. Nucl. Eng. Des. 162, 223–232.

Yeoh, G.H., Tu, J.Y., 2002. Implementation of a two-phase boiling model into the RELAP5/MOD2 computer code to predict void distribution in low-pressure subcooled boiling flows. Nucl. Sci. Eng. 140, 181–188.

TH-831_05610306